DEPARTMENT OF BIOLOGICAL SCIENCES

EARLY TROPHOBLAST PATTERNING AND DIFFERENTIATION DURING MAMMALIAN DEVELOPMENT: *IN VIVO, EX VIVO* AND STEM CELL STUDIES

DOCTOR OF PHILOSOPHY DISSERTATION

STAVROS NIKOLAOU

2017

DEPARTMENT OF BIOLOGICAL SCIENCES

EARLY TROPHOBLAST PATTERNING AND DIFFERENTIATION DURING MAMMALIAN DEVELOPMENT: *IN VIVO, EX VIVO* AND STEM CELL STUDIES

STAVROS NIKOLAOU

A dissertation submitted to the University of Cyprus in partial fulfillment of the requirements for the degree of Doctor of Philosophy

December 2017

VALIDATION PAGE

Doctoral Candidate: Stavros Nikolaou

Dissertation Title: Early trophoblast patterning and differentiation during mammalian development: *in vivo*, *ex vivo* and stem cell studies.

The present Doctoral Dissertation was submitted in partial fulfilment of the requirements for the degree of Doctor of Philosophy at the Department of Biological Sciences and was approved on the 15th of December 2017 by the members of the examination committee.

Examination committee:

Research Supervisor: Pantelis Georgiades, PhD, Associate professor, Head of Embryology and Stem Cells Laboratory, University of Cyprus.

_____

Committee member: Paris Skourides, PhD, Associate professor, Head of the Cell Biology and Molecular Embryology Laboratory, University of Cyprus.

_____

Committee member: Androniki Kretsovali, PhD, Professor, Institute of Molecular Biology and Biotechnology, Crete, Greece.

Committee member: Kleopas Kleopa, PhD, Professor, Cyprus Institute of Neurology and Genetics.

Committee member: Chrysoula Pitsouli, PhD, Assistant professor, Department of Biological Sciences, University of Cyprus.

DECLARATION OF DOCTORAL CANDIDATE

The present doctoral dissertation was submitted in partial fulfilment of the requirements of the degree of Doctor of Philosophy of the University of Cyprus. It is a product of original work of my own unless otherwise mentioned through references, notes, or any other statements.

..... [Full name of Doctoral Candidate]

..... [Signature]

Περίληψη

Η τροφοβλάστη του πλακούντα είναι ενας γενικός όρος ο οποίος περιλαμβάνει μια ομάδα κυτταρικών τύπων με κοινή αναπτυξιακή καταβολή (το πολικό τροφεκτόδερμα του κυήματος πριν την εμφύτευση στην μήτρα) οι οποίοι αποτελούν εξολοκλήρου τον πλακούντα κατά την διάρκεια των πρώιμων σταδίων του σχηματισμού του και οι οποίοι εν τέλει θα αποτελέσουν τον κύριο κορμό κυτταρικών τύπων του όταν αυτός σχηματιστεί πλήρως.

Ο πλακούντας είναι ένα επιστημονικώς ελκυστικό και ιατρικώς σημαντικό όργανο το οποίο αποτελείται από κύτταρα δύο ανθρώπων (της μητέρας και του αναπτυσσόμενου κυήματος) και το οποίο είναι απαραίτητο για την επιβίωση και αύξηση του εμβρύου στα θηλαστικά. Η παρούσα μελέτη επικεντρώθηκε στην χρήση του ποντικίσιου εμβρύου για την διερεύνηση άγνωστων πτυχών των πρώτων γεγονότων προτυποποίησης της τροφοβλάστης τα οποία συμβαίνουν κατά την πρώιμη μετεμφυτευτική περίοδο. Χρησιμοποιήθηκαν επίσης βλαστοκύτταρα της τροφοβλάστης (πολυδύναμα κύτταρα με απεριόριστο δυναμικό αυτό-ανανέωσης και τα οποία μπορούν να διαφοροποιηθούν σε κάθε κυτταρικό τύπο τροφοβλάστης) ως εργαλείο για την βαθύτερη κατανόηση του τρόπου διαφοροποίησης τους στον σωλήνα.

Διερευνήθηκαν δυο ασθενώς κατανοητά γεγονότα διαφοροποίησης. Πρώτον, ταυτοποιήθηκε το όριο μεταξύ των δύο ιστών της πρώιμης τροφοβλάστης: του εξω-εμβρυϊκού εκτοδέρματος (ExE; Επιθηλιακός ιστός προοριζόμενος να διαφοροποιηθεί στα κυτταρικά παράγωγα του χοριονικού εκτοδέρματος του πλακούντα) και του εκτοπλακουντικού κώνου (EPC; Μη επιθηλιακος ιστός με κωνική δομή, ο οποίος αποτελεί τον πρόδρομο ιστό όλων των υπολοίπων τροφοβλαστικών κυτταρικών τύπων του πλακούντα). Συνεκτικά, το εξω-εμβρυϊκό εκτόδερμα και ο εκτοπλακουντικός κώνος αποτελούν τους πρόδρομους ιστούς όλων των κυττάρων τροφοβλάστης στον ώριμο πλακούντα. Παρόλο που η ταυτοποίηση του ορίου μεταξύ των δύο ιστών είναι ένα σημαντικό προαπαιτούμενο για την κατανόηση της πρώιμης προτυποποίησης στην τροφοβλάστη, ο ακριβής εντοπισμός του δεν είχε επιχειρηθεί άμεσα προηγουμένως. Έτσι, ταυτοποιήσαμε αυτό το όριο για πρώτη φορά, βασιζόμενοι σε γνωστές μοριακές και λειτουργικές διαφορές μεταξύ του εξω-εμβρυικου εκτοδέρματος και του εκτοπλακουντικού κώνου, χρησιμοποιώντας διάφορες πειραματικές προσεγγίσεις που περιελάμβαναν

καλλιέργειες τροφοβλαστικών έκφυτων. Επιπλέον αυτού, ελέγξαμε κατά πόσον η γονιδιακή έκφραση καινούριων ή καθιερωμένων γονιδίων-δεικτών υπακούει αυτό το όριο, με αποτέλεσμα να επικυρώσουμε την χρηστικότητα τους ως δεικτών εξω-εμβρυικου εκτοδέρματος ή εκτοπλακουντικού κώνου. Δεύτερον, διερευνήθηκαν άγνωστες πτυχές της πρώιμης προτυποποίησης εντός του εξω-εμβρυικου εκτοδέρματος κατά μήκος του ΄΄εγγύτερου-απώτερου΄΄ άξονα (ως εγγύτερο σημείο ορίζεται το πιο κοντινό σημείο στον εκτοπλακουντικό κώνο και ως απώτερο, το πιο μακρυνό σημείο από αυτόν). Έτσι η εργασία αυτή παρήγαγε διάφορα καινούρια ευρήματα τα οποία περιλαμβάνουν τα ακόλουθα: (α) ανάλυση της γονιδιακής έκφρασης, *in vivo*, 6.5 μέρες μετά την γονιμοποίηση (E6.5, η εμφύτευση συμβαίνει κατά την E4.0) έδειξε ότι το εξω-εμβρυϊκό εκτόδερμα μπορεί να υπο-διαιρεθεί σε τουλάχιστον τρείς μοριακά διακριτές περιοχές (απώτερη, ενδιάμεση, εγγύτερη) κατά μήκος του ΄΄εγγύτερου-απώτερου΄΄ άξονα του εν αντιθέσει με τις δύο που υποστήριζε προηγουμένως η διεθνής βιβλιογραφία. (β) ο εντοπισμός των περιοχών τροφοβλάστης που αποκρίνονται στην σηματοδότηση Fgf και Nodal/Activin (σηματοδοτικά μονοπάτια που είναι απαραίτητα για την διατήρηση βλαστοκυττάρων τροφοβλάστης στον σωλήνα) πραγματοποιήθηκε σε σχέση με την νεο-ανακαλυφθείσα υποπεριοχή του εξω-εμβρυϊκού εκτοδέρματος. (γ) Ανίχνευση της χωρο-χρονικά ρυθμιζόμενης γονιδιακής έκφρασης στην πρώιμη τροφοβλάστη συνδυαζόμενης με *ex vivo* καλλιέργειες έκφυτων απώτερου εξω-εμβρυϊκού εκτοδέρματος παρουσία ή απουσία πρωτεϊνών Fgf και/ή Nodal/Activin, ή *ex vivo* καλλιέργειες ολόκληρων εμβρύων με ή χωρίς αναστολή των μονοπατιών Fgf και/ή Nodal/Activin, οδήγησε στην περιγραφή ενός νέου μοντέλου για την πρώιμη προτυποποίηση της τροφοβλάστης: (γ1) Οι τρείς περιοχές του εξω-εμβρυϊκού εκτοδέρματος εμφανίζονται κατά σειρά με την απώτερη περιοχή να είναι η πρώτη που εμφανίζεται κατά την ανάπτυξη, να παρουσιάζει θετική απόκριση και στα δύο μονοπάτια Fgf/Activin και να είναι παρούσα πριν τον σχηματισμού του εκτοπλακουντικού κώνου. (γ2) Ο χαρακτήρας της απώτερης περιοχής διατηρείται παρουσία και των δύο σηματοδοτικών μονοπατιών, ενώ ο εκτοπλακουντικός κώνος (ο οποίος δεν αποκρίνεται σε κανένα από τα δύο σηματοδοτικά μονοπάτια) σχηματίζεται απευθείας από την απώτερη περιοχή του εξω-εμβρυϊκού εκτοδέρματος στην απουσία των Fgf και Activin. (γ3) Η εγγύτερη περιοχή του εξω-εμβρυϊκού εκτοδέρματος (η οποία παρουσιάζει απόκριση στο μονοπάτι Activin αλλά όχι στο μονοπάτι Fgf), σχηματίζεται

από την απώτερη περιοχή εξω-εμβρυϊκού εκτοδέρματος διαμέσου της ενδιάμεσης περιοχής (η οποία επίσης παρουσιάζει απόκριση στο μονοπάτι Activin αλλά όχι στο μονοπάτι Fgf) παρουσία Activin αλλά όχι Fgf.

Εν τέλει, δημιουργήθηκε ένα σύστημα λέντι-ιών για να δημιουργήσουμε διαγονιδιακά βλαστοκύτταρα τροφοβλάστης τα οποία εκφράζουν την πράσινη φθορίζουσα πρωτεΐνη με πυρηνικό εντοπισμό, έτσι ώστε αυτά να χρησιμοποιηθούν ως ένα νέο εργαλείο για την απεικόνιση των βλαστοκυττάρων σε ζωντανές συνθήκες. Το εργαλείο αυτό, χρησιμοποιήθηκε για να συσχετίσουμε για πρώτη φορά την μορφολογία ζωντανών βλαστοκυττάρων τροφοβλάστης με τις αλλαγές στο μέγεθος του πυρήνα τους καθώς επίσης και στο περιεχόμενο της χρωματίνης τους που συμβαίνουν κατά την διάρκεια της διαφοροποίησης τους.

Συνεκτικά, τα ευρήματα αυτής της εργασίας αναμένεται να οδηγήσουν στην καλύτερη κατανόηση της πρώιμης προτυποποίησης της τροφοβλάστης *in vivo* και να παράσχουν ένα χρήσιμο εργαλείο για την διερεύνηση της κυτταρικής συμπεριφοράς των βλαστοκυττάρων τροφοβλάστης, υπό ζωντανές συνθήκες.

Abstract

Placental trophoblast is a term that encompasses a group of cell types with a common origin (the polar trophectoderm of the preimplantation conceptus) that make up the entire placenta during the initial stages of its formation and eventually comprise most cell types of the fully formed placenta. The placenta is a scientifically fascinating and medically important organ that contains cells from two individuals (mother and the developing conceptus) and is required for the viability and growth of the mammalian fetus. The main focus of this work was to use the mouse conceptus as a model to investigate unknown aspects of the earliest patterning events within the trophoblast compartment during the initial stages of placenta formation at around the early postimplantation period. Trophoblast stem cells (TS cells; established multipotent stem cells with indefinite self-renewal that can specifically differentiate into all trophoblast cell types) were also used as a tool to further our understanding of their mode of differentiation *in vitro*.

Two poorly understood trophoblast patterning events were investigated here. First, was the identification of the boundary between the first two compartments of early trophoblast, the extraembryonic ectoderm (ExE; an epithelial tissue fated to form the chorionic ectoderm derivatives of the placenta) and the ectoplacental cone (EPC; a non-epithelial, cone-like structure, which is the progenitor of the remaining placental trophoblast cell types). Collectively, ExE and EPC are the progenitors of all placental trophoblasts. Although identification of ExE-EPC boundary is an important prerequisite for understanding early trophoblast patterning, its location has not been directly addressed previously. This boundary was identified here for the first time based on known molecular and functional differences between ExE and EPC using various experimental approaches including culture of various trophoblast explants. Moreover, known and new ExE/EPC gene expression markers were assayed to test whether they respect this boundary, thereby validating their usefulness in distinguishing ExE from EPC character. Second, was the investigation of unknown aspects of early patterning within ExE itself, along its proximal-distal (PD) axis (proximal is closest to EPC and distal furthest away from it). In this regard, this work produced several novel findings that include the

following. (a) *In vivo* gene expression analysis at embryonic day 6.5 (E6.5; implantation begins at around E4.0) showed that ExE can be subdivided into at least three molecularly distinct regions (distal, intermediate and proximal) along its PD axis, as opposed to only two according to current literature. (b) The location of active FGF and Nodal/Activin signaling (signaling pathways necessary for maintaining TS cells *in vitro*) was identified in relation to the newly discovered ExE subdivision. (c) Detection of spatio-temporally regulated gene expression within early trophoblast combined with *ex vivo* culture of distal ExE explants in the presence or absence of FGF and/or Activin proteins, or *ex vivo* culture of whole conceptuses with or without inhibition of FGF and/or Activin signaling, led to a novel model of early trophoblast patterning: (c1) The three ExE regions appear in a step-wise manner with distal ExE character being the earliest, showing active FGF/Activin signaling and appearing in the first-formed ExE (at around E5.0), before EPC formation. (c2) Distal ExE character is maintained in the presence of both FGF and Activin signaling, whereas EPC (which lacks active FGF/Activin signaling) forms directly from distal ExE character in the absence of both FGF and Activin signaling. (c3) Proximal ExE (which displays active Activin, but not FGF, signaling) forms from distal ExE via intermediate ExE (displays only Activin signaling) in the presence of Activin, but not FGF.

Lastly, a lentivirus-based system was employed to generate novel transgenic TS cells that express green fluorescent protein (GFP) specifically in their nuclei, so as to be used as a new tool for TS cell live imaging. This tool was used here to correlate for the first time live TS cell morphologies with changes in their nuclear size and chromatin content during TS cell differentiation.

Taken together, the findings of this work are expected to lead to a better understanding of early trophoblast patterning *in vivo* and provide a useful tool for investigating cell behavior in live TS cells.

Acknowledgements

The requirements for this PhD degree took about 8 years to get completed. During these years several people had contributed towards its successful completion; to these people I want to express my honest thankfulness:

First of all, I want to thank my teacher and supervisor, associate professor Pantelis Georgiades, for the fruitful discussions, his scientific and moral help and advices as well as for triggering my scientific interest towards several difficult-to-approach questions. From him I took many lessons regarding the scientific approach and also lessons that will help me during my scientific career as well as my life.

I am also thankful to my teacher, associate professor Paris Skourides, for his valuable comments during the entire duration of my PhD studies, his many friendly advices regarding science or social life, his valuable help for the confocal imaging and several experimental approaches and for contributing in my examination committee. From him I learned that science and life can be more productive when you are focused and you think simply and practically.

I want to thank the examination committee composed (in addition to Drs Pantelis Georgiades and Paris Skourides) by professor Androniki Kretsovali (Institute of Molecular Biology and Biotechnology, Crete, Greece), professor Kleopas Kleopa (Cyprus Institute of Neurology and Genetics) and assistant professor Chrysoula Pitsouli (University of Cyprus) for taking the time to evaluate this work and for their very friendly comments for the better presentation and writing of this thesis. I appreciate it and thank all of them by heart.

The long time it took me to complete this study, had as a result to make a lot of good friends and colleagues. Although it is impossible to mention them all here, I want to personally thank, by heart, my good friends Christophoros Odiatis, PhD and Katerina Drakou, PhD for the many days and nights we spent thinking, discussing and experimenting towards finding the best solution for the issues we were facing. I am

thankful and obliged to my friends Artemis Elia, Xenia Hadjikipri, Giasemia Ioannou and Antrea Aristotelous for helping me by doing some of the required or supplementary experiments (Xenia Hadjikipri has performed some of the *in situ* hybridization reactions in pcEPC and ppExE explants; Artemis Elia and Giasemia Ioannou have performed some of the supplementary experiments).

Most of all I want to thank my beloved parents, Christophoros and Kalia for standing by me, not only during the many years my studies lasted but also during my entire life. Their strong belief on my abilities and their encouragement were the reasons I stayed focused on my studies and did not break up by the several issues that emerged during all these years. In addition, I want to thank them for teaching me that all problems exist to get solved.

Lastly, I want to thank the many people that had helped me in any possible way. I appreciate their help and I hope to help them back one day.

To my parents
with love

Table of contents

List of figures

List of tables

List of abbreviations

AC: Amniotic cavity

ACF: Amniochorionic fold

Al: Allantois

Al-bud: Allantois bud

Am: Amnion

AmEc: Amnion's ectoderm

AmM: Amnion's mesoderm

ASP: Anterior separation point

attR (or attL): Attachment site right (or left, respectively)

AVE: Anterior visceral endoderm

BM: Basement membrane

BMP: Bone morphogenetic protein

CA: Capsid

Ch: Chorion

Ch-TGCs: Channel trophoblast giant cells

CMV: Cytomegalovirus

C-TGCs: Canal trophoblast giant cells

DBA: Dolichos biflorus agglutinin

DIG: Digoxygenin

DTA: Diptheria toxin A

DVE: Distal visceral endoderm

EC: Exocoelomic cavity

EMT: Epithelial mesenchymal transition

emVE: embryonic visceral endoderm

Env: Envelope

EPC: Ectoplacental cone

EpiSCs: Epiblast stem cells

ExE: extraembryonic ectoderm

exVE: extraembryonic visceral endoderm

EPCa: Ectoplacental Cavity
ES: Embryonic stem cells
FBS: Fetal bovine serum
FCM: Fibroblast conditioned medium
Fgf: Fibroblast growth factor
FITC: Fluorescein isothiocyanate
GAG: glucozaminoglucan chains
Gag (for lentiviruses): Group specific antigen
GFP: Green fluorescence protein
GlyT: Glycogen trophoblast cell
HIV: Human immunodeficiency virus
HS: Heparan sulfate
HSC: Haematopoietic stem cell
HSPGS: Heparan sulfate proteoglycans
JZ: Junctional zone
IN: Integrase
IVT: *In vitro* transcription
LaTP: Labyrinth Trophoblast Progenitor
LTR: Long terminal repeat
MA: Matrix
MEFs: Mouse embryonic fibroblasts
MEF-CM: mouse embryonic fibroblast conditioned medium
MGI: Mouse genome informatics
NC: Nucleocapsid
PAC: proamniotic cavity
PAS: Periodic acid-Schiff
PaE: Parietal endoderm
pcEPC: putative core EPC
PCP: Planar cell polarity
PD: Proximodistal
PIC: preintegration complex

Pol: Polymerase
ppExE: putative proximal ExE
PS: Primitive streak
P-TGCs: Parietal trophoblast giant cells
R: Repeat region
RI: type I receptor (TGFb signaling)
RII: type II receptor (TGFb signaling)
RM: Reichert's membrane
RT: Reverse transcriptase
PCR: Polymerase chain reaction
PR: Protease
RRE: Rev response element
RT: Reverse transcriptase
SAR: Spiral artery remodeling
SCM: Stem cell medium
SEM: Scanning electron microscopy
SpA: Spiral arteries
SpA-TGCs: Spiral artery trophoblast giant cells
SpT: Spongiotrophoblast cell
S-TGCs: Sinusoidal Trophoblast Giant Cells
Syn-I: Syncytiotrophoblast layer I
Syn-II: Syncytiotrophoblast layer II
TGF: Transforming growth factor
TS: Trophoblast stem cells
uNK: uterine Natural killer cells
UTR: Untranslated region
VE: Visceral Endoderm
VYS: Visceral yolk sac
wISH: whole mount *in situ* hybridization
XEN: Extraembryonic endoderm cells
ZA: Zonular adherence

CHAPTER 1:

INTRODUCTION

1. Introduction

1.1 An introduction to the mature placenta with emphasis on its trophoblast cell types

The placenta (flat cake in latin) is a vital organ for intra-somatic development of the mammalian embryo as is necessary for the embryo to develop, grow and survive within the uterine environment. Its physiological function is really broad as (i) it mediates the exchange of nutrients and oxygen from the mother to the fetus as well as metabolic by-products and CO2 from the fetus to the mother, (ii) via the synthesis and secretion of hormones, it regulates the maternal physiology and uterine environment so that it meets fetal requirements for a healthy pregnancy and (iii) it mediates maternal immune system modulation to protect the semi-allogenic embryo from rejection and (iv) it is a hematopoietic site. Interestingly, the placenta is the only known organ that is structured by tissues from two different organisms: the fetus (trophoblast and endothelial cells) and mother (decidual stromal cells, uterine Natural Killer and endothelial cells). The term “trophoblast” is collectively used to describe an embryo-derived group of cell types with a common lineage, the fate of which is to become the main cellular component of the placenta by forming the embryo-derived parts of that organ. The clinical importance of the placenta is made clear in several diseases with defective placenta development and functionality like preeclampsia (Al-Jameil et al., 2014), intrauterine growth restriction (Nardozza et al., 2017) and miscarriages (Zhu et al., 2017).

1.1.1 General placenta anatomy

The better understanding of placenta development and physiology during health and disease, requires the detailed description of its architectural structure. The definitive placenta (i.e. the developmental stage where the organ is fully developed and functional; occurs by the embryonic day E10.5-E12.5) is characterized by radial symmetry, (that means any midsaggital sections whose plane passes through the central axis of the organ will look similar to each other) is composed by three morphologically and functionally distinct regions (Fig. 1) (Georgiades et al, 2002;

Mesometrial site **mother** **Proximal**

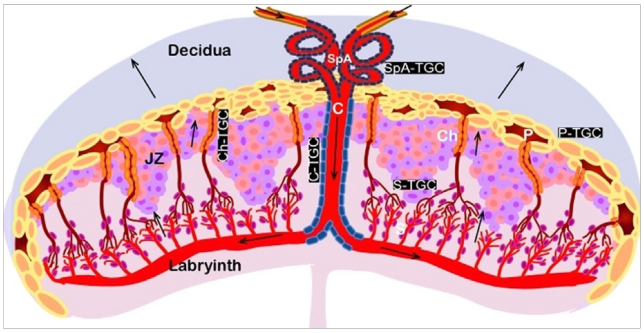

Anti-mesometrial site **fetus** **Distal**

Figure 1: Placenta architecture showing the three different regions composing the placenta and their relation to the mother (mesometrial or proximal side) and the fetus (antimesometrial or distal side). The localization of the Trophoblast Giant Cells is also depicted. SpA: Spiral Arteries, SpA-TGCs: Spiral Artery Trophoblast Giant Cells, C: Central Canal, C-TGCs: Canal Trophoblast Giant Cells, S-TGCs: Sinusoidal Trophoblast Giant Cells, Ch: Channels (venous), Ch-TGCs: Channel Trophoblast Giant Cells, P: Parietal layer, P-TGCs: Parietal Trophoblast Giant Cells (secondary), JZ: Junctional Zone. Modified from Rai and Cross, 2014

Simmons, 2014). These regions are apparent in sections along the midsaggital plane of the organ.

Located closest to the fetus (antimesometrially) is the “labyrinthine area”, the most distal compartment of the placenta. Directly overlying the labyrinthine layer, is the “junctional zone” which is itself followed by the “maternal decidua", the most proximal compartment of the placenta, located closest to the mother (mesometrially). In order to mediate its physiological function, placenta is composed by a delicate network of blood spaces which bring the maternal and the fetal blood in close apposition, yet completely separated, in order for the gases and nutrients to be exchanged without intermixing.

Depending on the tissue structure between the maternal blood and the fetal blood, we can discriminate placentas into three categories: epitheliochorial, endotheliochorial and hemochorial (Fig. 2). The human, as well as the mouse placentas are hemochorial, that means, the maternal blood is in direct contact with embryo-derived cells (trophoblast) (Simmons, 2014; Rai and Cross, 2014).

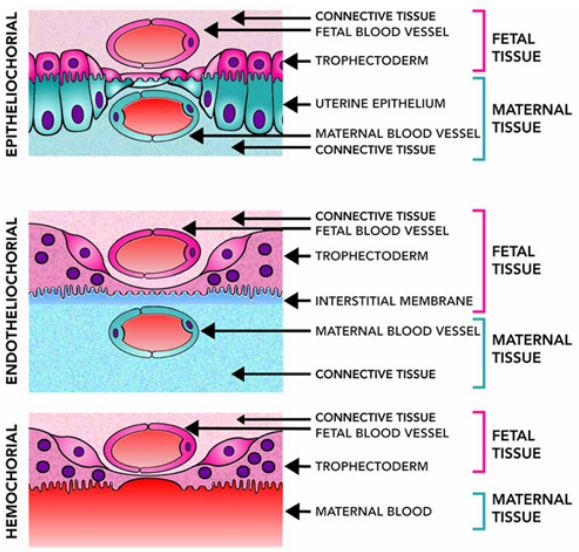

Figure 2: Placentas can be discriminated into three main categories. The human and mouse placenta belong to the hemochorial category, that is the maternal blood is in direct contact with the trophoblast. Adopted from http-//www.frontiersin.org/files/Articles/52035/fnana-07-00022-HTML/image_m/fnana-07-00022-g002

1.1.2 Vessel structure and blood flow through the placenta

The definitive placenta (E12.5) is characterized by two different blood circulations: the maternal and the fetal. In the maternal circulation, the oxygenated, rich in nutrients maternal blood after leaving the uterine artery, enters the spiral arteries (5-10 in number) of the maternal decidua through the radial arteries and radial artery branching (Fig. 3). At the level of junctional zone, spiral arteries exit the maternal decidua converging into one or two large in diameter central canals which transfer the blood through the junctional zone to the base of the labyrinth (Fig. 3 and 4A). From the basal canals, maternal blood abruptly enters into smaller sinusoids which drive it upwardly into the labyrinth, close to the junctional zone, through spiral and highly anastomosing sinuses which are trophoblast-lined (Fig. 4A' and 4D). During this time, maternal blood exchanges the carried oxygen for fetal-derived carbon dioxide as well as nutrients for fetal metabolic by-products. Sinusoids then coalesce into several channels (venous channels) traversing the junctional zone and coalescing into lacunae at the interface between the junctional zone and the maternal decidua (Fig. 4B - Adamson et al, 2002). From the lacunae, the blood is now driven into larger maternal venous sinuses which are lined by maternal endothelium, into the decidua basalis. In the fetal circulation, the fetal blood enters the umbilical artery which branches into several arterioles at the base

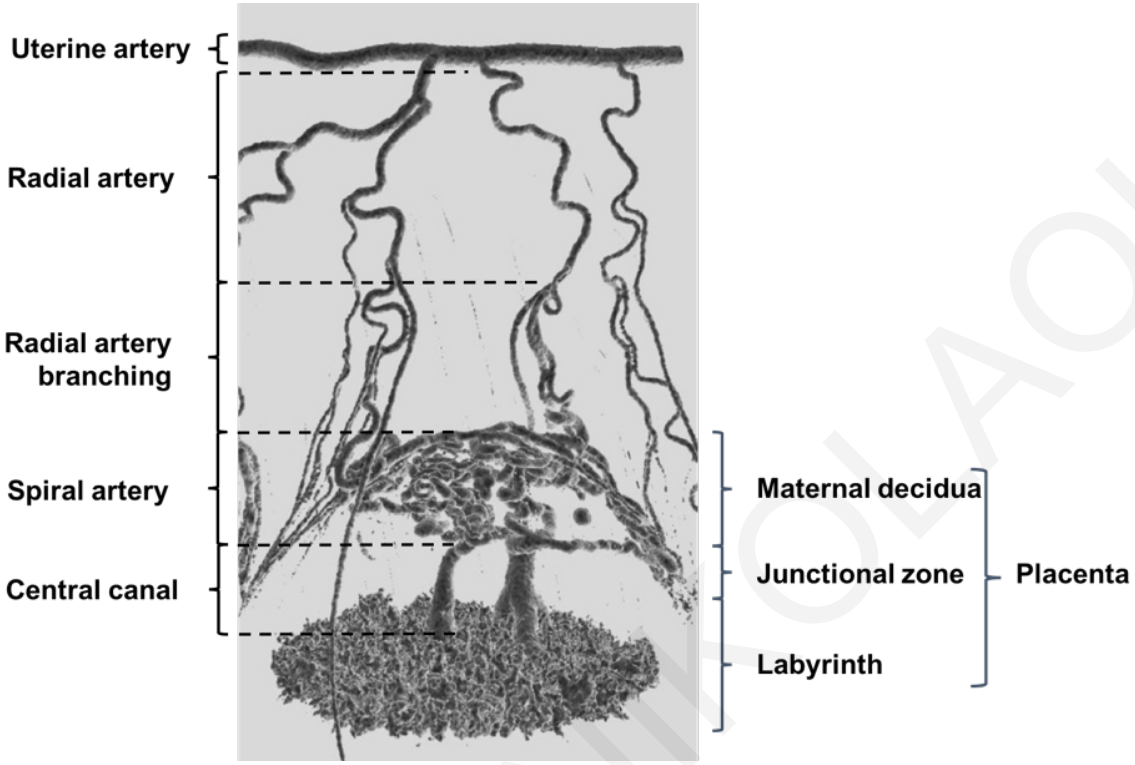

Figure 3: micro Computer Tomographic image visualizing maternal arterial system in the placenta. Modified from Venditti et al, 2013

of the placenta (Fig. 4D). Arterioles course the blood towards the anterior side of the labyrinth, close to the junctional zone. At this point, they abruptly branch into a dense network of capillaries which direct the blood back towards the fetal part of the labyrinth (Fig. 4C). At this point, the fetal blood's flow is counter to the maternal blood's and this favors the exchange of gases and compounds (Adamson et al, 2002). The oxygenated, nutrient rich fetal blood is then directed into placental venules and eventually it enters the umbilical vein.

1.1.2.1 Examples of trophoblast giant cells associated with maternal blood flow within the placenta

During the course of maternal blood through the placenta, the blood is not always in contact with maternal endothelium. In contrast, by approximately 300um prior entering the junctional zone and during the entire course into the "fetal portion" of the placenta

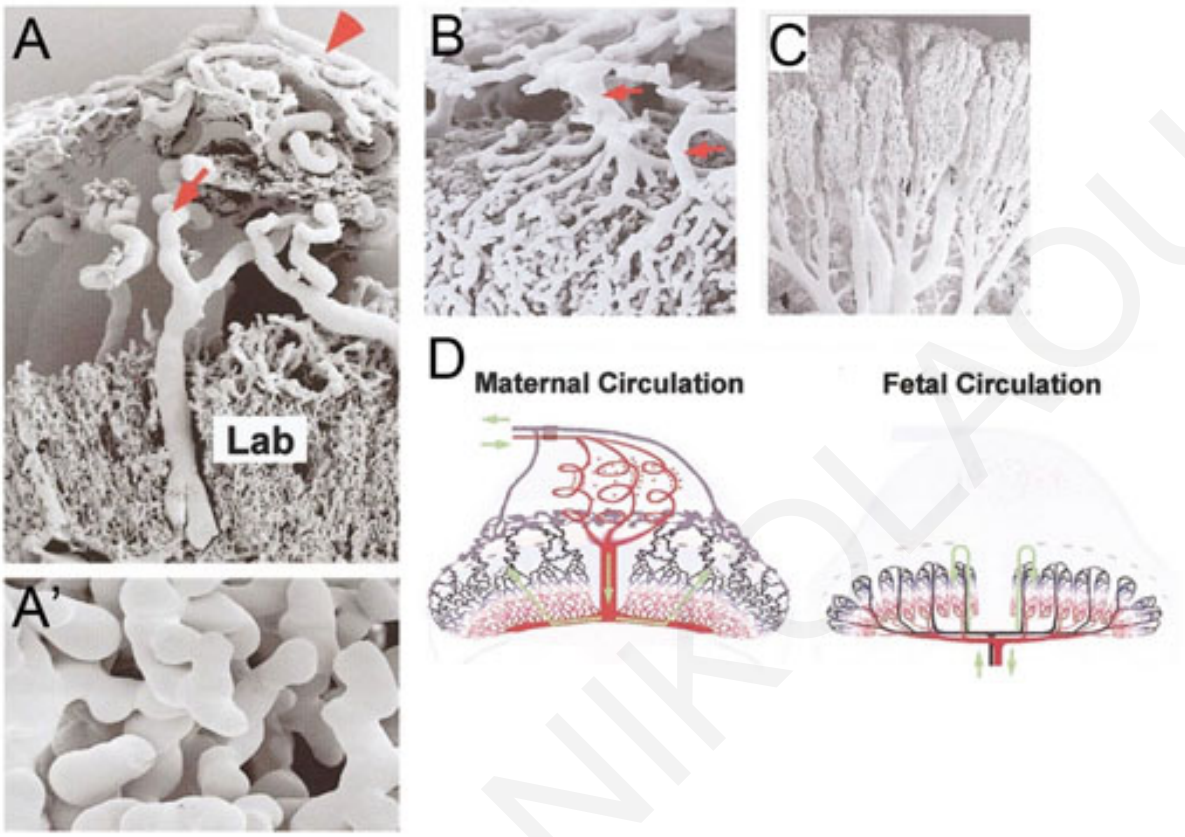

Figure 4: The placenta arterial system and blood flow A: Scanning Electron microscopy (SEM) of a vascular cast indicating the arterial system of the placenta. The red arrow and arrowhead indicate the spiral arteries, A': high magnification SEM indicating the labyrinthine sinusoid spaces, B: SEM of a maternal vascular cast indicating the venous system in the labyrinth and the junctional zone. Arrows indicate the venous channels and the lacunae at the interface between junctional zone and decidua, C: Fetal arteries branching into a dense network of capillaries in the labyrinth, D: Flow of the maternal or the fetal blood from arterial system (red color) to the venous system (grey color) through the placenta. Modified from Adamson et al, 2002

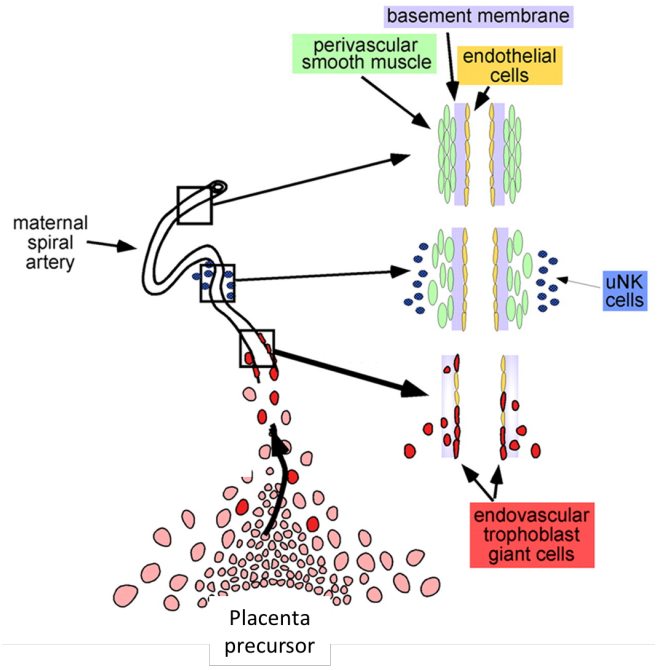

Figure 5: Diagram indicating SpA-TGCs migration from the developing placenta precursor, to the lowest region of the maternal spiral artery, where they completely substitute artery's endothelial cells. Modified from Screen et al, 2008

(i.e. distal most part of the spiral arteries, canal, labyrinthine sinusoids, venous channels and lacunae), the maternal blood is in direct contact with specialized, embryo derived trophoblastic giant cell types with distinct morphology, behavior, polyploid nucleus and transcriptional profile (Fig. 1 - Simmons et al, 2007).

Starting from the most distal part of the spiral arteries (approximately 300um from the junctional zone), the maternal endothelium is being invaded and eventually substituted by spiral artery associated trophoblast giant cells (SpA-TGCs) in a process recently described as "vascular invasion and endothelial mimicry" (Fig. 5 - Rai and Cross, 2014). This process is part of a more general process, known as spiral artery remodeling - SAR and results in a high, undisturbed blood flow from the mother to the embryo. SAR involves the loss of spiral artery contractility, a reduction to the thickness of the artery's wall and increase in lumen's diameter (artery dilation). Because SpA-TGCs have been found to line the spiral artery (Simmons et al, 2007), it was reasonable to speculate that these cells are implicated in SAR. In order to investigate that, Hu and Cross used a

transgenics approach to induce the expression of a cytotoxin (Diptheria Toxin A - DTA) in these cells, thus eliminating their population (Hu and Cross, 2011). Their results strongly suggest that these cells are involved at least in the initiation of SAR because in their absence, spiral artery lumen diameter as well as blood flow were significantly reduced. SAR is also regulated by uterine Natural Killer cells (please refer to section 1.1.5) so it is likely that these two cell populations work in cooperation (Fig. 5 – Chakraborty et al, 2011).

In addition to SAR, SpA-TGCs secrete several placental lactogen-related family members, such as *Prl5a1*, *Prl6a1*, *Prl4a1* (*Plp-A*), *Prl2a1*, *Prl2c* (*Proliferin - Plf*), *Prl7b1*, *Prl7c1* and *Prl7d1* (Simmons et al, 2008). Members of this family of proteins are hormones that play a significant role during pregnancy: they modify maternal metabolism through pancreas regulation, maternal behavior, corpus luteum development and mammary gland development (reviewed in Soares et al, 2007). Although a unique marker of SpA-TGCs has yet to be identified, these cells can be distinguished using a combination of markers, like the positivity for *Prl2c* and *Prl4a1* and negativity for *Prl3d1* (*Pl-I*), *Prl3b1* (*Pl-II*) and *Ctsq*.

Exiting the spiral artery, maternal blood enters the central canal whose wall is also made from another type of trophoblast giant cells, the so-called canal trophoblast giant cells (C-TGCs) (Simmons et al, 2007). Interestingly the lining of canals (as well as the lining of venous channels and lacunae) was not initially composed by maternal endothelium which was then substituted by trophoblast but they were constructed *de novo* by trophoblast cells (vasculogenic mimicry, a process recently reviewed by Rai and Cross, 2014). The ability of trophoblast cells to behave like endothelial cells and form lumen *de novo* has been verified recently (Rai and Cross, 2015). Although it is generally believed that C-TGCs have just a structural role (Hu and Cross, 2010), these cells also secrete a series of Placenta lactogen-related proteins like Prl4a1, Prl2a1, Prl2c, Prl3b1, Prl8a6, Prl7b1, Prl7d1 and Prl7a2 so they should have some endocrine role as well (Simmons et al, 2008). It is also reasonable to speculate that due to their location, C-TGCs might regulate blood flow through the canal. C-TGCs can be distinguished by their positivity for *Prl2c* (*Proliferin - Plf*), *Prl3b1* (*Pl-II*) and *Ctsq* as well as for their negative expression of *Prl3d1* (*Pl-I* - Simmons et al, 2007).

Within the labyrinth, maternal blood is in close contact with a third trophoblast giant cell type, sinusoidal trophoblast giant cells - S-TGCs (please refer to section 1.1.3.). From the labyrinthine sinusoids, the maternal blood is carried into the junctional zone through specific channels (venous channels) which lead into lacunae at the interface between the junctional zone and the maternal decidua. As mentioned earlier, the walls of these blood spaces are not lined by maternal endothelium but instead, they are lined by a fourth trophoblast giant cell type, known as channel trophoblast giant cells (Ch-TGCs). These cells express their own unique combination of marker genes (i.e. *Plf*, *Pl-II*, *Ctsq*, *Tle3*) (Gasperowicz et al, 2013). Unfortunately, not any specific marker gene has been identified so far. E12.5 placentas of mouse embryos null for *Tle3* display defective spiral arteries and canal architecture but also total absence of channels and lacunae with only a few and small Ch-TGCs lining their walls. Most of these embryos die before E15.5 (Gasperowicz et al, 2013).

1.1.3 The Labyrinthine region of the placenta: The site of maternal-fetal exchange

Labyrinth is the region where the exchange of oxygen (O2) for carbon dioxide (CO2) and nutrients for fetal metabolic by-products takes place. In scanning electron microscopy studies, the three-dimensional structure of this area has been elucidated: it is composed of a complex network of branched and anastomosed fetal capillaries and maternal sinusoid (blood) spaces lined with trophoblast (Detmar et al, 2008; Kulandavelu et al, 2013; Adamson et al, 2002) (Fig. 4).

Although the general structure of the labyrinth is maintained during gestation, several changes can be observed as gestational age advances. For example, the thickness of labyrinth area increases while the size of maternal sinusoid spaces become decreased (Adamson et al, 2002). This is believed to be responsible for the dramatic increase in placental functional efficiency observed during late gestational stages (Moll, 1985). This is evidenced by the observation that although embryo weight increases by two-fold during this period, placenta's weight remains relatively constant (Iguchi et al., 1993; Louvi et al., 1997).

Transmission electron microscopy studies aiming to uncover the light structure of fetal capillaries and maternal sinusoid spaces have identified the existence of four cellular

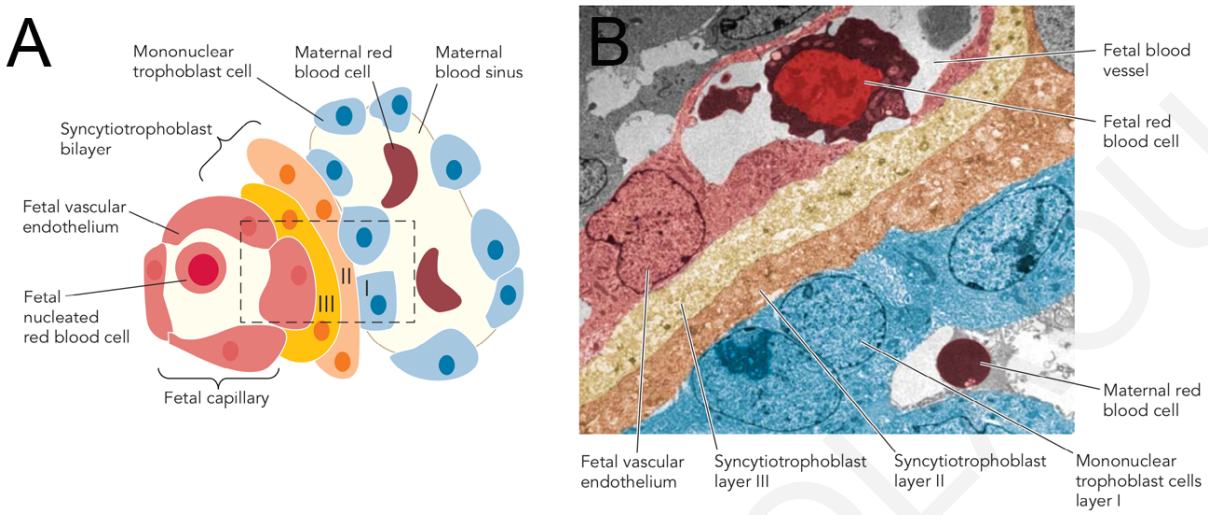

Figure 6: The light structure of the mouse placenta is composed by three trophoblastic layers followed by a fetal endothelium. A: Diagram depicting the architecture of the three layers relative to the mother and the fetus. Note that maternal blood is in direct contact to both trophoblast layers I and II but not layer III. B: Transmission electron microscopy of the labyrinth structure. Blue color indicates S-TGCs (layer I), orange color indicates Syn-I (layer II) and yellow color indicates Syn-II (layer III). Light red color marks the fetal endothelium encloding a fetal red blood cell. Modified from Watson and Cross, 2005

layers separating the fetal from the maternal blood circulations (Adamson et al, 2002; Georgiades et al, 2002; Watson and Cross, 2005 – Fig. 6). Directly facing the maternal sinusoid is a layer of loosely connected, mononuclear giant cells of trophoblast origin (trophoblast layer I - Georgiades et al, 2002) known as sinusoidal trophoblast giant cells (S-TGCs) (Simmons et al, 2007). The basal site of S-TGC is loosely attached to a syncytial layer of trophoblast cells known as syncytiotrophoblast layer I - Syn-I (or trophoblast layer II - Georgiades et al, 2002). A second trophoblast-derived syncytial layer, known as syncytiotrophoblast layer II (Syn-II) lies directly under Syn-I (or trophoblast layer III - Georgiades et al, 2002). Of these three trophoblast layers, only the layer III (Syn-II) is situated onto a basement membrane. The same basement membrane is also the site of attachment of the fetal endothelial cells lining the lumen of fetal capillaries. Due to the loose intercellular attachment of S-TGCs between themselves as well as with the underlying Syn-I, maternal plasma can be in direct contact with layer II. This excludes a role in nutrient transport for S-TGCs. The strategic

location of these cells, at the exact interface between mother and fetus, makes it possible that these cells are involved in the regulation of placenta's transport efficiency, possibly by the secretion of hormones and other molecules. Indeed, in an expression study of the prolactin hormone gene family members, S-TGCs were found to be positive for the expression of at least three known members of this family (Prl2b1, Prl3b1, Prl7d1) (Simmons et al, 2008). Interestingly, Prl7d1 has been found to have anti-angiogenic effects on endothelial cells (Jackson et al, 1994). S-TGCs appear to have a single large nucleus with intensive DAPI staining, an indicator of polyploidy. In addition, these cells appear to be positive for *Cathepsin Q* (*Ctsq*), *Hand1* and *Prl3b1* expression (Simmons et al, 2007). The role of S-TGCs has been addressed directly by linking DTA under the control of *Ctsq* promoter, thus eliminating S-TGCs (Outhwaite et al, 2015). Thus, in the absence of S-TGCs, embryos are growth retarded and die by late gestation (E18.5).

In strict contrast to the discontinuous localization of S-TGCs, the undisturbed, continuous nature of the two syncytial layers (Syn-I and Syn-II) emphasizes the importance of the complete separation of maternal from fetal circulation. To mediate their role in maternal-fetal exchanges the two layers can be permeated either by active or by passive diffusion means (reviewed in Watson and Cross, 2005). Both layers express transmembrane molecules required for transport of nutrients and ions such as the glucose transporters GLUT1 (SLC2A1) and GLUT3 (SLC2A3), the gap junction protein connexin 26 (cx26 - required for glucose diffusion – Gabriel et al, 1998) and the monocarboxylate transporters of lactate MCT1 (SLC16A1) and MCT4 (SLC16A3). The subcellular localization of these molecules appears to be highly polarized since GLUT1 is localized at the apical membrane of Syn-I and the basal membrane of Syn-II while GLUT3 is exclusively localized to the apical membrane of Syn-I (Shin et al, 1997, 1996). In addition, MCT1 is localized to the apical membrane of Syn-I while MCT4 is located at the basal membrane of Syn-II (Nagai et al, 2010). These data strongly suggest that both syncytiotrophoblast layers are polarized epithelial barriers that can mediate maternal-fetal exchanges. In fact, disruption of this polarity, as is the case of c-Met signaling attenuation (by *c-Met* knock-out), resulted in defective subcellular distribution of the transferrin receptor (CD71), a protein necessary for the uptake of iron from the embryo (Ueno et al, 2013). This suggests that disrupted polarity could lead to defective

transport capacity of the labyrinth. Since the apical and basal membranes of a polarized epithelial cell have distinct molecular signature (Nelson, 2009), it would be of interest to identify the molecular mechanisms that control the localization of same-family proteins or even the same protein in one of the two compartments.

Permeabilization efficiency of syncytial layers is regulated by growth factors as in the absence of insulin-like growth factor II (*Igf-II*), an alteration in the function of system A amino acid transporter is observed, resulting in fetal growth restriction (Constancia et al, 2002). Furthermore, reduced expression of *Igf-II* is associated with reduced expression of *Cx26* but enhanced expression of lipid transport proteins such as the fatty acid transporter CD36 and the cholesterol transporter ABCA1 (Kuehnel et al, 2017). Similarly, attenuation of parathyroid hormone/parathyroid hormone-related peptide receptor is linked with reduced active transport of calcium (Kovacs et al, 1996). Passive diffusion is also an important means for maternal-fetal transport: the thickening of the trilaminar trophoblastic layer observed in a placental specific *Igf-II* knock-out, increases the diffusional distance and therefore reduces placental permeability (Constancia et al, 2002). Similar findings were obtained in the attenuation of a subgroup of the vertebrate-specific ESCC microRNA family (Paikari et al, 2017).

Syn-I layer can be identified not only by the apical localization of MCT1 but also by the expression of *Syncytin A* (*Syna*) (Dupressoir et al, 2009) as well as by the expression of *Ly6e* (Hughes et al, 2013). Interestingly, Syncytin A is a protein produced by the envelope region of an endogenous retrovirus that has infected the germ line of murine ancestors about 20 million years ago and has cell-cell fusogenic properties (Dupressoir et al, 2005). *Syna* knock-out embryos display disruption of their labyrinthine architecture with Syn-I cells failing to fuse in order to make a syncytium. Furthermore, cell overexpansion in the fetal blood vessels is observed followed by apoptosis, fetal growth retardation and eventually embryo death between E11.5-13.5 (Dupressoir et al, 2009). Syn-II layer can be identified by the expression of *Gcm1*, *Cebpa* and *Syncytin B* (*Synb*) (Simmons et al, 2008). Syncytin B, just like Syncytin A, is derived from an endogenous retrovirus and displays cell-cell fusion activity (Dupressoir et al, 2005). Electron microscopy examination of *Synb* knock-out placentas reveals defective formation of Syn-II with failed cell-cell fusion but embryos survive to term with minor

growth retardation (Dupressoir et al, 2011). This finding suggests that maternal-fetal exchange is not significantly affected in *Synb* knock-out placentas. This could possibly be explained by a compensatory mechanism of the ectopic over expression of *Connexin 30* observed in these placentas. Double knock-out of *Syna* and *Synb* has as a result the early death of embryos, by E9.5-E10.5, which is earlier than in single *Syna* knock-out. This strongly suggests that (i) Syncytin B has an early effect on placenta formation provided that Syncytin A is also absent and (ii) Syn-I and Syn-II cooperate during development.

In addition to the differentiated trophoblast cells, recently it was found that the labyrinth at least from E14.5, also contains progenitor trophoblast cells capable of giving raise to all three labyrinthine trophoblast cell types described so far (S-TGCs, Syn-I and Syn-II) both *in vitro* and *in vivo* (Ueno et al, 2013). This population of cells (labyrinth trophoblast progenitor - LaTP) resides in clusters, is BrdU positive, expresses high levels of epithelial cell adhesion molecule (Epcam) and *Gcm1* and is dependent upon c-Met signaling for its maintenance (but not specification) and proper terminal differentiation into polarized syncytiotrophoblast (Ueno et al, 2013). A subpopulation of Epcam positive cells, also expresses high levels of the *stem cell antigen I* - *Sca-I*. This subpopulation is also negative for *Gcm1* but positive for *Eomes* and *Cdx2* and upon its culture under permissive conditions, it is able to switch its phenotype into an undifferentiated trophoblast stem cell-like population (trophoblast stem cells are multipotent proliferative epithelial cells which under appropriate conditions can differentiate in all trophoblast cell types- please refer to section 1.3) (Natale et al, 2017; Tanaka et al, 1998) Interestingly, these results were reproduced from *Sca-I*+ cells derived up to E18.5 placentas (Natale et al, 2017).

Other cell types in the labyrinth which are not of trophoblast origin are the lumen endothelial cells which are characterized by the expression of *Flt1*, *Cd34* and *Pdgfb* (Nelson et al, 2016) and pericytes, which are perivascular cells located between endothelial cells and Syn-II. Although pericytes have been shown to regulate vascular morphogenesis and function, their role in the placenta still remains elusive (Armulik et al, 2011). Since they can be identified by the expression of alpha smooth muscle actin

and chondroitin sulfate proteoglycan (NG2), is expected that more interest will be focused on these cells (Simmons, 2014).

Recently it was found that placenta labyrinth in addition to its role as a maternal-fetal exchange interface and endocrine region, is also a site of hematopoietic stem cell (HSC) generation, maintenance and expansion (Rhodes et al, 2008). The maintenance (prevention of differentiation) of HSC is dependent on the responsiveness of S-TGCs on PDGF-B signaling from the fetal endothelium as in the absence of PDGF-B, S-TGCs ectopically produce and secrete erythropoietin, which results to the ectopic erythropoiesis in the fetal vasculature (Chhabra et al, 2012).

1.1.4 The junctional zone of the placenta

By E12.5, the junctional zone appears as a binary sheet of cells sandwiched between the labyrinth layer and the maternal decidua. The layer closer to maternal decidua is relatively homogeneously composed of giant cells (parietal trophoblast giant cells - P-TGCs) thus is denoted as the “Giant cell layer” while the layer closer to the labyrinth is mostly composed of two cell types, the spongiotrophoblast (SpT) and the glycogen trophoblast cells (GlyT). Because SpT are more abundant, the layer is often denoted as the “spongiotrophoblast layer”.

The exact role of spongiotrophoblast layer in mouse development is yet ill defined but its importance was made obvious in knock-out embryos lacking the expression of the maternally expressed imprinted gene *Mash2* which totally lack this layer to the favor of the giant cell layer (Guillemot et al, 1994) or of the *trophoblast specific protein alpha - TpbpA* which lacks this layer but the giant cell layer is unaffected (Hu and Cross, 2011). Such embryos do not survive post E10.5. So, this finding shows that the presence of this layer is vital for embryo survival. In contrast, absence of another maternally expressed imprinted gene, the *Phlda2,* causes dramatic expansion of spongiotrophoblast layer without affecting embryo viability (in fact, embryos at birth weight as wild type embryos) (Frank et al, 2002). The presence of even reduced volume of spongiotrophoblast layer seems to be sufficient to maintain embryo survival until term as it happens in partial loss or overexpression of *Mash2* (Oh-McGinnis et al, 2011; Tunster et al, 2016).

The two main cell populations (i.e. the SpT and GlyT) in the spongiotrophoblast layer can be distinguished by their morphology, their behavior and their transcriptional profile:

- SpT cells have a compact and dense appearance and they remain within the contour of the spongiotrophoblast layer. Their role is currently poorly understood but it seems like they have an endocrine role because they express a series of genes of the prolactin family of hormones (i.e. *Prl3b1*, *Prl8a8*, *Prl8a9*, *Prl8a6*, *Prl8a1*, *Prl7a1*, *Prl7a2*, *Prl7d1*, *Prl3c1*, *Prl3a1*, *Prl2c*, *Prl5a1*, *Prl2b1*, *Prl4a1*) as well as *Mash2*, *TpbpA* and *Psgs* (Tunster et al., 2016; Simmons et al, 2008; Guillemot et al, 1994).

- GlyT cells appear to be vacuolated cells, within the spongiotrophoblast layer with stored glycogen as indicated by positive Periodic acid-Schiff (PAS) staining (Fig. 7). Within the spongiotrophoblast layer, GlyT cells are not randomly localized but instead they form wrapping layers around every maternal blood space (central canal and channels, also in lacunae of the giant cell layer and around the spiral arteries in maternal decidua) (Gasperowicz et al, 2013). By E14.5, GlyT cells migrate interstitially the giant cell layer, reach the maternal decidua and concentrate around the spiral arteries where they release their stored glycogen (Coan et al, 2006). Their number is reduced to the half by two to four days later (E16.5 - E18.5) (Coan et al, 2006). In this way, it is believed that they contribute to embryo growth. The role of GlyT cells is currently elusive because there are no models of specific elimination of these cells, likely because until recently there was not any GlyT specific marker gene which could be used to study them and as a driver of cre-mediated DTA expression. However, in a model of partial loss of *Mash2*, although the SpT is reduced (as already said) and the GlyT are totally absent, embryos are still developed to term, albeit growth retarded (Oh-McGinnis et al, 2011). This finding indicates that GlyT cells are not responsible for embryo viability but likely for embryo growth. In addition, in models of enhanced expression of either *Mash2* or *Phlda2*, glycogen cells are present but are mislocalized into the labyrinth layer instead of the maternal decidua, failing to release their glycogen stores. This failure in glycogen release

is believed to be the reason for the growth retarded embryos observed at term (Tunster et al, 2016; Tunster et al, 2010). Fortunately, it is now known that the protocadherin 12 (*Pcdh12*) is a specific marker for GlyT cells so is expected that more light will be shed up on this mysterious cell population (Rampon et al, 2005). *Pcdh12*$^{-/-}$ embryos are growth retarded at birth with their placentas having several morphological alterations like reduced cell density and vascularization in the labyrinth, increased glycogen content in the GlyT cells and mislocalization of these cells into the labyrinth (Rampon et al, 2008). In addition to *Pcdh12* glycogen cells express *TpbpA*, *Gjb3*, *Gys1*, *Igf2*, *Prl6a1*, *Prl4a1*, *Prl2a1*, *Prl8a9*, *Prl7b1*, *Prl7c1*, *Prl7d1* (Tunster et al, 2016). The high number of hormones produced and secreted by GlyT cells, strongly suggests that they contribute to placenta's endocrine activity.

The giant cell layer is a sheet of phagocytic cells with large size and enlarged, polyploid nuclei locating above the spongiotrophoblast layer (Hu and Cross, 2010) known as the Parietal Trophoblast Giant Cells - P-TGCs (secondary, to distinguish them from another population of transcriptionally and phenotypically similar but not identical cells, which appears earlier in development, on a different embryonic site and is known as primary P-TGCs).

The significant role of this layer in embryo development can be extracted by the phenotype of *Hand1* (*Heart and neural crest derivatives expressed 1*) knockout embryos which arrest in development and die by E7.5 (Riley et al, 1998). In these embryos, the giant cell layer is highly eliminated but markers of the spongiotrophoblast layer are still present at levels comparable to the control (i.e. *TpbpA* - Riley et al, 1998). A similar phenotype is seen in *Sak*-null embryos with highly reduced giant cell layer and embryos arrested at E7.5 (Hudson et al, 2001; Martindill et al, 2007). Recent studies have shown that Sak-mediated phosphorylation of Hand1 induces its nucleolar release and subsequent accumulation into the nucleus to induce differentiation into secondary P-TGCs (Martindill et al, 2007). In contrast, in mutants where P-TGCs are present, even at ~40-50% of the control, embryos are being born albeit growth retarded, as is the case for *Jak1*-null embryos (Rodig et al, 1998, Takahashi et al, 2008). P-TGCs express a wide series of Placenta lactogen-family hormones like *Prl3d1*

(*Pl-I*, prior E12.5 - Simmons et al, 2007), *Prl3b1* (*Pl-II*, post E12.5 - Simmons et al, 2007), *Prl7a2*, *Prl2c* (*Plf*), *Prl4a1* (*PlpA* - a specific marker of secondary P-TGCs - Ma and Linzer, 2000), *Prl2a1*, *Prl3d3*, *Prl8a9*, *Prl8a1*, *Prl7d1*, *Prl7a1*, *Prl7a2* (Simmons et al, 2008). This finding strongly suggests an endocrine and paracrine role for P-TGCs.

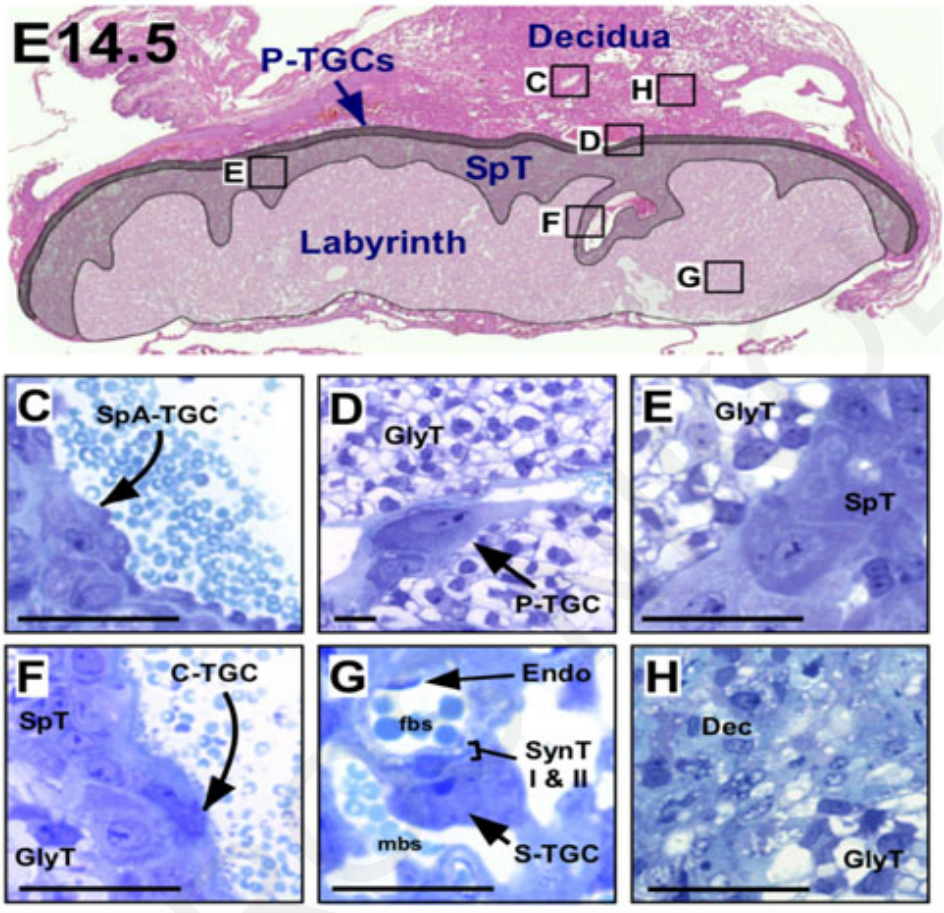

Figure 7: Light micrograph of the placenta at E14.5 depicting the different locations of placental cell types relative to placenta's regions. The numbered squares are shown in high magnification: C: spiral artery trophoblast giant cells (SpA-TGC) lining maternal spiral artery's lumen. D: glycogen trophoblast cells (GlyT) having migrate interstitially through the giant cell layer (P-TGCs) into the decidua while other GlyTs still remain into the spongiotrophoblast layer. E: GlyT and spongiotrophoblast (SpT) cells within the spongiotrophoblast layer. Note the distinct cellular morphology of the two cell types with GlyT being vaculated and SpT being compact and dense. F: canal trophoblast giant cells lining the canal lumen, within the spongiotrophoblast layer. G: light structure of the labyrinth. H: Decidual (Dec) cells are morphologically distinguishable than GlyT cells. Modified from Simmons et al, 2008

Indeed, Prl3d1 (Pl-I) and Prl3b1 (Pl-II) have been shown to regulate the functionality of several maternal organs, like the brain, corpus luteum, pancreas and mammary glands to better adapt to pregnancy (Hu and Cross, 2010). Additionally, *Prl2c* (*Plf*) has been linked to angiogenesis (Jackson et al, 1994). Furthermore, Prl4a1 (PlpA) inhibits the ability of NK cells to secrete interferon-gamma (INFg) which has been shown to induce spiral artery dilation (please refer to 1.1.5) (reviewed in Hu and Cross, 2010).

1.1.5 The decidua basalis region of the placenta

The decidua basalis (refers to here by its alternative name, 'maternal decidua') is the most distal part of the placenta and is largely composed of cells with maternal origin. Two are currently the main known maternal cell types: decidual stromal cells (which contribute to ~90% of the total decidua mass) and uterine Natural Killer cells (uNK - which contribute to about 10-15% of the total decidua mass (Croy et al, 1985). However, as already described, two more cell types, of trophoblast-origin, also exist in the maternal decidua: GlyT (which migrate interstitially and concentrate around spiral arteries) and SpA-TGCs (which migrate and substitute maternal endothelium of the spiral arteries).

The role of the decidual stromal cells remains largely unexplored but in a recent single cell RNA-sequencing study, it was found that they express factors responsible for angiogenesis (*Angiopoietin 4* - *Angpt4*) and vasodilation (*Adrenomedulin* - *Adm*). Moreover, *Adm* has been shown to attract uNK cells (Li et al, 2013). In addition to this role, it seems that stromal cells have endocrine function because they are positive for the expression of several Prolactin-related hormones like *Prl6a1*, *Prl3c1*, *Prl8a9*, *Prl8a2* (Simmons et al, 2008). Interestingly, *Prl8a2* (*decidual prolactin-related protein - Dprp*) is exclusively decidual stromal cell-specific and the *Prl8a2*-null phenotype has been reported (Alam et al, 2007). Under physiological conditions, wild type and mutant embryos are indistinguishable, however under hypoxic conditions, pregnancy failure is observed around E17.5. This failure is associated with enlarged lacunae at the interface between P-TGCs and maternal decidua, expanded giant cell layer, reduction of maternal decidua thickness and decreased invasion of endovascular trophoblast cells (presumably SpA-TGCs).

Pregnancy-associated uterine Natural Killer (uNK) cells exist in two subpopulations, based on *Dolichos biflorus agglutinin* (DBA - a lectin with specificity for α-linked N-acetylgalactosamine) positivity (Paffaro et al., 2003). DBA^- cells express *Interferon gamma* (*Ifng*) while DBA^+ cells express the angiogenic factors *Il22* and *Pgf* as well as *Eomes*, *Cd122, Perforin* (Chen et al, 2012; Nelson et al, 2016). Studies performed in immunocompromised mice which lack uNK cells have provided strong positive association of uNK cells with spiral artery remodeling as uNK-deficient mice fail to remodel their spiral arteries (spiral arteries characterized by narrow lumen, thick wall and presence of vascular smooth muscle actin) while this phenotype is rescued in bone marrow transplanted-uNK deficient mice (Ashkar and Croy, 2001). Because the key molecule responsible for this behavior seems to be the IFNgamma ($Infg^{-/-}$ bone marrow transplanted - uNK deficient mice do not rescue their phenotype) it turns out that it is the DBA^- subpopulation that is involved in spiral artery remodeling. In addition to their role in spiral artery remodeling, DBA^- uNK cells might also be involved in the regulation of trophoblast (GlyT and SpA-TGCs) invasion into the maternal decidua because this process appears to be uNK and IFNg-dependent (Ain et al, 2003). A possible function of the DBA^+ subpopulation is the angiogenesis as they express known angiogenic factors like the *Placenta growth factor* - *Pgf* (reviewed in Gaynor and Colucci, 2017).

1.2 Early trophoblast development and its relation to early mouse embryonic development

1.2.1 Early post implantation mouse development: a period of rapid morphogenetic processes

The first four days after fertilization of the mouse oocyte is a period of cell proliferation and morphogenetic events which have as a result the formation of a vesicular structure known as the blastocyst which attaches onto the uterine epithelium (a process known as implantation). Implantation occurs by the attachment of a specialized cell type of embryonic origin, the primary Parietal Trophoblast Giant Cells (primary P-TGCs). A few

hours after implantation of the blastocyst onto the uterine epithelium (which occurs by E4.5), the mouse embryo has adopted a relatively simple structure, radially symmetric

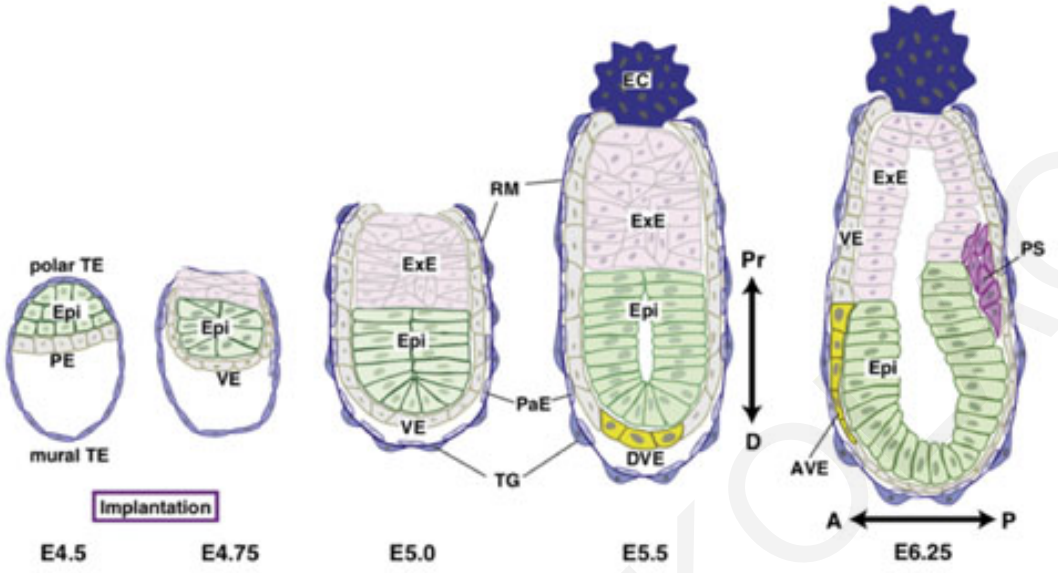

Figure 8: Early post-implantation mouse development (from implantation to PS initiation). Until E5.0 the embryo is composed of only three epithelial tissues, the ExE (light pink color), the Epiblast (green color) and the VE (light green) which are encapsulated within the Reichert's Membrane (RM - light blue-grey color). A few hours later, EPC (dark blue with spots - denoted as EC in the picture) appears at the most proximal point of ExE and DVE (yellow color) appears at the most distal point of Epiblast. Until this developmental stage, the embryo is characterized by a radial symmetry with proximal to distal polarity. One day later, the appearance of PS (magenta color) in the epiblast marks the future posterior site of the embryo. ExE's symmetry however remains radial with proximal to distal polarity. ExE and its first differentiated derivative, EPC are the precursors of the entire trophoblast population of the placenta. PE: Primitive Endoderm, Epi: Epiblast, ExE: Extraembryonic Ectoderm, TG: primary Parietal Trophoblast Giant cells, the trophoblast component of RM, PaE: Parietal Endoderm, the second component of RM, EC: Ectoplacental Cone (EPC in the text), DVE: Distal Visceral Endoderm, AVE: Anterior Visceral Endoderm, PS: Primitive Streak, D: Distal, Pr: Proximal, A: Anterior, P: Posterior. Adopted and modified from Matsuo and Hiramatsu, 2016

with a proximal to distal pattern, composed by three epithelial tissues: the embryonic ectoderm (or epiblast) at the distal half, the extraembryonic ectoderm (ExE) at the proximal half and the Visceral Endoderm (VE) encapsulating the other two tissues (E5.0) (Fig. 8). The whole structure is encaged within a membrane composed of the P-

TGCs and a differentiated derivative of the VE, the Parietal Endoderm (PaE), which lines the membrane's interior surface. This membrane is known as the Reichert's membrane (RM).

The three tissues enclosed within RM will eventually differentiate into all tissues of the adult body as well as all the necessary embryo-derived tissues required for the *in uterus* physiological development. For example, the epiblast's fate is to differentiate into all somatic tissues, ExE's fate is to differentiate into the trophoblastic portion of the definitive placenta and Visceral Endoderm will eventually give the yolk sac placenta, a tissue necessary for the nourishment of the developing embryo for the period prior definitive placenta is functioning (Georgiades et al, 2002). The border between epiblast and ExE can be easily distinguished by a morphological constriction on the overlaying VE. This constriction is known as the "embryonic-extraembryonic junction". Accordingly, the VE associated with epiblast is defined as embryonic VE (emVE) while the one associated to ExE is defined as the extraembryonic VE (exVE).

By this time, a cavity develops at the center of epiblast and expands proximally towards the embryonic-extraembryonic junction (Coucouvanis and Martin, 1995). Cavity's appearance is the result of apoptosis (the process of cavitation) and/or epithelial morphogenetic events (process of hollowing) occurring within the epiblast (Coucouvanis and Martin, 1995; Bedzhov and Zernicka-Goetz, 2014). Shortly afterwards, by E5.5, a new hollowing appears within the proximal part of ExE this time, growing distally and eventually the embryonic and extraembryonic hollows fuse together into a single cavity, known as the proamniotic cavity.

Although by this time the embryo has grown in size and is elongated, its overall structure and radial symmetry has remained essentially the same, except of the proamniotic cavity which spans along the epiblast and the ExE. This embryonic architecture is termed as "the egg cylinder" (although it is not truly a cylinder nor an egg) because it looks like an egg with a lumen to the inside. Between the transition from E5.0 to E5.5, two morphological alterations occur to the egg cylinder, without breaking the symmetry: (i) The formation of a cellular outgrowth on the proximal-most part of the ExE (known as the Ectoplacental Cone – EPC), growing distally and out of

the confines of exVE and (ii) the thickening of the distal-most group of cells of the Visceral Endoderm (known as the Distal Visceral Endoderm - DVE).

Within the next 24 hours, DVE cells actively migrate anteriorly until they reach the embryonic extraembryonic junction (Stower and Srinivas, 2014); DVE is now known as Anterior Visceral Endoderm –AVE. Thus, the initiation of this anterior movement of DVE (which occurs after E5.5), is the first morphological sign of symmetry breaking and by the end of this process (E6.0), the epiblast underneath AVE will be the future anterior site of the embryo, but as yet, no morphological changes occur within the epiblast.

Slightly later, by E6.25 - E6.5, the cells of the epiblast being on the opposite direction of the anterior site of the embryo undergo an epithelial-to-mesenchymal transition (EMT) and delaminate, with the cells specified to a mesodermal fate localizing themselves between the Epiblast and the VE as mesenchymal cells while cells specified through an endodermal fate engressing into the overlaying VE cells (Nowotschin and Hadjantonakis, 2010).

The ingression of the cells has as a consequence the formation of a cleft on one site of the Epiblast, known as the Primitive Steak (PS); the appearance of the PS is considered as the initiation of gastrulation. The Epiblast has now its anterior-posterior and left-right axes fully defined with its anterior end being the site directly underneath the AVE while its posterior end being the site of PS initiation. The end of gastrulation will have as a consequence the embryo to adopt the characteristic of all metazoans triploblastic structure (presence of mesoderm sandwiched between the ectoderm and endoderm). It is important to note that the restriction of AVE at the junction between Epiblast and ExE has as a consequence the maintenance of ExE's radial symmetry and the proximal-to-distal polarity of the extraembryonic half of the embryo.

1.2.2. Epiblast and embryonic Visceral Endoderm

At E5.0 the entire Epiblast is positive for *Oct4* (Chazaud and Rossant, 2006; Chu and Shen, 2010), and *Sox2* (Adachi et al, 2013). Both of these transcription factors are markers of pluripotency and are required during the early stages of development for

the establishment of a pluripotent population in the embryo, in a dose dependent manner (Niwa et al, 2000; Masui et al, 2007; Kopp et al, 2008). During the same time, the TGFb superfamily member Nodal is expressed in a uniform fashion along the entire epiblast and VE (Mesnard et al, 2006). *In vitro* experiments involving epiblast stem cells (EpiSCs – epithelial stem cells derived from the E6.5 epiblast and considered to be the *in vitro* equivalent of epiblast) suggest that Nodal is necessary for the maintenance of pluripotency because in its absence, EpiSCs cease proliferating and differentiate towards the neural lineage (reviewed in Papanayotou and Collignon, 2014). Additionally, *in vivo* experiments in the mouse embryo have shown that in *Nodal*$^{-/-}$ embryos, not only *Oct4* is significantly downregulated but also the posterior identity (i.e. the expression of PS marker genes such as *Eomes*, *Wnt3* and *Lefty2*) is not induced (Brennan et al, 2001). Similar findings were found when both Nodal receptors Cripto and Cryptic, were eliminated from the embryo: *Oct4* is significantly reduced by E5.5 and totally absent by E6.5 (Chu and Shen, 2010).

In addition to *Nodal*, early epiblast is also positive for the expression of *Fibroblast growth factor 4* (*Fgf4*) (Georgiades and Rossant, 2006). *Fgf-4* knockout embryos do not develop significantly post implantation (Feldman et al, 1995). Interestingly, Fgf as well as Nodal protein have to be provided in the culture medium in order to successfully derive epiblast stem cells.

By E5.5, DVE appears at the distal point of the embryo, within the VE as a group of tall columnar cells, expressing *Hex*, the BMP antagonist *Cer1*, the Nodal antagonist *Lefty1*, and the Wnt antagonist *Dkk1* (Rossant and Tam, 2007). In *ex vivo* experiments, where the ExE was microsurgically removed from the epiblast/emVE followed by culture, the DVE (as defined by marker gene expression) was expanded around the entire epiblast. This indicates a role for ExE in restricting the formation of DVE to the distal tip of the egg cylinder (Richardson et al, 2006). It was later found that this ExE-derived signal is the Bone Morphogenetic Protein 4 - BMP4 (Soares et al, 2008). It is likely that BMP4 prevents the formation of DVE via the wnt-signaling member Wnt3 because mutants with enhanced wnt signaling responsiveness (APC$^{-/-}$) fail to form DVE (Chazaud and Rossant, 2006) and because BMP4 has been found to induce *Wnt3* expression at the epiblast (Ben-Haim et al, 2006). In turn, Wnt3 induces Nodal expression in the epiblast

(Ben-Haim et al, 2006) and Nodal induces DVE formation in a Smad2-dependent manner because *Nodal*$^{-/-}$ or *Cripto*$^{-/-}$;*Cryptic*$^{-/-}$ embryos do not form DVE (Brennan et al, 2001; Chu and Shen, 2010). (Fig. 9).

Between E5.5 and E6.0, DVE cells migrate towards the anterior site as a result of differential proliferation within the DVE cell population (Yamamoto et al, 2004), extensive cell rearrangement within the epithelial sheet of VE with planar cell polarity (PCP) signaling (Trichas et al, 2011) and by Rac1-dependent extension of long lamellipodia by the leading cells towards the direction of movement (Migeotte et al, 2010). This movement is prevented to proceed through the embryonic extraembryonic junction because the cells of the exVE display differential localization of the F-actin and the PCP signaling component Dishevelled 2 – Dvl-2 (i.e. both are apically enriched in exVE while they are lateraly enriched in emVE - Trichas et al, 2011).

The current position of AVE cells at the future anterior site of the embryo has as a consequence the regionalized localization of the signaling antagonists they express so that, the expression and responsiveness of the epiblast cells directly underneath AVE to BMP, Nodal and Wnt signals is eliminated. However, the future posterior site of the embryo is still responding to these molecules. The Nodal signaling from the epiblast induces *Bmp4* expression in ExE which, in turn, induces the expression of *Wnt3* back to the posterior epiblast.

Ex vivo experiments involving epiblast explant culture in the presence of exogenously provided Wnt3A or BMP4 have shown that both Wnt3A and BMP4 alone were able to induce the expression of the PS marker *Brachyury – T* (Ben-Haim et al, 2006). In fact, both *Wnt3*$^{-/-}$ and *Bmp4*$^{-/-}$ embryos lack PS induction (Liu et al, 1999; Winnier et al, 1995). Because by E6.5 *Wnt3* is expressed in both the posterior epiblast and the posterior VE, more recent studies aiming to identify the exact tissue that was responsible for the induction of PS, specifically deleted *Wnt3* expression from either tissue and found that nor the epiblast-derived neither the posterior VE-derived Wnt3 were sufficient to induce PS initiation (Tortelote et al, 2013; Yoon et al, 2015). These data suggest that Wnt3 from both tissues is necessary for PS induction in the epiblast

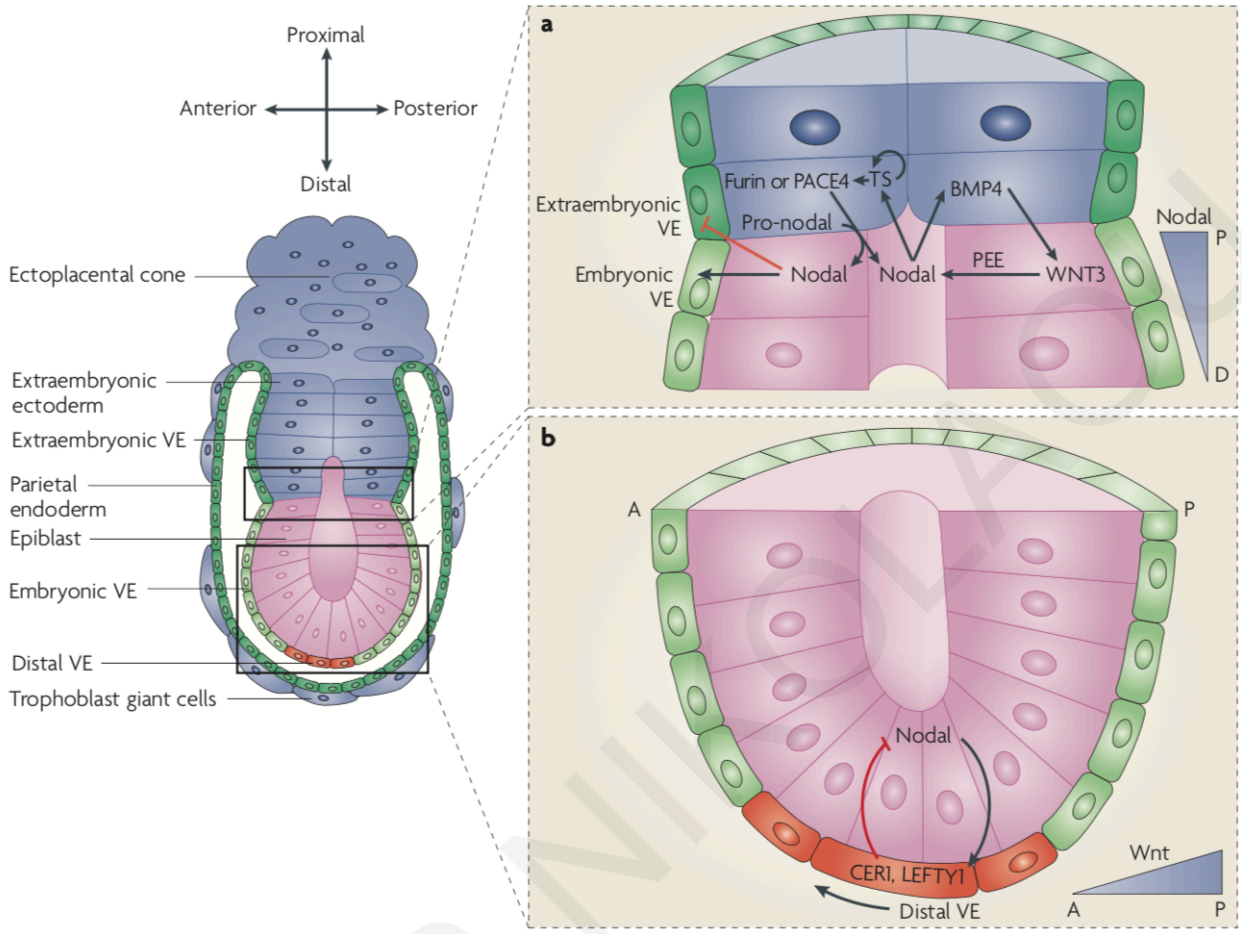

Figure 9: Signaling communication between Epiblast and ExE (a) and Epiblast and DVE (b). (a) Nodal expressed in the Epiblast in a precursor form (pro-Nodal) diffuses to the ExE where it maintains a Trophoblast Stem cell microenvironment (Guzman-Ayala et al, 2004) and the expression of BMP4. Nodal convertases Furin and PACE expressed in the ExE are then cleaving pro-Nodal to provide Epiblast with mature Nodal. In addition, trophoblast derived BMP4 induces the expression of Wnt3 in the epiblast which then induces back the expression of *Nodal*. (b) Epiblast derived Nodal induces the expression of its antagonists in the DVE (Distal VE), which has as a result the formation of a proximal to distal Nodal gradient. The movement of DVE to the future anterior site of the embryo has as a result the formation of a Wnt (and also Nodal) gradient from the anterior to posterior site of the embryo. Adopted and modified from Arnold and Robertson, 2009.

1.2.2.1 The Primitive Streak: a model for epithelial-to-mesenchymal transition studies

The cells comprising the epiblast are polarized epithelial cells of the pseudostratified epithelium type (Williams et al, 2012). Epithelial cells are relatively static and are characterized by a high degree of intercellular adhesions and the presence of an extracellular proteinaceous membrane at their basal region (basal lamina or basement membrane – Lamouilee et al, 2014). Based on the intracellular protein localization, we can determine three morphological states into which cells can belong: (i) the polarized epithelial, (ii) the non-polar intermediate state and (iii) the mesenchymal state (Lamouilee et al, 2014).

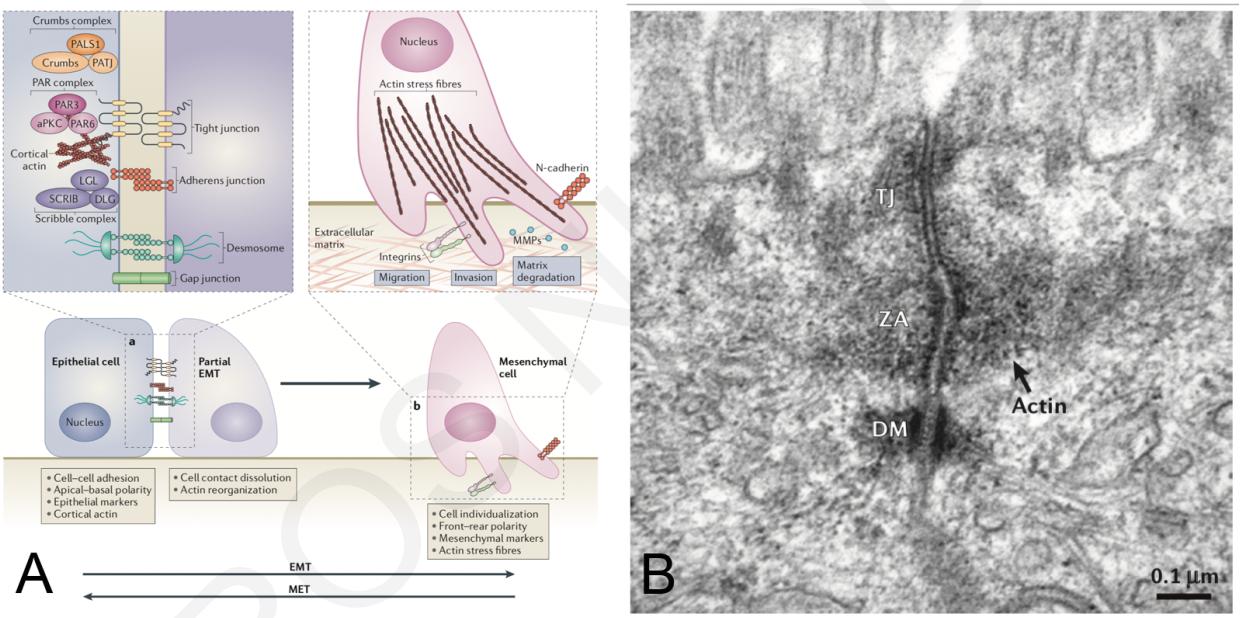

Figure 10: Cells appear in three main morphologies: epithelial, non-polarized and mesenchymal. A) Epithelial cells exist in cell sheets and are characterized by a polarized localization of specific intercellular junctions like tight junctions, adherence junctions and desmosomes as well as the presence of cortical actin. Please note the presence of Par6 in tight junctions. On the other extreme lies the mesenchymal type of cells, which are individual and motile cells characterized by lack of apical-basal polarity, existence of actin stress fibers and expression of mesenchymal markers like N-Cadherin. In between the two cell morphologies is the non-polarized morphology (here denoted as "Partial EMT") characterized by the absence of apical-basal polarity but some degree of intercellular adhesion still remains, albeit not in a polarized manner. B) Transmission electron microscopy demonstrating the existence of intercellular adhesions at the most apical part of the lateral membrane in an epithelial cell. Note the existence of fibrillar actin emanating from the zonular adherence (ZA). Adopted and modified from Lamouille et al, 2014 and Takeichi, 2014

For example, polarized epithelial cells have a squamous, cuboidal or a columnar shape with a primary cilium at their apical membrane, facing the external environment, usually a lumen and a basement membrane at the basal site. This type of cells, contain specialized multi-protein structures known as tight junctions, formed at the most apical site of their laternal membrane and containing proteins like the tight junction protein ZO-1, Claudins (i.e. Cldn4), members of the Par complex (i.e. Par6B) and aPKC. In addition to tight junctions, epithelial cells contain a second type of multi-protein structures, known as adherence junctions which are composed of proteins like E-Cadherin and Lgl (Bedzhov et al, 2014; Williams et al, 2012; Bulganova and Knust, 2009; Li et al, 2015 – Fig. 10). Polymerized actin filaments (fibrillary actin) begin from the adherence junctions, forming a belt-like structure underneath the apical membrane (at the cell cortex), spanning the entire cellular circumferential (Takeichi, 2014).

The physiological function of tight and adherence junctions is (i) to tightly link together two neighboring epithelial cells, (ii) to provide a sealing barrier between the cellular environment facing the apical membrane and the one facing the basolateral membrane and (iii) to maintain the polarized nature of epithelial cells (Gunzel and Yu, 2013).

In the non-polar cells, tight junctions are disrupted and the polarized localization of proteins like E-Cadherin and Par6 disappears as they are now uniformly distributed around the entire cellular membrane. In addition, the cell shape is changing and becomes circular-like but still maintains a high degree of intercellular adhesions, although the actin-belt disappears (Williams et al, 2012; Vinot et al, 2005).

Mesenchymal cells, in contrast, display a reduced degree of intercellular adhesions and high cell mobility with a stellate shape. Epithelial proteins like E-Cadherin and Par6 are not present and the actin cytoskeleton forms long filamentous bundles along the entire cell, known as stress fibers (Lamouille et al, 2014). In addition, mesenchymal-specific proteins like N-Cadherin and Vimentin are now being expressed. Transition of epithelial cells into mesenchymal and vice versa is a very important process during development, but also during disease (Thiery et al, 2009).

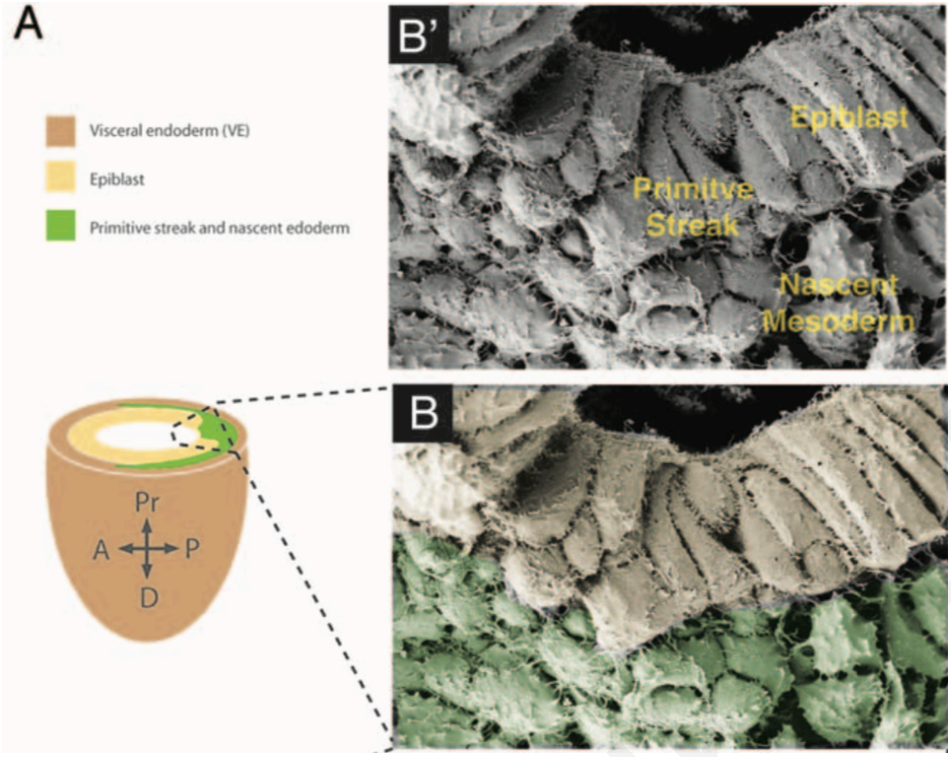

Figure 11: Primitive streak is a site of an epithelial to mesenchymal transition. B (pseudocolorized) and B' is a scanning electron microscopy image whose location in the embryo is shown in A. Polarized epithelial cells (epiblast) move towards the streak, gradually losing their intercellular adhesions to become mesenchymal cells (nascent mesoderm) through a non-polar cellular morphology (the group of cells located below the primitive streak). Adopted from Ferrer-Vanquer et al, 2010

Epiblast cells located at the posterior site of the embryo, are responsive to Nodal, BMP4 and Wnt3, as well as the Nodal induced Fgf8. These cells, progressively start losing their basement membrane and undergoing an Epithelial-to-Mesenchymal Transition (EMT) (Williams et al, 2012). During this process, epiblast cells undergo an apical constriction, ingress through the epiblast, lose their apical-basal polarity and becoming non-polarized cells with E-Cadherin localizing around their entire membrane (Williams et al, 2012). These cells will eventually silence genes for *aPKC*, *Par6* and *E-Cadherin* and will become stellate cells with upregulated *N-Cadherin*, migrating away from the streak as the mesodermal layer of the developing embryo Fig. 11.

Once EMT has initiated, its maintenance is depended on the epiblast-derived Wnt3 signaling as well as the Nodal-induced *Fgf8* (Tortelote et al, 2013; Beck et al, 2002;

Sun et al, 1999). Fgf8 induces the expression of the zinc finger transcriptional repressor *Snail1* at the primitive streak. *Snail1* overexpression in the epithelial cell-line MDCK cells causes disruption of the apical-basal polarity by repressing a member of the Crumbs family (Whiteman et al, 2008) while in the absence of *Snail1 in vivo*, epiblast cells ingress through the streak but they do not lose their apical-basal polarity as shown by electron microscopy studies (Carver et al, 2001). Using cell lines, it has been shown that *Snail1* binds on three specific regions of *E-Cadherin* promoter (E-box sequences) and mediates its downregulation hence enforcing epithelial cells to adopt a mesenchymal morphology (Batlle et al, 2000; Cano et al, 2000).

1.2.3. Extraembryonic ectoderm (ExE): The precursor of all trophoblast cell types

The early (E5.0) ExE is a uniform epithelial tissue in physical contact with the epiblast (reviewed in Nowotchin and Hadjantonakis, 2010). Electron microscopy studies suggest that ExE cells are of irregular shape, with darkly stained nucleus containing a large nucleolus with most of their chromatin concentrated into compact areas around the nuclear envelope (Reinius, 1965; Ahmet et al, 2010).

The close physical association with the epiblast is necessary for the continual distal growth of ExE because isolated ExEs heterotopically explanted or *in vitro* cultured fail to maintain their identity and differentiate (Gardner et al, 1973; Rossant and Ofer, 1977).

Although early ExE is positive for epithelial markers like aPKC, Par6B, F-actin, these molecules appear not to be polarized to the apical surface of the cells, neither there is any lumen formation within it (Bedzhov and Zernicka-Goetz, 2014). These data strongly suggest that the early ExE is a proliferative epithelium comprised of non-polarized cells which grow distally, towards the site of the epiblast. *In situ* hybridization experiments identified the homogeneous expression of several trophoblast multipotency marker genes such as the *Caudal type homeobox 2* - *Cdx2* (Strumpf et al, 2005), *Eomesodermin* – *Eomes* (Russ et al, 2000; Strumpf et al, 2005), *Bone morphogenetic protein 4* - *Bmp4* (Uez et al, 2008) and *ETS proto-oncogene 2* - *Ets2* (Georgiades and

Rossant, 2006). Trophoblast of *Cdx2, Eomes* and *Ets2* knockout embryos is defective and fails to self-renew (Strumpf et al, 2005; Georgiades and Rossant, 2006).

At a slightly later developmental point (by ~E5.5), the cells localizing at the proximal half of ExE initiate epithelial maturation by polarizing the subcellular localization of the epithelial marker proteins Par6B, aPKC and podocalyxin – PCX (now localizing at the apical surface of the cell), rearranging their actin cytoskeleton and initiating lumenogenesis by creating a small hollow between the apical membranes of the distal ExE cells (Bedzhov and Zernicka-Goetz, 2014). The distal half of ExE remains as a non-polarized epithelium in close contact with the epiblast.

ExE is still positive for multipotency marker genes albeit the expression of some of these genes is localized to its distalmost region, close to the epiblast while some others display a more uniform expression across the entire ExE. For example, *Errb*, *Cdx2*, *Eomes*, *Sox2*, *Bmp4* and *PletI* were all found to be distally expressed (Donnison et al, 2015, Luo J et al, 1997, Georgiades and Rossant, 2006; Frankenberg et al, 2007) while genes like *Fgfr2*, *Elf5*, *Ets2* and *Tcfap2c* are still expressed across the entire length of ExE (Georgiades and Rossant, 2006; Donnison et al, 2005, Auman et al, 2002, Donnison et al, 2015).

The same bias of gene expression is retained one day later, at E6.5 with the same genes following the same pattern of expression (including the expression of the *ETS domain-containing transcription factor* - *Erf* along the entire ExE – Papadaki et al, 2007). However, by this time, the proximal ExE cells (i.e. those located closest to the EPC) although retaining their polarized epithelial phenotype, they initiate the expression of a differentiation-associated group of genes like *Achaete-scute homolog 2 – Mash2* and *Keratin 8 – Ker8* (Spruce et al, 2010; Li et al, 2013). At the same time, the previously formed lumen has now expanded distally and fused with the epiblast's lumen, thus creating the proamniotic cavity (Bedzhov and Zernicka-Goetz, 2014). Thus, by E6.5 the ExE is composed of at least two cell populations of polarized epithelial cells: a distally located one, expressing markers of multipotency (and therefore it is considered to be the "trophoblast stem cell storage") and a proximally

located one which expresses simultaneously markers of differentiation and multipotency (Donnison et al, 2015).

A strict balance in the levels of expression of these genes is necessary for their optimal interaction and maintenance of multipotency. For example, low concentration of Elf5 and Tcfap2c is required in order to form a complex with Eomes and promote the expression of multipotency associated genes while increased concentration of Elf5 results to a preferable interaction only with Tcfap2c and the induction of differentiation associated genes (Latos et al, 2015). Overexpression of *Elf5*, as expected causes premature differentiation towards the giant cell phenotype (expansion of *Prl2c*$^{+}$ and complete absence of *TpbpA*$^{+}$ trophoblasts as well as structural defects in the chorion – a derivative of ExE and precursor tissue of labyrinth in the definitive placenta, please refer to section 1.2.7) while *Elf5* knockout embryos fail to maintain their ExE but they have an EPC (Donnison et al, 2005).

A similar dose-dependend relationship was found for *Elf5* and *Ets2* where double heterozygous embryos (i.e. *Elf5*$^{+/-}$; *Ets2*$^{+/-}$) display delayed phenotype of single homozygous embryos. Since both proteins are transcription factors of the same family this behavior was attributed to the regulation of the same genes and therefore the partial absence of each protein was rescued by the partial presence of the other (Donnison et al, 2015). Other studies identified the *Sox2* as a gene regulated by *Elf5* while *Ets2* regulates the expression of *Elf5*, *Cdx2*, *Eomes* and *Bmp4* (Pearton et al, 2014; Polydorou and Georgiades, 2014). In addition to the above *in vivo* studies, in an *in vitro* study using trophoblast stem cells (TS cells – undifferentiated epithelial stem cells which are considered to be the *in vitro* equivalent of ExE - please refer to section 1.3.) the function of the *Placenta-expressed transcript 1* - *Pletl* was found to induce giant cell formation when overexpressed and syncytiotrophoblast formation when downregulated (Murray et al, 2016). Interestingly, *Plet1* is weakly expressed at the distal ExE and strongly in the EPC (Frankenberg et al, 2007). *Mash2*$^{-/-}$ embryos, as already described, present an overexpanded giant cell layer at the expense of spongiotrophoblast layer, but also, they present a reduced chorionic ectoderm (Guillemot et al, 1994).

1.2.4 The formation of ectoplacental cone: the first differentiated derivative of ExE

As ExE expands, EPC appears between E5.0 and E5.5 as an overgrowth of ExE-derived trophoblast cells at its proximal tip which is not surrounded by VE and grows mesometrially, towards the uterine lumen (Robertson, 1942). This event is a very important step during placenta development because it constitutes the first differentiation event towards that. The induction of EPC from ExE is believed to be caused by the continual antimesometrial growth of ExE which has as a result the removal of its proximal-most cells from the effect of the epiblast-derived signals required to maintain ExE's identity.

Currently only one gene has been identified that affects the transition from ExE to EPC. Embryos deficient for the *POU domain, class 2, transcription factor 1 – Oct1* although developing a small ExE, they don't develop EPC (Sebastiano et al, 2010). The small size of ExE is in agreement with the model described, that in order for the EPC to develop, it is necessary by ExE to increase in size. EPC continues to grow, expanding in size, into the uterine lumen.

Electron microscopy studies performed at E6.5 (although the author mentions that the specimens are of E8, the diagram and the developmental stage of the sample seems to be ~E6.5. This discrepancy could be due to strain-specific differences) have identified the existence of 3 microscopically distinguishable areas: (i) the basal area, (ii) the central area (which is itself composed of two subareas) and (iii) the peripheral area (Mehrotra, 1984).

The cells of the basal area have all the aspects of a "stem cell" population: they are proliferative (have mitotic figures), polyhedral, have an oval or kidney-shaped nucleus with a single large nucleolus, rich in ribosomes and their mitochondria are having a discoid shape.

The cells of the central area are divided into two subareas: a region with trophoblast cells having an oval nucleus with nucleoli, well-developed golgi apparatus and secretory granules and a region with trophoblast cells with irregular size and

dimensions, with heterophagosomes and a big and pleomorphic nucleus. The presence of heterophagosomes strongly suggests that these cells are phagocytotic.

The cells of the peripheral area had an elongated nucleus, possessed large cytoplasmic extensions penetrating the maternal tissue in depth and were rich in lysosomes strongly suggesting intensive phagocytotic activity. Furthermore, these cells displayed morphological aspects of secretory cells.

Work by others include the presence of extensive cell-cell adhesion structures like desmosomes in the cells of the basal area while the cells in the other areas are larger, have irregular shape and are more distantly located from each other, maintaining minor cell-cell contacts through cytoplasmic projections (Bevilacqua et al, 2014). The above mentioned cellular characteristics are indicative of a non-polarized nature of the basal cells while the cells in the other regions are mesenchymal.

In situ hybridization studies as well as ingenious fate mapping techniques have shed light into the fate of some of these areas. For example, the cells at the periphery of EPC are positive for *Pll* (*Prl3d1*) as well as *PlpA* (*Prl4a1*) (Screen et al, 2008; Martindill et al, 2007). These findings along with the morphological data provided by the electron microscopy studies, suggest that the cells at the periphery of the EPC are the secondary P-TGCs found in the junctional zone of the definitive placenta.

Mash2 and *Snail* are also expressed in EPC albeit not at the peripheral cells (Tanaka et al, 1999; Scott et al, 2000; Nakayama et al, 1998; Ben-Haim et al, 2006). Interestingly, although *Mash2* is a maternally expressed, imprinted gene (Guillemot et al, 1995), in a minority of central (or basal) cells it appears to be biallelicaly expressed (Tanaka et al, 1999). The reason for this, from the developmental point of view, is currently unknown however *Mash2* overexpression *in vivo* resulted to significant reduction of P-TGCs and spongiotrophoblasts (Tunster et al, 2016) while *in vitro* it appears to promote proliferation under conditions assuming to mimic the EPC environment (Hughes et al, 2004). If this is so, it is in agreement with the observation that basal EPC cells are proliferative. The absence of *Mash2* at the peripheral cells is required to allow the differentiation of EPC cells into P-TGCs (Scott et al, 2000).

Similarly to *Mash2*, *Snail in vivo* is expressed in the central and/or basal areas of EPC but not in the peripheral. *Snail* overexpression in TS cells induces a mesenchymal phenotype but it does not prevent the expression of the giant cell marker *Pll* as one might expect (Abell et al, 2011). These authors however did not examine more trophoblast giant cell indicators, like the presence of a polyploid nucleus. Indeed, embryos doubly knocked out for the *Cyclin E1* and *Cyclin E2* (important mediators of the endoreduplication – the process which mediates the increase in ploidy without cell division) have Pll^{+} cells which contain significantly reduced genetic material relative to control wild type (Geng et al, 2003; Parisi et al, 2003). So, it is likely that *Snail* is required to the central/basal cells to prevent premature endoreduplication and it must be silenced in the peripheral cells in order to allow the physiological giant cell phenotype to emerge.

Plet1 however displays widespread expression across the entire EPC (also weakly expressed in distal ExE - Frankenberg et al, 2007). In a recent *in vitro* study involving overexpression of this gene in TS cells (to mimic the *in vivo* situation) it was found that the role of this gene is to promote differentiation towards EPC – giant cells and prevent differentiation towards labyrinthine trophoblast (Murray et al, 2016).

Another gene that displays an EPC-specific expression is *Secretin* (*Sct*). It was identified in a microarray-based screen and verified by *in situ* hybridization that is expressed in the EPC (Pearton et al, 2014). Secretin is a hormone with an as yet unidentified role in the trophoblast but in other systems it was found to inhibit apoptosis (Jukkola et al, 2011).

EPC cells not only give rise to secondary P-TGCs but also to all cells of the junctional zone (GlyT, SpT and SpA-TGCs) and possibly to cells of the labyrinth (i.e. S-TGCs). For example, cells containing glycogen and having the typical vacuolated appearance of GlyT can be identified by PAS staining as early as the E6.5, located in aggregates at the proximal third of EPC (Tesser et al, 2010). In agreement to the above findings, *TpbpA*, a marker of both SpT and GlyT cells is expressed at the proximal region of the E7.5 EPC (Lescisin et al, 1988). In an effort to identify whether cell types other than

SpT and GlyT are derived from a *TpbpA*$^{+}$ precursor population, Simmons and coworkers (2007) employed an elegant approach. By mating female mice carrying the expression of Cre recombinase under the control of *TpbpA* promoter with male mice carrying a dual reporter (a cre-recognition-flanked *lacZ* fused to *Alkaline Phosphatase*), they were able to observe the Alkaline Phosphatase activity not only in all SpT and GlyT as expected but also to all SpA-TGCs, none S-TGCs and ~half of C-TGCs and P-TGCs of the embryos (Simmons et al, 2007).

A similar but not identical pattern of expression at the proximal half of E7.5 EPC was found for the *PR domain zinc finger protein 1 - Blimp1*. Fate mapping analysis using a similar approach to Simmons and co-workers (2007) the authors were able to find that the cell types derived from *Blimp1*$^{+}$ precursors were the SpA-TGCs, GlyT and C-TGCs. In addition, they found that by E9.5, a ~10-20% of the *Blimp1*$^{+}$ population is proliferative (Mould et al, 2012). It would be interesting to perform a double *in situ* hybridization staining with *TpbpA* and *Blimp1* to identify a part of the C-TGCs precursor area within the EPC.

1.2.5 Signaling pathways controlling ExE maintenance: the role of Nodal/Activin and Fgf pathways

As has been mentioned earlier, maintenance of ExE's identity requires the close association with epiblast cells. One of the central signaling molecules in the epiblast is Nodal. Furthermore, a positive interplay between Nodal and Fgf signaling pathways has already been documented in epiblast explants where it was shown that *Fgf4* expression is induced if Nodal is supplemented into the culture medium and also in *Nodal*$^{-/-}$ embryos where *Fgf8* is not induced (Guzman-Ayala et al, 2004; Brennan et al, 2001).

Nodal and Activin belong to the same family of secreted signaling proteins; the Transforming Growth Factor (TGF-β) superfamily. Nodal is secreted as a precursor dimeric protein which is then cleaved by its convertases Furin and PACE4 into a matured form of Nodal (Beck et al, 2002). Activin appears in three dimeric forms, the B_AB_A, B_BB_B and the B_AB_B (Matzuk et al, 1995). Other members of this family are the BMP and TGF-β proteins. Several reports have linked this superfamily with the

regulation of cell proliferation, apoptosis, differentiation and specification (reviewed in Goumans and Mummery, 2000). Dimeric ligands bring together and bind on two heterodimeric complexes of receptor serine-threonine kinases. The resulting hexameric complex is composed by two type I receptors (RI) and two type II receptors (RII) in addition to the dimeric ligand. In turn, the active kinase domain of RII, phosphorylates and activates the previously inactive kinase domain of RI thus rendering it capable of phosphorylating the receptor-regulated Smads (Smad2 and Smad3 in TGF-β, Nodal and Activin; Smad 1/5/8 in BMP ligands). Phosphorylated Smads then bind to Smad4 and this complex is transported to the nucleus where it regulates gene expression. One of the genes often responding to TGF-β, Nodal and Activin signaling (excluding BMP signaling) is *Smad7* as it acts as a negative feedback to fine-tune signal intensity (Nakao et al, 1997). Nodal and Activin bind on the same receptors, with ALK4 or ALK7 (Nodal only) being the RI and ActRII being the RII. *In situ* hybridization analysis has identified the presence of *Alk4* transcripts along the entire epiblast and ExE at E5.5 and E6.5 (Gu et al, 1998). Similarly, *ActRII* is found to be expressed along the entire embryo (including the EPC) except the VE at the same developmental stages (Manova et al, 1995). *Alk4*$^{-/-}$ embryos show defective egg cylinder formation with disorganized epiblast and ExE (Gu et al, 1998). *Smad2* and *Smad3*, the signal transducers and response mediators are also found to be expressed in the embryo albeit *Smad2* was ubiquitously expressed (de Sousa Lopes et al, 2003) while, interestingly, *Smad3* was ExE-specific (Tremblay et al, 2000). Cripto and Cryptic are coreceptors of Nodal signaling (but not Activin signaling) but none of them is expressed in the trophoblast (Brennan et al, 2001; Chu and Shen, 2000). As already mentioned, *Nodal* transcripts are found in the epiblast and emVE but *Activin* transcripts of the B_A and B_B subunits have been identified in the surrounding decidua around gastrulation stages (Manova et al., 1992; Albano et al., 1994). *In vivo* studies have provided significant evidence that, in the absence of Nodal or its co-receptors (both Cripto and Cryptic) or molecules involved in its maturation (like the Nodal convertases Furin and PACE4) has as a result the differentiation of ExE towards an EPC-like phenotype as verified by the absence of *Errb*, *Bmp4*, *Cdx2*, *Eomes*, reduced growth of the ExE and expression of *Mash2* across the entire ExE (Brennan et al, 2001; Guzman-Ayala et al, 2004; Chu and Shen, 2010). Surprisingly, Nodal effect on the ExE appears to be Smad2-independent because in *Smad2*$^{-/-}$ embryos *Bmp4* and *Eomes* are present

(Brennan et al, 2001; Waldrip et al, 1998). On the other extreme, although *Smad3* expression is ExE-specific and a phenotype would be possibly expected, *Smad3*$^{-/-}$ embryos are born alive (Yang et al, 1999b). Embryos with double deletion for both Smad2 and Smad3 (Smad2$^{-/-}$; Smad3$^{-/-}$) still have a *Bmp4*$^{+}$ and *Sox2*$^{+}$ ExE (Dunn et al, 2004). Deletion of all Activins has not any obvious embryonic phenotype (Matzuk et al, 1995; Vassali et al, 1994). Thus, although the presence of ALK4 and ActRII in ExE strongly suggests that ExE can respond to both Nodal and Activin molecules, it is likely that *in vivo*, Nodal is the key molecule controlling ExE's identity. This is in contrast to the expression of Nodal's co-receptors *Cripto* and *Cryptic* which is epiblast and emVE-specific respectively. This discrepancy can be explained by the finding that the specific ligand in the ExE is the Nodal precursor protein and not Nodal itself that acts to maintain its identity (verified by *Bmp4* expression). Nodal precursor only requires the presence of Alk4 and ActRII as verified by *ex vivo* cultures in the presence of SB431542 (a small molecule inhibitor of ALK4 - Ben-Haim et al, 2006).

TGF-β superfamily members act as morphogens; this means that the phenotypic response of the target tissue is prone to concentration differences of the signaling molecule (reviewed in Tabata and Takei, 2004). In the case of Nodal activity in the mouse embryo, this is evidenced in the case of a Nodal hypomorph where Nodal levels in the epiblast are reduced and the anterior-posterior axis fails to be established (DVE fails to migrate anteriorly and markers of the primitive streak fail to posteriorize – Norris et al, 2002). Interestingly, in this case, ExE markers like *Bmp4* and *Eomes* appear to be normally expressed. On the other hand, *Ectodermin* mutants display enhanced responsiveness on Nodal, specifically at the ExE and the VE and this enhanced responsiveness results to the absence of expression of ExE markers such as *Eomes*, *Cdx2* and *Bmp4* (Morsut et al, 2010). Another important consideration in morphogens, is the distance from their source that they can be active. In the case of Nodal, this distance, depends on post-translational modifications like N-glycosylation which stabilize Nodal by preventing its proteolytic maturation and the subsequent degradation. Thus, the matured form of Nodal acts at short distance from the epiblast while the precursor, non-matured form of Nodal can be active at longer distance (Le Good et al, 2005).

Fibroblast growth factors (FGFs) are encoded by a large family of 22 genes in the mouse and human and 5 genes encoding for FGF-receptors (FGFRs - Ornitz and Itoh, 2001). FGFRs consist of an extracellular ligand-binding domain connected to an intracellular tyrosine-kinase domain via a transmembrane domain. Context-dependend alternative splicing can increase the heterogeneity and ligand-specificity of receptors. For example, in the case of *Fgfr 2*, the inclusion of exon 8 and exclusion of exon 9 renters the receptor as epithelial-type specific (now designated as Fgfr2b) while the inverse process renters it as mesenchymal-type specific (receptor is now designated as Fgfr2c) (reviewed in Brewer et al, 2016).

A necessary factor for the assembly of the Fgfr-ligand complex is the presence of the highly glycosylated proteins Heparan sulfate proteoglycans (HSPGs) as co-receptors (Ornitz, 2000). These are proteins with covalently attached polysaccharide chains known as glycosaminoglycan chains (GAGs). Tissue specific chemical modifications of these molecules facilitate ligand-receptor interactions, affect their chemical affinity thus shaping ligand concentration gradients and because they can be cleaved, they can spread the ligand to nearby cells (Shimokawa et al, 2011). An example of the importance of HSPGs during mouse early embryogenesis is the mutation of *Ugdh* a gene encoding for the UTP-glucose dehydrogenase, an enzyme required for the synthesis of GAG chains. An ENU-mediated mutagenesis of *Ugdh*, caused defects in mesoderm and endoderm migration which closely resembles those of *Fgf8*$^{-/-}$ and *Fgfr1*$^{-/-}$ embryos (Garcia-Garcia and Anderson, 2003).

Activation of Fgf signaling is mediated via the binding of the ligand on the extracellular domain of a monomeric receptor followed by a pairing (dimerization) of two ligand-receptor complexes (reviewed in Brewer et al, 2016). Receptor dimerization brings the intracellular kinase domains of each receptor close to each other, allowing complexes' autophosphorylation. These phospho-groups can then serve as recruitment points of scaffold proteins which then interact with additional signaling proteins, depending on the pathway to be followed **(**Fig. 12).

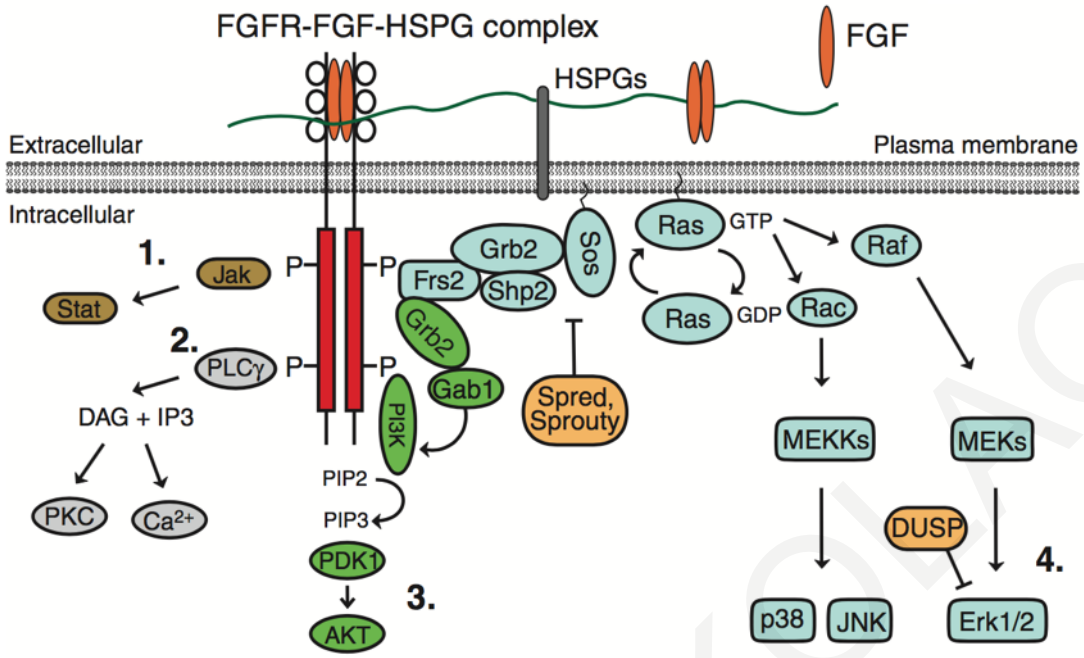

Figure 12: Fgf signaling pathway and the intracellular molecular braches it induces. 1: Jak-Stat pathway, 2: Phospholipase C - Diacylglycerol pathway, 3: PI3K – AKT pathway, 4: protein38/Janus Kinase and phospho Erk1/2 pathway. Activation of the fourth branch induces the expression of Sprouty and DUSP proteins which act in a negative feedback loop to regulate Fgf-mediated responses. Adopted from Lanner and Rossant, 2010

Four distinct pathways can be engaged in Fgf-signal transfer: the Jak-Stat pathway, Plc-gamma, PI3K-AKT, and the fourth which is divided in two branches: p38/Janus Kinase pathway and Erk1/2 pathway. Of these pathways, the best characterized in the ExE and in its *in vitro* equivalent trophoblast stem cells, is the fourth pathway. In this pathway, receptor phosphorylation induces the binding of several scaffold proteins like the Frs2a, Grb2, Shp2 and Sos which mediate the phosphorylation and activation of Ras. Ras phosphorylates either Rac or Raf. In turn, Rac activation results to the activation of p38 and Janus Kinase while Raf activation results to the phosphorylation of Erk 1 or Erk2 (pErk). Phosphorylation of these proteins can modify cell behavior via several ways with one of these ways being gene transcription. Two main responsive genes have been identified as being induced by Fgf-signaling: *Spry2/4* and *DUSP4/6* (Lanner and Rossant, 2010). Both of them act in a negative feedback loop to fine tune Erk activity (Fig. 12).

One of the main Fibroblast growth factors identified in the early mouse embryo is Fgf4 which is expressed along the entire epiblast (Georgiades and Rossant, 2006). *Fgf4*$^{-/-}$ embryos fail to develop postimplantation (Feldman et al, 1995). The most predominant Fgf receptor in the early embryo is the Fgfr2 which is expressed in the entire ExE (Ciruna and Rossant, 1999). Targeted disruption of the *Fgfr2* locus causes lethality of the embryo a few hours after implantation similarly to the phenotype obtained in *Fgf4*$^{-/-}$ (Arman et al, 1998). Other ligands and receptors identified in the early embryo such as Fgf5, Fgf8 and Fgfr1 have late phenotypes and therefore they are not expected to be involved during ExE development (reviewed in Lanner and Rossant, 2010).

Whole-mount immunofluorescence analysis of the localization of pErk in the embryo has revealed that by E5.5 the entire trophoblast (both ExE and EPC) is positive for strong pErk staining while one day later the positive area is restricted to the distal region of ExE and is persistent in the EPC (Corson et al, 2003). However, exposure of the embryos in the FGFR inhibitor SU-5402, has revealed that only the ExE-localized signal is FGF-dependent (Corson et al, 2003).

Similar findings were obtained by *in situ* hybridization analysis of *Spry4* and *DUSP6*, with and without culturing the embryos in the presence of SU-5402 (Shimokawa et al, 2011). These data strongly support a model where Fgf-signaling is activated exclusively at the distal portion of the ExE. This is further supported by the finding that by E6.5, *ribosomal S6 kinase 4* - *Rsk4*, a gene involved in the negative regulation of receptor tyrosine kinase signaling, is expressed in the proximal ExE and the base of the EPC (Myers et al, 2004).

One of the scaffold proteins involved in Fgf signal relay to the Erk is Frs2alpha which is expressed throughout the embryo but is particularly strong in the entire ExE (Gotoh et al, 2005). The deletion of *Frs2alpha*, results to embryos with defective anterior posterior patterning and absence of the distal ExE markers *Bmp4* and *Eomes*. This defect is caused due to defective extraembryonic tissue development as verified by tetraploid complementation assay. Biochemical analysis using trophoblast stem cells and *in situ* hybridization strongly suggests that Frs2a complexes with Grb2 and Shp2

upon activation with Fgf4, and this induces Erk phosphorylation followed by *Cdx2* and *Bmp4* expression (Gotoh et al, 2005; Murohashi et al, 2010).

Deletion of the gene encoding for a second scaffold protein (Shp2) of the Erk pathway, the *Ptpn11*, resulted to a phenotype closely resembling the *Fgf4*$^{-/-}$ and *Fgfr2*$^{-/-}$ (Yang et al, 2006) with blastocysts implanting but failing to survive (Yang et al, 2006). *In vitro* studies in trophoblast stem cells which had abolished *Ptpn11* as a result of Cre-mediated gene ablation, provided evidence that Shp2 is necessary for survival and that this is due to pErk-mediated depletion of the pro-apoptotic protein Bim, thus uncovering a linkage between Fgf4 signaling through Erk to prevent apoptosis. The *Erk* gene responsible for Fgf-mediated responses in the ExE is the *Erk2* because *Erk1*$^{-/-}$ blastocysts implant and develop normally while *Erk2*$^{-/-}$ display a phenotype similar to *Fgf4*$^{-/-}$, *Fgfr2*$^{-/-}$ and *Ptpn11*$^{-/-}$ (Saba-El-Leik et al, 2003).

In addition to *Cdx2* and *Bmp4*, *Sox2* and *Errb* have recently been identified as early targets of the Fgf4/pERK axis (Adachi et al, 2013; Latos et al, 2015). In fact, lentivirus-mediated simultaneous overexpression of *Sox2* and *Errb* could renter FGF4 unnecessary for trophoblast stem cells maintenance (Adachi et al, 2013). Detailed gene expression analysis of trophoblast stem cells upon *Errb* shRNA-mediated depletion has revealed that *Errb* forms stem cell type transcriptional networks by inducing the expression of *Sox2*, *Cdx2*, *Elf5*, *Eomes*, *Bmp4* and *Tcfap2c*. The conclusion from the data presented until now is that Fgf signaling in the ExE is activated at the distal part of this tissue and that when signaling is relayed via phosphorylated Erk, is necessary to maintain the transcriptional profile of ExE as well as to prevent apoptosis.

Fgf signaling might have additional roles relayed by signaling branches other than the pErk branch, like for example the branch of p38/Janus Kinase. Indeed, in mutant embryos for the MEKK4 (mitogen-activated protein kinase kinase kinase), an Fgf-responsive protein that regulates Janus N-terminal Kinase and p38, the spongiotrophoblast layer appears to be dramatically increased. *In vitro* studies involving trophoblast stem cells have revealed that Fgf-mediated activation of Janus N-terminal Kinase and p38 via MEKK, maintains the epithelial status of the trophoblast

by maintaining the expression of *E-cadherin* and preventing *Snail* expression and migration without affecting the self-renewal and multipotency properties of these cells as verified by chimera construction (Abell et al, 2009; Abell et al, 2011).

The distal localization of Fgf-responsive area of ExE is in agreement with the epiblast-derived source of Fgf4. Although Fgf4 ligands can be detected by immunofluorescence to be bound on the cell membranes along the entire length of ExE, the responsiveness of ExE's cells is likely to be depended on the local concentration of heparan sulfates because the *Cdx2*-positive area of ExE expands when culturing the embryos in the presence of exogenously supplied heparin (Shimokawa et al, 2011). This is explained by the finding that the proteolytic activity of a secreted serine protease is necessary to release Fgf4 ligands that are bound on cell-surface-tethered HS chains (which are not receptor-bound) thus allowing their spreading and activation of nearby cells (Shimokawa et al, 2011). Although these studies shed some light on the local retention of Fgf4 it is yet unknown how exactly the Fgf signaling is restricted to the distal region of ExE.

In an effort to directly examine the effect of Fgf4 and Nodal/Activin signaling on ExE, Guzman-Ayala and coworkers, 2004, cultured ExE explants (shielded by their exVE) in the presence of each factor alone, in combination or in the absence of both. Their findings indicate that it is necessary for both factors to simultaneously act of ExE in order to induce multipotency marker genes such as *Cdx2*, *Eomes* and *Errb* while in their absence, after 24 hours in culture, explants had differentiated towards an EPC phenotype, as indicated by the expression of *Mash2* and downregulation of *Cdx2*, *Eomes* and *Errb*. When Fgf4 was used alone, no expression of *Mash2*, neither multipotency marker genes was detected. In contrast, when Nodal (or Activin) were used alone, *Mash2* expression was detected with simultaneous absence of multipotency genes. These data strongly suggest that epiblast-derived Fgf4 is necessary (i) to induce multipotency marker genes in collaboration with Nodal and (ii) to prevent ExE from differentiation towards an EPC-like phenotype. Nodal is only necessary to act in collaboration with Fgf4 to induce multipotency marker genes (Guzman-Ayala, et al, 2004).

1.2.6 **The extraembryonic Visceral Endoderm**

Extraembryonic Visceral Endoderm (exVE) is morphologically and functionally a distinctive tissue from embryonic VE as it is composed by tall, columnar epithelial cells rich in microvilli while emVE is composed of squamous epithelial cells devoid of microvilli (Ishikawa et al, 1986; Kawamura et al, 2012) as well as it envelops the ExE instead of the epiblast. ExVE cells develop an extensive system of cytoplasmic vesicles close to their apical surface, in contrast to the emVE cells which under electron microscopy appear to lack the extent of cytoplasmic vesicles occurring in exVE (Kawamura et al, 2012). The function of these vesicles is currently unknown but it is likely to serve nutritional and signaling requirements (Aoyama et al, 2012).

Although both VE populations share common gene expression markers like *Hnf4* and *Gata6* (Tam and Loebel, 2007) and positivity for lectins like DBA and BS-I lectin (Charalambous et al, 2013), they have molecular differences, at least before PS initiation, which prevent the intermixing of these populations (Trichas et al 2011). For example, during the anterior migration of AVE cells (which are a cellular subpopulation of emVE cells), the AVE stops at the embryonic-extraembryonic junction due to differential subcellular localization of Disheveled-2 and F-actin in the exVE (both molecules are localized at the apical membrane of exVE cells while they are lateraly localized in emVE - Trichas et al, 2011).

The exVE can also be distinguished from the parietal E (PaE), a third VE population covering the inner portion of the RM. These cells can be morphologically distinguished by exVE and emVE cells by their non-polarized, flattened appearance (Gardner, 1983).

Interestingly, based on gene expression analysis, Ninomiya and co-workers, 2005 suggest the existence of a neck-like structure around the EPC and/or proximal ExE during primitive streak stages which is positive for the RM marker gene *Sparc* (Ninomiya et al, 2005). The position of RM initiation from the egg cylinder can be defined as the point of enhanced Collagen IV thickness as PaE cells secrete large amounts of this extracellular molecule contributing to the construction of RM (Salamat et al, 1995).

exVE's role in ExE has not been investigated in detail but is likely nutritional (Kawamura et al, 2012). Another possible role is the provision of a basement membrane onto which the ExE can attach and grow.

1.2.7. Attachment of chorion to EPC: how to make a cake

Early after PS initiation, extraembryonic mesoderm emanating from the steak is directed proximally accumulating between the ExE and the exVE, hence detaching the two epithelia from each other. As a result, the posterior part of ExE (i.e. ExE's region located directly over the PS) is pushed towards the proamniotic cavity while the opposite part of ExE (the anterior ExE) remains closely associated with its exVE. This process has as a result the formation of a fold on the posterior ExE; this fold with the accumulated extraembryonic mesoderm is known as the amniochorionic fold (ACF) (Fig.13).

As the ACF expands, a cavity will form within it as the result of the fusion of several small lacunae; this cavity is known as the exocoelomic cavity (EC). The expansion of EC has as a result the eventual fusion of the posterior ExE with the anterior ExE at the anterior separation point (ASP) and their detachment from the exVE. This process has three consequences: (i) the formation of the chorion, a tissue comprised by the "released ExE" together with the underlying extraembryonic mesoderm, (ii) the formation of the ectoplacental cavity (EPCa) and (iii) the enclosure of the developing embryo into a separated cavity, known as the amniotic cavity. At the same time, a new mesodermal tissue emanates from the primitive streak, initially as a bud and then as a solid mass of mesodermal cells growing into the EC towards the chorion; this tissue is known as the allantois (Al); the cells comprising Al will differentiate into the umbilical cord connecting the fetus with the definitive placenta.

The single-cell thick trophoblast layer of the chorion continues to express whole ExE marker genes such as the *Erf* and *Fgfr2* as well as distal ExE marker genes like *Eomes* and *Cdx2* at the folding point close to the exVE (Arnold and Robertson, 2009). The continuous expansion of EC, pushes chorion proximally, eliminating the EPCa and

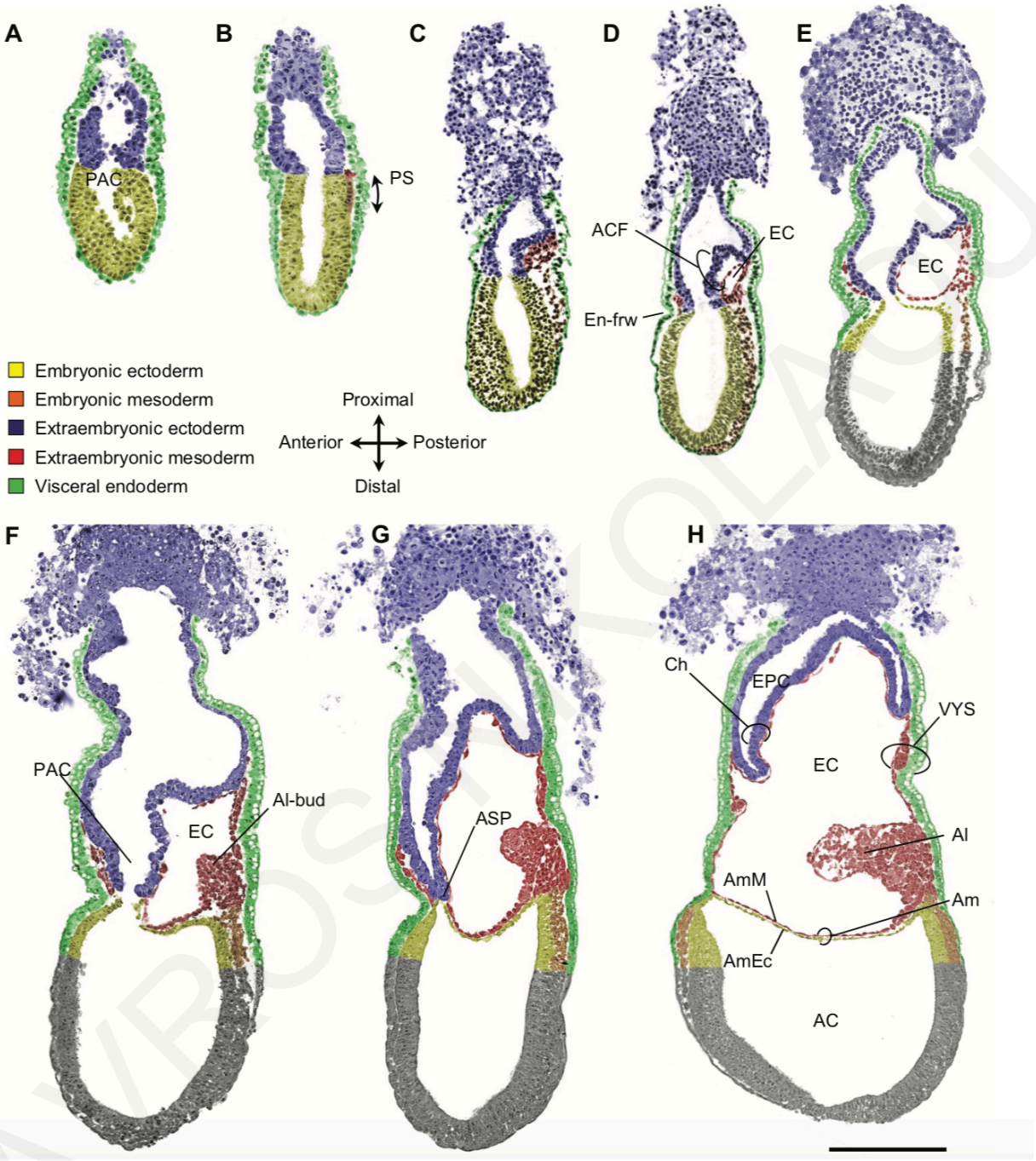

Figure 13: Formation of chorion from ExE respects trophoblast's radial symmetry and involves the formation of the short living ectoplacental cavity. ACP: Amniochorionic fold, EC: Exocoelomic cavity, Al-bud: Allantois bud, PAC, Proamniotic cavity, ASP: Anterior separation point. AC: Amniotic cavity, Am: Amnion, AmEc: Amnion's ectoderm, AmM: Amnion's mesoderm, Al: Allantois, VYS: Visceral yolk sac, Ch: Chorion, EPC: Ectoplacental Cavity (denoted as EPCa in text to distinguish it from EPC). Adopted from Pereira et al, 2011

eventually by ~E7.75 the chorion attaches on the base of the EPC, occluding the EPCa. Slightly later, Al fuses with the attached chorion (Pereira et al, 2011). Whether chorion actually attaches on the base of EPC or on pre-existing ExE (which is itself attached on the base of EPC) is currently controversial with some workers favoring the one at the expense of the other (Simmons et al, 2007; Bevilacqua et al, 2014).

1.3. Trophoblast stem cells: the *in vitro* equivalent of ExE

Trophoblast stem cells (TS cells) were first isolated almost 20 years ago by the group of Janet Rossant in the Mount Sinai Hospital, Toronto, Canada (Tanaka et al, 1998). TS cells is one of the three types of embryo-derived stem cells; the other two being extraembryonic endoderm stem cells (XEN cells) and the embryonic stem cells (ES cells) (Kunath et al, 2003; Evans and Kaufman, 1981). They are diploid cells growing in tight epithelial colonies with morphologically indistinguishable cell:cell borders. Injection of single TS cells within blastocyst cavities resulted to the formation of chimeric placentae with TS cells contributing to all placenta regions (labyrinth, junctional zone and decidua - Tanaka et al, 1998; Abell et al, 2011).

TS cells have been derived from E6.5 ExE after near single-cell trypsinization followed by culture in the presence of exogenously supplied Fgf4 and heparin as well as mitotically inactivated mouse embryonic fibroblasts (MEFs) or MEF-conditioned medium (MEF-CM). In addition to E6.5 ExE, TS cells have been successfully derived from E3.5 blastocysts as well as the E7.5 chorion, prior the occlusion of the EPCa (Uy et al, 2002). Although the study of Uy and coworkers, has shown that the ability to derive TS cells was lost after the occlusion of the EPCa, recently, Natale and coworkers, 2017, have successfully isolated TS cells from definitive placenta (Natale et al, 2017).

Although when cultured under normal stem cell conditions they express distal ExE marker genes like *Errb*, *Cdx2*, *Eomes*, *Bmp4* and *Sox2*, microsurgery experiments verified that TS cells can also be derived from both distal and proximal ExE with the same efficiency (Uy et al, 2002). The factor contained in the MEF-CM was later identified by studies from Erlebacher and coworkers as well as by Natale and

coworkers as the TGF-β or Activin (Erlebacher et al, 2004; Natale et al, 2009). The authors had also examined Nodal's effect but contrary to what would be expected, Nodal could not substitute MEF-CM. This is likely because the authors had used the matured form of Nodal instead of the precursor Nodal because precursor Nodal is able to maintain the expression of the distal ExE marker gene *Bmp4* in ExE explant cultures (Ben-Haim et al, 2006).

The presence of serum in the culture medium, is a complicating factor because the heterogeneous and variable nature of this component could be masking the presence of important regulators of the trophoblast lineage (Drakou and Georgiades, 2015). During the last years, it was made possible to derive and maintain TS cells in a serum-free, chemically defined culture medium in the presence of Fgf4 and TGF-β1 in two independent cases provided that a substratum was used as a cell attachment site. In the first case, the authors examined the suitability of several commercially available substrates, like matrigel, fibronectin, gelatin and others. The most optimal adhesiveness was obtained in the presence of matrigel (~15% of the seeded cells had attached) while adhesion in the presence of fibronectin or other compounds, was highly compromised. Although the authors do not mention the adhesiveness efficiency in serum conditions, cells grown under serum-free conditions on matrigel, display a more homogeneous live appearance under phase contrast microscopy, normal proliferation rate, transcriptional profile and diploid karyotype as well as they could contribute exclusively to placentas upon chimera formation (Kubaczka et al, 2014).

In an independent approach, Ohinata and Tsukiyama, 2014, used fibronectin instead of matrigel to succesfully derive and maintain TS cells under chemically defined conditions in the presence of Fgf2 and Activin, however they also included the presence of the Wnt/β-catenin-signaling inhibitor XAV939 as well as the ROCK-inhibitor Y27632. In the absence of XAV939, the authors observed induction of differentiation at the colonies' periphery while Y27632 was necessary for survival because in its absence, significant apoptosis had emerged (Ohinata and Tsukiyama, 2014). Their data suggest that under normal conditions, an unknown extracellular matrix compound inhibits ROCK in order to prevent apoptosis.

TS cells share several similarities with ExE: a similar epithelial status, transcriptional profile and chromatin architecture and the same differentiation potency as verified by chimera and *in vitro* differentiation analysis (Tanaka et al, 1998; Ahmed et al, 2010; Rayon et al, 2016; Donnison et al, 2015); for this reason, they are considered to be the *in vitro* equivalent of ExE. This consideration is further supported by the recent technological achievement of embryo synthesis entirely from ES and TS cells combined together *in vitro* (Harrison et al, 2017). TS in these synthetic embryos had successfully formed a polarized, epithelial tissue with ExE-specific transcriptional profile and were able to induce a PS-like formation within the ES-derived epiblast.

Upon the removal of both Fgf4 and MEF-CM or Activin (differentiation conditions), TS cells initially respond by losing their epithelial morphology and initiating an EMT process by adopting mesenchymal characteristics like *E-Cadherin* downregulation and *Snail* upregulation, as well as an invasive phenotype (Abell et al, 2011), while after 7 days in differentiation conditions, the majority but not all of the cells appear to be trophoblast giant cells by morphology (Tanaka et al, 1998). Time-point gene expression analysis suggests that TS respond by quickly losing expression of the Fgf-responsive gene *Spry4* and multipotency marker genes like *Errb*, *Sox2, Cdx2* and *Eomes*. The expression of the whole ExE marker gene *Fgfr2* persists for somewhat longer but eventually is substituted by the transient upregulation of the proximal ExE/EPC specific *Mash2*. 7 days post-differentiation induction, markers of trophoblast terminal differentiation can be identified, like the *TpbpA* (spongiotrophoblast marker), *Pll, Ctsq, Plf,* (TGC markers), low levels of *Gcm1, Syna, Synb* (SynT markers) and *Pcdh12* (GlyT marker) (Donnison et al, 2015; Tanaka et al, 1998; Murray et al, 2016). *Secretin*, which is considered to be an EPC marker (Pearton et al, 2014), is also highly expressed by 7 days in differentiation conditions. It is currently unknown whether *Secretin* is also expressed in any terminally differentiated trophoblast cell type (Donnison et al, 2014). Similar findings were derived after differentiating TS in serum-free conditions either on matrigel or fibronectin (provided the continuous supplementation of Y-27632 in the case of fibronectin-based differentiation - Kubaczka et al, 2014; Ohinata and Tsukiyama, 2014).

In a study aiming to identify the several trophoblast giant cell types existing *in vivo* and *in vitro*, Simmons and coworkers, 2007, using double color ISH experiments on differentiated TS in serum-containing cultures identified the co-existence of P-TGCs, SpA-TGCs, C-TGCs and S-TGCs in the same culture. The presence of Ch-TGCs was not investigated as they were yet unknown by this time. Similar findings were reproduced by other investigators, using serum-free culture conditions with the only difference between the two conditions being the higher percentage of S-TGCs obtained in serum-culture conditions and the higher percentage of the other types in serum-free, matrigel containing medium (Simmons et al, 2007; Kubaczka et al, 2014). The above findings suggest the existence of a S-TGCs' inducer in serum, at the expense of the other three cell types. Surprisingly little is known about the live morphology of TGCs. In fixed samples, a large, polyploid nucleus within a prominent cytoplasm is a shared characteristic of all TGCs. The nuclear size and ploidy as well as the cell size varies between the different TGC types. For example, P-TGCs have the biggest nucleus and DNA content of all cell-types while the other three have a similar size of nucleus and DNA content (Simmons et al, 2007).

The presence of syncytiotrophoblast cells can be easily distinguished by the characteristic appearance of these cells (multiple nuclei, closely localized and enclosed within the same cell membrane), however the low representation of these cells under normal differentiation conditions makes it difficult to identify them. Overexpression of *Gcm1* in TS cells induces a dramatic arrest in cell proliferation and prevention of differentiation towards a TGC phenotype. Although due to the rapid arrest of proliferation the physical separation of the cells did not allow cell fusion to occur, it is likely that *Gcm1* overexpression induces syncytiotrophoblast formation (Hughes et al, 2004). Similar findings were obtained by low levels of *PletI* expression. Under these conditions, TS cells promote the formation of syncytia as shown by immunofluorescence analysis and upregulate the Syn-I marker genes *Syna* and *Ly6e* (Murray et al, 2016).

In the presence of Fgf4 alone TS cells respond by quickly downregulating multipotency-associated genes like *Errb*, *Eomes* and *Cdx2*, reducing their proliferation rate and eventually adopt a TGC-like morphology (Erlebacher et al, 2004). In contrast, in the

presence of Activin alone, TS cells respond by upregulating the syncytiotrophoblast marker *Gcm1* and *Synb*. Hence the *in vitro* data suggest a model were TS cells self-

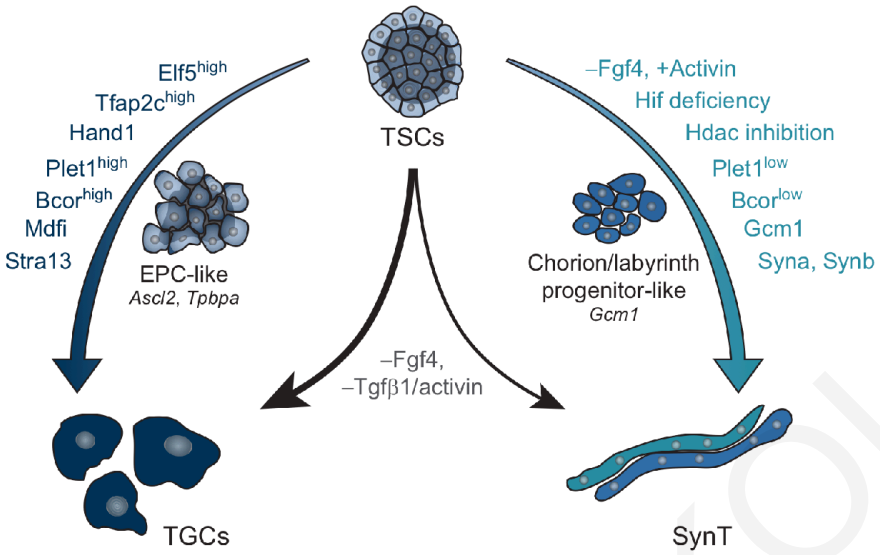

Figure 14: Trophoblast stem cells can be induced to differentiate *in vitro* into all trophoblast cell types in the presence or absence of the appropriate growth factors. In the absence of Fgf4 and Activin, TS cells differentiate mostly into the EPC derivatives TGCs while in the presence of Activin (with simultaneous absence of Fgf4) TS cells differentiate into Syncytiotrophoblast cells. Adopted and modified from Latos and Hemberger, 2016

renew in the presence of both Fgf4/Heparin and Activin while the absence of both factors promotes their specification towards an EPC/Giant cells phenotype while the presence of only Activin specifies these cells to differentiate towards a labyrinthine phenotype (Fig. 14).

1.4. Lentiviruses and lentivirus-based vector development: the good face of a dangerous enemy

1.4.1 Lentivirus architecture

Lentiviruses are slow-growing (hence the prefix “Lenti”), RNA viruses belonging to a subgroup of the *Retroviridae* family. *Retroviridae* is a family of single stranded RNA (+) viruses which replicate through a DNA intermediate, the latter being stably integrated into the host genome as a provirus. They are composed of a spherical, host’s membrane-enveloped virion, of ~80-100 nm in diameter which contains two copies of single stranded RNA (+) molecules enclosed within a proteinaceous capsid. A famous

example of a lentivirus is the human immunodeficiency virus 1 and 2 (HIV1 and HIV2) (Fig. 15).

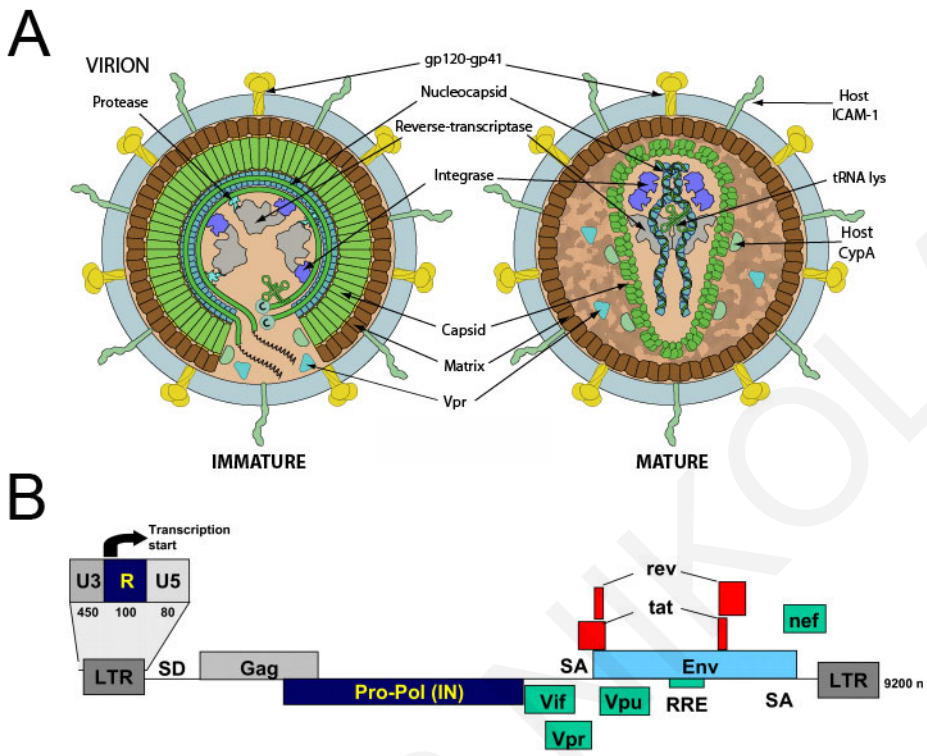

Figure 15: Structure of lentiviral virion and organization of their genome. A) Virions core is composed of a capsid (green color) enclosing two copies of their RNA genome. Capsid is itself enclosed within the Matrix protein and the whole structure is encaged within host's cell membrane which is spanned by the viral receptor proteins. B) The general lentiviral genome structure is composed of three main genes flanked by two Long Terminal Repeat (LTR) sequences. Several "accessory genes" regulate virus' physiology and life cycle. (from Swiss Genome Informatics, Viralzone and Dufait et al, 2013)

Lentiviral RNA genome size varies from 7 kb to 11 kb. It is flanked by two homologous regions containing repeat sequences, known as Long Terminal Repeats (LTRs). LTRs' size varies from 600-900nt and is required for viral replication, integration and expression. To meet these requirements, LTRs are divided into three functionally distinct regions: The "unique 3" (U3), the "repeated sequence" (R) and the unique 5 (U5) regions. The U3 region is responsible for the appropriate tissue-specific expression of the virus as it contains sequences with basal promoter and enhancer activities as well as modulatory sequences. In addition, U3 contains a sequence

required for the integration of the provirus into the host genome (*att*R) (Coffin, 1996). The R region is required during transcription as it has the transcription initiation codon and additionally, it is the region of capping (5'-end) and polyadenylation (3'-end) of the viral transcript. U5 region contains sequences necessary for the integration of the provirus into the host genome (*att*L) as well as part of the encapsidation signal - psi element - ψ (Coffin, 1996; McBride *et al*., 1997). The in-between region, contains three groups of sequences: (i) cis-acting elements necessary for the reverse transcription process (for example the Primer Binding Site - PBS), the encapsidation of the viral RNA into the viral capsid and the efficient viral RNA transcription (Rev Response Element – RRE (Coffin, 1996; Freed, 2002), (ii) three genes encoding for the major viral proteins and (iii) several regulatory genes necessary for the efficient lentiviral life cycle. The three genes for the major viral proteins are named as the *Gag* (*Group-specific antigen*), *Pol* (*Polymerase*) and the *Env* (*Envelope*).

All three genes are translated as precursor proteins with the two of them cleaved by a viral protease (PR) and the other by a cellular enzyme. For example, Gag precursor polypeptide is spliced into three proteins with structural function, the Matrix (MA), the Capsid (CA), the Nucleocapsid (NC) and the protein 6 (p6). Pol polypeptide is cleaved into Protease (PR), Reverse Transcriptase (RT) and Integrase (IN). In contrast to Gag and Pol, the Env is not cleaved by the PR but by a cellular enzyme into two products, the Surface (SU) and the Transmembrane (TM) which upon incorporating into the viral membrane, are determining its tropism.

1.4.2. Lentivirus life cycle

Lentiviral life cycle initiates as the result of receptor mediated fusion of the viral membrane with the host-cell membrane. The entrance of the viral capsid into the host's cytoplasm is followed by a microtubule-mediated transfer towards the nuclear periphery (McDonald et al, 2002; Arhel et al, 2006b). During this transfer, the viral RT mediates the reverse transcription of the viral RNAs into a double stranded, complimentary DNA (Telesnitsky and Goff, 1997). The complex of the cDNA with viral proteins like IN, is known as the preintegration complex (PIC). PIC enters the nucleus and cDNA is permanently incorporated into the host genome as the result of IN activity. The genomic positions of DNA integration appear to be random but transcriptionally active regions

(Wang et al, 2007). Transcription from the viral genome results to the assembly of new viral particles at the host's membrane; these particles are then released into the cellular environment. The ability of the viral cDNA to pass through the nuclear pore and get permanently incorporated into the host DNA gives to lentiviruses the ability to infect not only dividing cells (like the rest of retroviruses) but also non-dividing ones (Lewis *et al.*, 1992).

1.4.3. Lentivirus-based vector (lentivector) development

The ability of lentiviruses to infect dividing or non-dividing cells and permanently incorporate their genetic material into the host's genome was the excellent reason for the researchers to construct lentivirus-based vectors for easy, efficient and targeted transgenesis of cells and whole organisms.

An important aspect to consider during this process is safety and efficiency. In order to achieve that, researchers segregated the *cis*-acting elements of a lentivirus (i.e. the two LTRs, the ψ element, PBS, RRE and the two attachment sites) into a single plasmid (named as "vector plasmid") and all *trans*-acting elements (*Gag* and *Pol*) into a second plasmid (named as "packaging plasmid"). *Env* was substituted by a gene encoding a protein derived from another virus and displaying wide tropism, the vesicular stomatitis virus protein G (VSV-G). *VSV-G* was subcloned into a third plasmid ("envelope plasmid") (Cockrell and Kafri, 2007).

A second layer of safety was added (i) by deleting the ψ-element and PBS from the packaging plasmid, a modification which ensures the inability of Gag-Pol to get incorporated into the viral particle in the form of RNA and (ii) by substituting the most part of the U3 region with a heterologous promoter like the human cytomegalovirus immediate-early promoter (CMV). This strategy makes the lentiviruses replication-incompetent because of the absence of all *trans*-acting factors required for their replication into the host cell but also due to the absence of U3 from the vector plasmid (Cockrell and Kafri, 2007). The transgene (the gene of interest) can be subcloned into the vector plasmid along with all the necessary sequences required for transgene expression (i.e. promoter/enhancer) provided that lentivector's genome length will not exceed the physiological size of lentiviral genome of 11 kb.

CHAPTER 2:

SCIENTIFIC AIMS

2. Scientific Aims

Although the current knowledge regarding placenta development is continuously expanding, it still lacks important information regarding the earliest steps of this organ's development. The general aim of this study was to better understand the process of placenta development at its earlier stages, focusing on its trophoblast component. In order to do that, we used the mouse as a model organism and employed *in vivo*, *ex vivo* and *in vitro* approaches. This work had three main aims.

2.1. Aim 1:

The aim here was to identify the exact boundary between ExE and EPC at E5.5-E6.5 and to correlate this with anatomical features of the conceptus. Although knowledge of this is crucial for understanding early trophoblast patterning, the location of this boundary (and hence the validity of current markers of ExE/EPC) is unknown, as this issue has not been addressed directly.

The background to this aim is as follows: EPC appears as an outgrowth of the proximal-most ExE cells as early as ~E5.3 (Robertson, 1942). During this time and until E6.5 proximal ExE and EPC are contiguous tissues but they don't share any morphological aspect which can be easily used for their distinction. Because the EPC grows mesometrially, and is not shielded by a VE layer it is arbitrarily assumed that EPC initiates at the turning point where the VE becomes PaE (Rossant and Ofer, 1977). Interestingly however, a study performed by Ninomiya and coworkers, 2005, has identified a region of VE, prior the turning point, which has PaE characteristics, like the expression of the RM-component *Sparc* (Ninomiya et al, 2005). In a more recent approach, Donnison and coworkers, 2015, used a morphological constriction occurring on the exVE as the separation point of EPC-ExE but these authors did not provide any supporting evidence that this point is indeed the correct border of the two tissues.

The specific aims here were to: (i) identify the exact border between ExE and EPC based on cellular and functional assays (ii) use this knowledge in order to test whether known and putative ExE/EPC gene expression markers respect this boundary.

2.2. Aim 2:

The aim here was to describe in more detail proximodistal (PD) patterning within the ExE and to investigate the role of Fgf and Nodal/Activin signaling (Fgf and Nodal/Activin signaling are necessary and sufficient for the maintenance of TS cells) in relation to distinct ExE regions along its PD axis. Although this is an important aspect for the understanding of early trophoblast patterning, it is largely unexplored.

Specific aims:

1. To investigate whether there are more than two distinct regions within ExE along its PD axis using gene expression at E6.5 (a time when ExE is considered fully formed). Although current literature suggests that there are only two distinct regions (Donnison et al, 2015), our pilot experiments suggested that there are at least three (distal, intermediate and proximal, the latter being closest to the EPC and the first being furthest away from the EPC). Knoweledge of this is a prerequisite for understanding PD patterning within the ExE.

2. To investigate the sequence of appearance of the aforementioned ExE regions based on gene expression profiles from E5.0 to E5.5.
   Although it is known that early ExE is uniformly positive for distal ExE markers like *Cdx2* and *Eomes* (Adachi et al, 2013; Donnison et al, 2015), it is yet unknown when these genes become distally localized as well as when the expression of the proximal ExE markers is induced. Moreover, if an intermediate area exists by E6.5 (as our pilot experiments suggested), we wanted to know when this putative novel ExE region firstly appears.
   The aim here therefore was to employ single and double *in situ* hybridization analysis of known markers of the distal and proximal ExE to investigate how their expression changes E5.0 (a time just before EPC appearance) and E5.5 embryos (when the EPC is established). This would alow us to make suggestions as to the sequence with which these ExE regions appear.

3. To associate the sequence of appearance of ExE regions discovered in the previous section with the appearance of the EPC.

Although it is known that EPC appears by ~E5.25, it is yet unknown whether this tissue arises from the distal, the proximal or intermediate ExE (the latter was discovered during this work). This section was expected to give clues as to the identidy of the ExE region giving rise to EPC. This involved single and double *in situ* hybridization analysis of known markers of the distal and proximal ExE/EPC performed at E5.25 embryos.

4. To correlate the localization of Fgf and Activin/Nodal signaling in relation to our newly discovered ExE PD pattern (proximal, intermediate and distal ExE).

It is currently known that Fgf signaling is active at the distal part of ExE but the exact region of ExE responding to Fgf signaling (especially in relation to the intermendiate region) is yet unknown. Moreover, the localization of Nodal/Activin signaling within the ExE along its PD axis is currently unknown. Although pSmad2 localization (an indicator of Nodal/Activin signaling) was reported to exist within the ExE (Aoyama et al, 2012; de Souza Lopez et al, 2003), whether its presence within the ExE is indicative of Nodal/Activin signaling has not been confirmed and its spatial relation to distal, intermediate or proximal ExE is unknown. The aim here therefore was to correlate distal ExE (marked by *Errb* gene expression*)* and the rest of ExE (*Errb* negative ExE) with (a) Fgf signaling detected by the expression of the Fgf-responsive gene *Spry4* and the localization of Fgf signaling indicator pErk and (b) Nodal/Activin signaling detected by the expression of Nodal/Activin responsive genes *Smad7* and *Nodal,* as well as with pSmad2. In all cases, the activity of this signaling was confirmed by culturing embryos in the presence or absence of small molecule inhibitors of these signaling patways.

5. To investigate the role of Fgf and Activin/Nodal signaling in the maintainance of ExE PD patterning.

Although this is an important issue, global inhibition of either or both of these signaling pathways has not been investigated directly. In an approach to investigate the effect of Nodal and Fgf signaling in the embryo, Guzman-Ayala and coworkers, 2004 used *Nodal* knockout embryos to investigate their phenotype in the ExE. They

concluded that ExE in *Nodal* knockout embryos had differentiated into EPC (Guzman-Ayala et al, 2004). However, this study did not involve a sufficient number of marker genes since *Mash2* is a marker of both EPC and proximal ExE. Furthermore, although *Nodal* knockout embryos by definition lack Nodal activity, it is possible that maternally derived Activin can mask the data obtained from these embryos. Moreover, *Fgfr2* knockout embryos have an early death prior to the full establishement of the PD ExE pattern described here, thereby precluding their usefulness in this respect. In order to effectively study the effect of Fgf and Nodal/Activin on the maintenance of ExE's pattern, we used a recently described serum-free culture medium developed in our lab (Drakou and Georgiades, 2015) under mock conditions or in the presence of specific small molecule inhibitors of the Fgf pathway (SU-5402) and the Nodal/Activin pathway (A-8301) for 12 hours. The use of the serum-free culture medium also allowed us to avoid the effect of unknown serum-derived factors that could possibly mask our results.

6. To investigate the role of Fgf and Activin/Nodal signaling on the ability of distal ExE (the earliest ExE region to appear) to generate the other ExE regions as well as EPC.

The role of these two signaling pathways in the induction of pattern *in vivo* is currently ill-defined with most of the information coming from *in vitro* data involving TS cells. In order to investigate the role of these two signaling pathways on distal ExE, we employed an *ex vivo* methodology, culturing distal ExE explants in the presence or absence of Fgf2 or Activin A proteins alone or in combination, under chemically defined conditions on matrigel.

2.3. Aim 3:

The aim here was to develop a new tool for investigating cell behavior in live TS cells using lentivirues.

Currently there no TS cell lines that permanently display fluorescent nuclei and/or F-actin, thereby allowing one to follow changes in nuclei and/or F-actin under live conditions. The construction of such system would contribute to the better

understanding of TS behavior during their differentiation *in vitro*.

Specific aims:

1. To use a lentivirus-based approach to develop a TS cell line that simultaneously expresses Ruby-fused F-actin (fluorescing at the red spectrum) and GFP-fused Histone H2B (fluorescing at the green spectrum).

2. To use TS cells expressing GFP-fused Histone H2B to correlate changes in their nuclear size and chromatin content with live cell morphology, during their differentiation.

Induction of differentiation of TS cells mainly leads to the formation of TGCs which are characterized by an increased nuclear size and chromatin content (Simmons et al, 2007). However, the early morphological alterations occurring during this process have not been directly assessed in live TS cells and it is currently unknown whether increase in nuclear size always correlates with increase in DNA content during this process.

CHAPTER 3:

MATERIALS AND METHODS (For companies and catalog numbers please see Appendix)

3. Materials and Methods

3.1 Cell cultures

3.1.1 Trophoblast stem cell culture (stemness- and differentiation- promoting conditions)

Trophoblast stem cells (kindly provided by Dr Janet Rossant, Mount Sinai, Toronto, Canada) were cultured in TS medium (i.e. 80% RPMI 1640 1X, 20% Fetal Bovine Serum, Sodium Pyruvate, Penicillin/Streptomycin, L-Glutamine and β-mercaptoethanol) in the presence of 50ng/ml Fgf2 + 1ug/ml Heparin + 10ng/ml Activin A (these culture conditions will be hereafter denoted as stem cell medium - SCM). Fgf2 can be used instead of Fgf4 because they share the same receptors (Zimmer et al, 1993). In some cases, fibroblast conditioned medium (FCM) was used instead of Activin A (30% TS medium + 70% FCM) without any change in cell behavior or morphology (Natale et al, 2009). Cells were routinely passaged at 1/10 ratio every 3-4 days (i.e. when confluency was ~80%) by exposing them to 0.05% Trypsin-EDTA for 5 minutes at 37^{o}c. Cells were maintained in 35mm plates (SPL). For differentiation induction, stem cell colonies, previously grown for 24 hours under SCM, were gently washed two times with prewarmed PBS (pH 7.2, Ca^{2+}-Mg^{2+} free) and then they were cultured in TS medium with the exclusion of growth factors (i.e. without 50ng/ml Fgf2 + 1ug/ml Heparin + 10ng/ml Activin A). The time just prior switching culture media, it was considered as Day 0.

3.1.2 HEK293T cell culture

HEK293T cells were routinely cultured into 10cm plates in DMEM containing 10% FBS. Upon reaching ~80% confluency (i.e. every 2-3 days), cells were washing with prewarmed PBS (pH 7.2, Ca^{2+}-Mg^{2+} free) followed by trypsinization for 3 minutes at room temperature. Passaging was routinely performed at a 1/10 dilution.

3.1.3 STO cell culture – Fibroblast Conditioned Medium (FCM) production

STO cells were routinely cultured into 10cm plates in DMEM containing 10% FBS. Upon reaching ~80% confluency, cells were washing with prewarmed PBS (pH 7.2, Ca^{2+}-Mg^{2+} free) followed by trypsinization for 5 minutes at 37^{o}c. Passaging was routinely performed at a 1/10 dilution. For FCM production, 10 x 10cm plates were

prepaired with STO cells at 90-100% confluency. Then their culture medium was replaced with fresh culture medium containing 10ug/ml freshly made Mitomycin C and the plates were incubated at 37^{o}c for 3 hours. During this period, fresh 10 x 10cm plates were gelatinized with the addition of 5ml gelatin solution (0.1%) per plate, incubate all plates at 37^{o}c for 20 minutes and after aspiration of gelatin solution, plates were allowed to air dry until used. By the completion of the 3-hour mitomycin C-treatment of STO cells, medium was aspirated and cells were washed twice with prewarmed PBS (pH 7.2, Ca^{2+}-Mg^{2+} free). The cells were then trypsinized and 4 000 000 cells were added per gelatinized plate (i.e. 5 x $10^4/cm^2$). Cells were allowed to attach overnight by incubating at 37^{o}c and the following day the culture medium was replaced with freshly made TS medium. Every three days Fibroblast Conditioned Medium was collected from cells and replaced with fresh TS medium (no more than three harvests). FCM was spun down (1000g for 10 minutes, RT) to remove cell debris and then aliquoted at 10ml aliquots. It was stored at -20^{o}c until used.

3.2 Lentivirus production, measurement and usage

3.2.1. Lentivirus production by calcium phosphate transfection of HEK293T cells

(Odiatis and Georgiades, 2010 with modifications)

HEK293T cells were seeded in 75cm^2 cell culture flasks ~20 hours before transfection at a density of 3.5 x 10^6 cells per flask so that at the time of transfection their confluency was ~60-70%. Transfection reaction was performed by preparing two mixtures as follows:

Mixture 1:

- 12.5ug of vector plasmid (this was FG12.hisGFP or pLenti.PGK.LifeAct-Ruby.W - addgene #51009)
- 6.5 ug pCMV.delta8.91
- 3.5 ug pCMV.VSV-G
- H_2O
- $CaCl_2$ 2M

Mixture 1 was then transferred dropwise into 780 ul of 2x HeBs solution while vortexing at low speed. Reaction was left at RT in the dark for 20 minutes and then transferred

dropwise into the corresponding flask. After an overnight incubation at 37^{o}c, the cells were washed once with 10ml of prewarmed plain DMEM and then once again with prewarmed PBS (pH 7.2, Ca^{2+}-Mg^{2+} free). Finally, fresh culture medium was added and the flasks were returned to the incubator for 48 hours. After this, the first viral harvest was performed and then fresh medium was added for a second harvest 24 hours later. The virus-containing supernatant obtained from the first harvest was spun down at 500g for 5 minutes and then kept at 4^{o}c. The next day it was mixed with the second viral harvest (which had previously spun down under the same conditions) and filtered through a 0.45 um vacuum filter. The filtered supernatant was transferred into ultracentrifuge tubes and ultracentrifuged at 25000 rpm, 4^{o}c for 1 hour and 45 minutes. After this step, the supernatant was discarded and 100 ul of TS culture medium (lacking Fibroblast Conditioned Medium and Fgf2/Heparin or Activin A) were added to the pellet. The pellet was left overnight at 4^{o}c to resuspend and the following day the viral supernatant was transferred at -80^{o}c to be stored for no more than 6 months. A small amount (5ul) of supernatant was used for titration.

3.2.2. Lentivirus titration

A small aliquot of the concentrated lentivirus was used to measure its titer as follows: Decimal dilutions were prepaired (10^{-1}, 10^{-2}, 10^{-3}, 10^{-4} and 10^{-5}) by diluting concentrated virus into plain DMEM. After that, 2 ul of each dilution were used to inoculate one well of a 4-well plate containing 1.8 x 10^{4} HEK293T cells (the cells were seeded 8 hours earlier) growing in 500ul culture medium (DMEM supplemented with 10% FBS). Each transduction step was performed in duplicate. Three days after virus addition, several random pictures were taken from the dilution giving between 1-20% positive fluorescing cells (usually the 10^{-4} dilution) and fluorescing cells were measured (cell doublets, triplets or quadruplets were measured as one). Lentivirus titer (expressed as “Infectious Units per ml, IU/ml”) was measured using the formula: Virus titer = {(F × Cn) /V} × DF were F= frequency of fluorescing cells Cn= total number of cells in the well (1.8 x10^{4}) V=volume in ml, DF= dilution factor. The usual titer obtained was at the range of 1 - 5 x 10^{7}.

3.2.3. Trophoblast stem cells transduction (Odiatis and Georgiades, 2010 with modifications)

Trophoblast stem cells were seeded under stem-cell conditions approximately 16 hours before transduction at a density of 1500 cell particles (either single cells, doublets or triplets; occasionally particles of more than three cells were also observed) per well of a 4-well plate. Virus-containing medium was left on ice to thaw and then transferred directly into the corresponding well. Transduction took place overnight, under stem-cell conditions in the presence of 8 ug/ml of polybrene. The following day, transduced cells were washed twice with prewarmed PBS (pH 7.2, Ca^{2+}-Mg^{2+} free) and fresh stem cell medium was added.

3.2.4 Clonal derivation of transduced trophoblast stem cell colonies

Transduced cells were seeded under conditions favoring the formation of single, well isolated colonies, derived from a single cell. This was achieved by seeding 1000 cells in a 35mm plate followed by culture under stem cell conditions for 6-7 days. All colonies were examined for fluorescence positivity and colonies displaying 100% positivity were marked by a small scratch on the plastic directly below the colony. The medium was then aspirated and prewarmed PBS (pH 7.2, Ca^{2+}-Mg^{2+} free) was added to the plate. Under strictly sterile conditions, each colony of interest was selected under a stereoscope (Zeiss stereomicroscope) and transferred into a small drop of 0.05% Trypsin-EDTA, at 37^{o}c for 5 minutes. Then the cells were transferred into one well of a 4-well plate containing fresh stem cell medium.

3.2.5. Nuclear content measurement during differentiation using the hisGFP intensity (live)

5000 of lentivirus FG12.hisGFP-transduced, clonally expanded trophoblast stem cell particles (singlets, doublets or triplets) were seeded in a 35mm plate in the presence of TS medium + 50ng/ml Fgf2 + 1ug/ml Heparin + 10ng/ml Activin A. 24 hours later cells were switched into differentiation conditions for 6 days. On days 0, 1, 2, 4 and 6 pictures were taken from several random fields of view (both phase contrast and fluorescence) at a fixed exposure time (13.99ms) and magnification (10x, optovar 2.5). The plate was returned to the incubator until the next documentation day. Pictures were taken with a Zeiss Axiovert inverted microscope equipped with 10x phase contrast lens

and GFP filter. Nuclear area (in squared inches) and GFP intensity were measured by ImageJ. Statistical analysis and graphs were done using Microsoft excel. Student's *t*-test for independent variables was employed for statistical significance.

3.3. Mouse embryo isolation, explant derivation and cultures

3.3.1. Mice maintenance and plug derivation

All animals were provided with direct access to food, water and clean-quiet living conditions by cleaning twice a week throughout the completion of this study. Animals were living in a 12-hour dark – 12-hour light conditions. For "plug" derivation, female mice (at least 3 months old) were transferred into a stud the previous evening (usually at 17:00-18:00) and the following morning (prior 11:00) each female vagina was checked for the presence of a white "plug" (Fig. 3.1). Presence of a "plug" was considered as a successful mating.

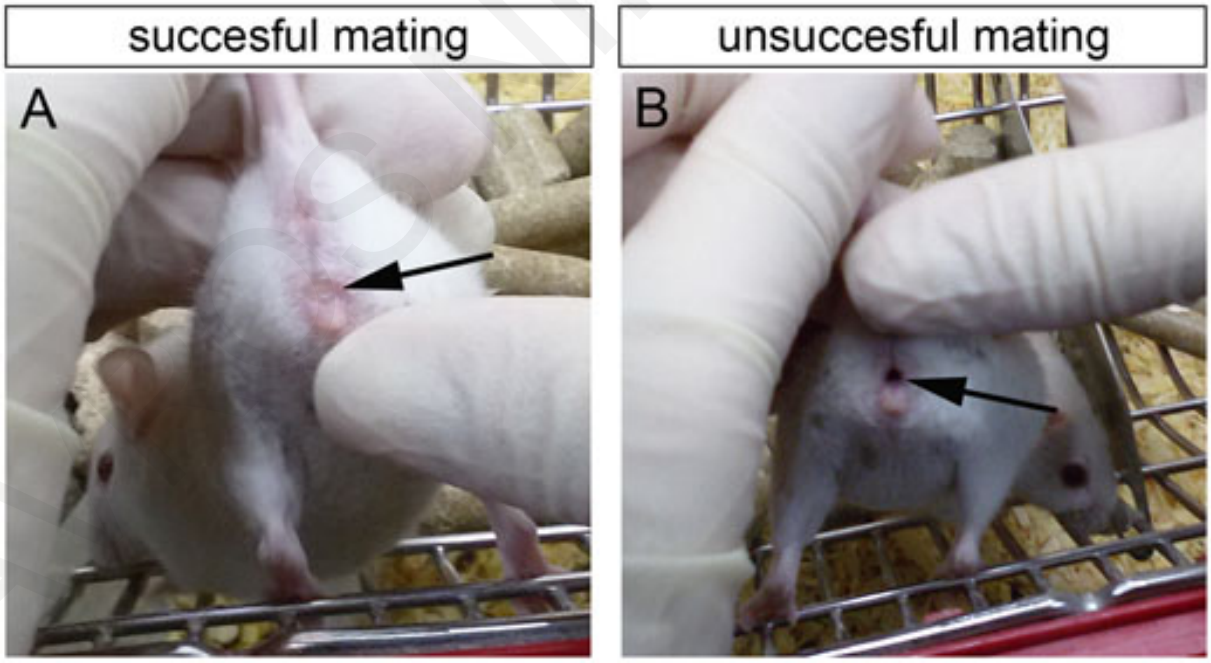

Figure 3.1: The presence of a white "plug" in mouse's vagina can be used as a determinant of pregnancy. A) successful mating, presence of plug is denoted with a black arrow, B) Unsuccessful mating denoted by the absence of plug (black arrow)

3.3.2. Mouse embryo derivation and fixation

Pregnant female mice of the ICR strain were sacrificed by cervical dislocation after a brief exposure to carbon dioxide at the desired stage of pregnancy. Noon of the day that a vaginal plug was observed was considered as embryonic day 0.5 (E0.5). Pregnant mice whose embryos would be derived at E5.5, E6.5 or E7.5 stages were sacrificed at ~11:30-12:00 am of the corresponding day. In the case of E5.0, pregnant mice were sacrificed at 00:00-01:00 am while for E5.25, pregnant mice were sacrificed between 04:00-05:00 am. Embryos were dissected out of the uterus, RM was removed using a pair of $30^{1/2}$ gauge needles and collected in Ham's F-12 Nutrient Mix, GlutaMAX™ medium supplemented with 10% fetal bovine serum (dissection medium). Following collection, embryos were fixed in 4% pfa overnight at 4^{o}c. After a gradual dehydration in methanol, embryos were stored in 100% methanol at -20^{o}c.

3.3.3. **Mouse embryo culture**

E6.5 embryos were dissected as described. Embryos were then transferred through two drops of serum-free medium prior transferring in the same medium for culture. Serum free medium was composed of 25% (v/v) DMEM, low glucose, pyruvate, no glutamine, no phenol red, 25% (v/v) Ham's F-12 Nutrient Mix, GlutaMAX™, 50% (v/v) Neurobasal™-A Medium (1X) Liquid without Phenol Red, 0.5X of N-2 Supplement (100X) liquid, 0.5X of B-27 Serum Free Supplement (50X) liquid, 100 U/ml of Penicillin-Streptomycin, 0.1mM of β-Mercaptoethanol. Cultures were performed in equilibrated culture medium for 8 and 12 hours in the presence of DMSO (mock conditions), 20uM A83-01 (selective inhibitor of TGF-bRI, ALK4 and ALK7), 20uM of SB431542 (selective inhibitor of TGF-bRI, ALK4 and ALK7), 40uM SU5402 (potent FGFR and VEGFR inhibitor), 3uM of PD161570 (selective inhibitor of FGFR) and combination of 20uM A83-01 + 40uM SU-5402.

3.3.4 Putative proximal ExE and putative core EPC explant derivation

E6.5 embryos were dissected as described. Once the RM was removed, two cuts were made using a custom-made glass needle. The first cut was made at the area proximally to the most proximal point of the opaque region (putative core EPC) and the second cut was made at the area distally to this point (putative proximal ExE). The explant corresponding to the putative proximal ExE was washed in a drop of 1 x PBS, Ca^{2+},

Mg^{2+} - free, pH 7.2 followed by incubation into ice-cold 0.5% Trypsin/2.5% Pancreatin, pH 7.6 for 10 minutes at 4^{o}c, standing. Following this reaction, the surrounding exVE was removed by gentle mouth pipetting. The explant corresponding to the putative core EPC was mechanically cleaned from the surrounding maternal blood. Explants of both types as well as very small fragments of exVE were cultured for 24 hours (only the putative proximal ExE and putative core EPC) or for 4 days in chemically defined culture medium an matrigel, in conditions favoring ExE maintenance (i.e. 50ng/ml Fgf2 + 1ug/ml heparin + 10ng/ml Activin A). Putative core EPC explants cultured for 4 days were fixed and stained with Hoechst (diluted 1:5000 in 1 x PBS, Ca^{2+}, Mg^{2+} - free, pH 7.2). Nuclear area (in squared inches) and hoechst intensity were measured by ImageJ. Statistical analysis and graphs were done using Microsoft Excel. Student's *t*-test for independent variables was employed for statistical significance.

3.3.5. E5.5 distal ExE explant derivation and culture on Matrigel

E5.5 embryos were dissected as described. Once the RM was removed, embryos were exposed to ice-cold 0.5% Trypsin/2.5% Pancreatin in PBS Ca^{2+}, Mg^{2+}-free, pH 7.2, at 4^{o}c, standing for 10 minutes. Enzymatic reaction was terminated by transferring the embryos into fresh dissection medium. A custom-made glass needle was made to cut the embryoning-extraembryonic region as well as to make a cut in the middle of ExE. The fragment corresponding to distal ExE was denuded from the surrounding VE by mouth pipetting and then this fragment was transferred into 500ul of serum-free medium to attach onto matrigel-coated 4-well plates under the following conditions: 50ng/ml Fgf2 + 1ug/ml heparin + 10ng/ml Activin A for 24 hrs, no growth factor for 24 hours, no growth factor for 6 hours, 50ng/ml Fgf2 + 1ug/ml heparin for 24 hours, 10ng/ml Activin A for 24 hours, 10ng/ml Activin A for 6 hours. Three explants (derived from three E5.5 embryos) were cultured under each condition.

3.4. Real Time PCR analysis

3.4.1 RNA derivation from E6.5 embryos and Reverse Transcription

Four E6.5 embryos per condition were pooled together and their EPC with the underlying proximal-most part of ExE was microsurgically removed. Remaining tissue was used as a source of total RNA which was extracted using the NucleoSpin® RNA

XS kit from Macherey Nagel. The whole process was repeated three times (three biological replicates). 63ng of total RNA were then used per reverse transcription reaction using random hexamers and oligo dT primer, according to the manufacturer (PrimeScript^{TM} RT reagent Kit – Perfect Real Time, TaKaRa). For a list of the Real Time primers used, please refer to the Appendix (table 8.1)

3.4.2. Real Time PCR

For each reaction (each gene was measured in duplicate for each condition, using three biological replicates), 7ng of cDNA were used per reaction in a total volume of 25ul as follows:

- 1.1ul template cDNA
- 10.6ul PCR grade H_2O
- 0.8ul 1:1 primer mixture (10uM each primer)
- 12.5ul KAPA^{TM} SYBR® FAST qPCR Kit (KAPABIOSYSTEMS)

Cycle thresholds (C_t) for each reaction were obtained and transformed into gene expression fold change according to the formula: Fold change=$2^{\text{delta delta Ct}}$, where delta delta C_t= delta C_t (*GOI* treated – *Gapdh* treated) – delta C_t (*GOI* mock – *Gapdh* mock). Where GOI = Gene of Interest.

3.5. General Molecular Biology techniques

3.5.1 Design, subcloning and *in vitro* transcription of riboprobes (*Spry4, Smad7*, *Cldn4* and *Secretin*)

3.5.1.1 Design

i) Design of *Spry4*, *Smad7* and *Cldn4* templates

The full mRNA sequence of *Spry4*, *Smad7* and *Cldn4* was derived from Mouse Genome Informatics (*Spry4* - MGI:1345144, *Smad7* - MGI:1100518, *Cldn4* - MGI:1313314) in FASTA format. A random sequence of each mRNA (between 0.5-1kb, usually at the 3' UnTranslated Region – 3'-UTR) was selected and used as a query sequence for a blast nucleotide alignment against all known mouse genomic and transcript sequences to verify its gene-specific specificity (Blastn algorithm). The query sequences

showing unique identity with the target sequence were selected and primers at their 5' and 3' ends were designed.

ii) Design of *Secretin*

The sequence of interest as well as the appropriate primer sequences were found from Allen Brain Atlas (http://mouse.brain-map.org, probe name: RP_050329_04_A02, experiment: 74357731)

3.5.1.2 Template derivation

Total RNA from 10 littermate E8.5 embryos (which were pooled together) was isolated using the NucleoSpin® RNA XS kit from Macherey Nagel. Following RNA isolation, 1ug of total RNA was used for full-length cDNA conversion using the SMARTer™ PCR cDNA Synthesis Kit from Clontech

3.5.1.3 Polymerase chain reaction

100 ng of template full-length cDNA were used per PCR reaction (KAPA HiFi HotStart ReadyMixPCR Kit from KAPABIOSYSTEMS) with gene specific primers (for a list of these primer pairs please refer to table 8.2 in the appendix), according to the protocol provided by the manufacturer (table 3.1):

Step	Temperature	Duration	Cycles
Initial denaturation	95°c	3 min	1
Denaturation	98°c	20 sec	
Annealing	Case depended (60-75°c)	15 sec	25 cycles
Extension	72°c	60 sec	
Final extension	72°c	5 min	1

Table 3.1: PCR conditions followed for template derivation

When the appropriate PCR conditions per case were set up, 4 PCR reactions were set up per gene and the products of all reactions were finally mixed together.

3.5.1.4. Subcloning – plasmid preparation

PCR products were electrophoresed on a 1% agarose gel and then the band of the correct size (often a single band) was gel extracted (NucleoSpin® Gel and PCR Clean-up kit). 10ug of the PCR product were then digested overnight in a restriction enzyme digestion reaction according to the recognizing sequences previously included into the PCR primers. A similar restriction enzyme reaction was also set up for the vector (often plasmid Bluescript SK-). After a second gel extraction, the isolated fragments took part in a ligation reaction (10ul total volume incubated at 14^{o}c, overnight). The ratio of vector:insert was kept constant at 1:3 with vector's total weight being 100ng per reaction. 5ul of the ligation reaction were used to transform competent DH5a bacteria (MAX Efficiency^{TM} DH5A^{TM} Competent Cells, Invitrogen^{TM}) and the transformed cells were then spread on ampicillin containing agar plates followed by an overnight incubation at 37^{o}c. 5 colonies were picked up the next morning and screened for the presence of the appropriate clone, using the same restriction enzymes used for the initial PCR product and vector digestion. The appropriate colony was then grown further and the plasmid DNA was isolated (NucleoBond Xtra Midi Kit, Mackerey Nagel). A portion of the grown colony was stored indefinitely at -80^{o}c in the presence of Glycerol (1:1 v/v ratio).

3.5.1.5. Plasmid Linearization - *In Vitro* Transcription (IVT) reactions

20ug of the appropriate plasmid were digested overnight at 37^{o}c using the specific enzyme required to get a linearized product for *in vitro* transcription. The digestion product was then phenol/chloroform extracted and ethanol precipitated. 1ug of the linearized plasmid was *in vitro* transcribed as follows:

- 1ug linearized plasmid
- 1ul buffer
- 1ul oligonucleotides with Digoxigenin (DIG) or Fluorescein isothiocyanate (FITC)-labeled dUTP
- 0.5ul RNase inhibitors
- 0.5ul T_3 or T_7 or SP6 RNA polymerase
- H_2O to 10ul final volume

Reactions were incubated at 37°c (except for reactions conducted by SP6 polymerase which were incubated at 40°c) for 3 hours and then each reaction was terminated by the addition of 90ul H_2O, precipitated with LiCl and ice-cold isopropanol and then resuspended in 45ul of DEPC-treated H_2O. All probes were stored at -80°c until used. In order to examine the quantity and quality of the probe, a sample (5ul) was taken later from each reaction and electrophoresed (Figure 3.2).

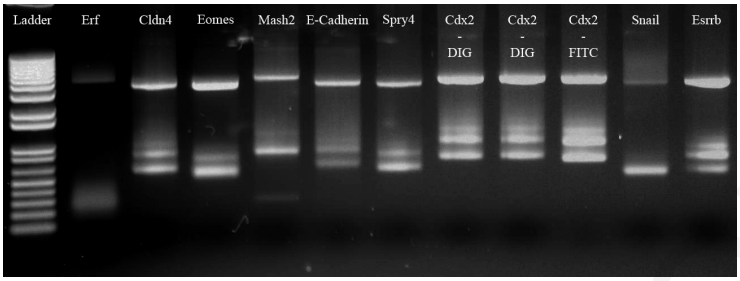

Figure. 3.2: Products of a series of *in vitro* transcription (IVT) reactions. RNA riboprobes appear as a single or double bright band. The upper bands (~3kb size) correspond to the linearized plasmid template. Samples displaying faint diffusive appearance like the case of *Erf* (second well) were discarded.

3.6. Whole-mount RNA *in situ* hybridization on mouse embryos and explants (single and double color wISH)

Mouse embryos of the desired developmental stage were isolated and fixed at freshly prepaired 4% ice-cold pfa, overnight at 4°c. The following morning embryos were dehydrated through an increasing concentration of methanol (PBST, 25%, 50%, 75% and 100% methanol) and then stored in 100% methanol at -20°c. Stored embryos were then rehydrated through a reducing concentration of methanol (100%, 75%, 50%, 25%, PBST). Rehydrated embryos were then penetrated by incubation in Proteinase K (20mg/ml). Exposure to Proteinase K was for 1.0 minute for E5.0 embryo, 1.5 minutes for E5.5 embryos and E2.5 minutes for E6.5 embryos. Penetrated embryos were then re-fixed in 0.2% glutaraldehyde/4%pfa for 20 minutes at room temperature to withstand the high temperature of the following hybridization step. After fixation, embryos were washed three times in PBST and incubated at 67°c in pre-hybridization solution for 6 hours. This step was followed by the addition of the probe solution (this solution was composed by 15 – 25 ul of probe diluted in 380ul of prewarmed at 67°c pre-hybridization solution). For a complete list of probes used in this study, see table 3.2. Embryos were then incubated in the presence of probe at 67°c for two overnights (occasionally for

three), in a hybridization chamber filled with 50ml of 50% SSC pH 7 and 50% formamide. The following day, each sample was washed three times for 30 min at 67°c with Solution I (1x SSC pH 4.5, 50% formamide, 0.1% Tween 20), treated with RNase I for 1 hour at 37°c and then washed three more times for 30 min at 67°c with Solution II. Each sample was blocked for three hours into blocking solution (MABT/Block/Sheep serum; MABT was composed of 100mM maleic acid, 150mM sodium chloride, 0.1% Tween 20, pH 7.5) and then incubated in 1:2500 anti-Digoxigenin antibody in blocking solution for 2 overnights at 4°c, rocking. Washes in MABT were performed over the entire next day and overnight at 4°c. Finally, after three washes in NTMT solution, color development followed using BM Purple AP Substrate (Roche). When color development was completed, reaction was terminated by washing in PBST and then post-fixing in 4% pfa for 20 min at room temperature. Embryos were finally cleared by transferring into 50 and then 70% glycerol for documentation and storage. In the case of double color experiments, the FITC-bound probe (often the most strongly expressed gene) was first developed (INT/BCIP was used which gives a reddish color instead of BM purple which gives a blue-purple color). Upon reaction was ready, embryos were gradually transferred into 70% glycerol, oriented, documented and then dehydrated and rehydrated through an increasing and decreasing concentration of methanol as described. Enzyme inactivation was conducted by incubating the embryos at 70°c for one hour, standing. Following enzyme inactivation, embryos were stained with BM purple to visualize the expression of the second gene, cleared by transferring into 50 and then 70% glycerol, oriented according to the orientation they had when the first gene was documented, and documented again, this time for the second gene.

Gene	Restriction enzyme for antisence probe	RNA polymerase
Errb	*Eco*RI	T_7
Sox2	*Eco*RI	T_3
BMP4	*Acc*I	T_7
Eomes	*Eco*RI	T_7
Cdx2	*Xho*I	T_7
Cldn4	*Xho*I	T_3
Erf	*Bam*HI	T_7
Snail	*Cla*I	T_7
Mash2	*Xho*I	T_7
Ker8	*Xba*I	T_3
Spry4	*Xho*I	T_3
Smad7	*Xho*I	T_3
Nodal	*Xho*I	T_7
Secretin	*Eco*RI	T_7

Table 3.2: List of plasmids used for *in vitro* transcription, their corresponding restriction enzymes and the RNA polymerase used

3.7. DBA-lectin staining (immunochemistry) following w*ISH* and embryo histology

Following wISH, embryos were transferred into PBST (0.01% Tween-20 in PBS Ca^{2+}, Mg^{2+}-free), penetrated using 0.3% TritonX-100 in the presence of 0.1M Glycine for 15 m, rocking at room temperature and blocked in blocking solution (10% goat serum in PBST) for 1 hour at room temperature, rocking. DBA lectin (1:400 in blocking solution) was added and embryos were incubated overnight at 4^{o}c, rocking. The embryos were then washed five times, 5 minutes each, in PBST and then peroxidase-conjugated streptavidin was added (1:2000; diluted in blocking solution) for 2 hours at room temperature. Following washing (five times in PBST for 5 minutes each), color development was conducted using DAB substrate. Color development often lasted for

~1 minute. After clearing by transferring embryos into 50 and then 70% glycerol, they were oriented according to the orientation they had during wISH documentation, and documented again, this time for DBA lectin. For embryo histology, embryos were dehydrated by exposing them in an increasing concentration of ethanol (50%, 70%, 90% 100%) and xylene prior to embed them in paraffin wax. Sagittal sections were cut at 7um intervals.

3.8. Whole mount immunofluorescence – confocal microscopy

Embryos were fixed in 2% pfa for 20 minutes at room temperature. Tissue penetration was performed using 0.3% TritonX-100 in the presence of 0.1M Glycine for 15 m, rocking at room temperature. After blocking (blocking solution: 10% goat serum, 0.01% Tween-20 in PBS Ca^{2+}, Mg^{2+}-free) for one hour at room temperature, primary antibody was added in the presence of blocking solution overnight, rocking, at 4^{o}c (rabbit anti-PAR6B 1:100, BS-I lectin 1:400, DBA lectin 1:400, rabbit biotin conjugated anti-Collagen IV 1:100, rabbit anti-phospho Erk 1:50, mouse anti-Cdx2 1:100). Corresponding secondary antibody (1:700) was added the following day in the presence of blocking solution for 2 hours, rocking at room temperature. Nuclei were stained with TOPRO^{TM}-3 Iodide, diluted 1:500 in PBS Ca^{2+}, Mg^{2+}-free, for 30 minutes at RT. Embryos were then post fixed in 2% pfa for 10 minutes at room temperature, cleared by transferring in 50% glycerol for 10 minutes and then in 70% glycerol. They were then mounted on glass coverslips, using 70% glycerol as a mounting medium, for confocal microscopy.

CHAPTER 4:

RESULTS

4. Results

4.1 Results for aim 1: To identify the exact boundary between ExE and EPC at E5.5-E6.5 and to correlate this with anatomical features of the conceptus. Although knowledge of this is crucial for understanding early trophoblast patterning, the location of this boundary (and hence the validity of current markers of ExE/EPC) is unknown, as this issue has not been addressed directly.

Identification of the exact boundary between the ExE and the EPC is often difficult because of the apparent lack of anatomical differences in the trophoblast within the transition region between ExE and EPC, as these two tissues are contineous during the early stages of development. As a first approach towards identifying this boundary, we observed live embryos at different developmental stages (i.e. the E5.5, E6.5 pre-streak, E6.5 early streak and E6.5 mid-streak). It was found that at E6.5, exVE is more opaque than other cells of the conceptus. This allowed us to identify the most proximal edge of exVE, which coincides with the area where it turns outward, before it eventualy turns distally and becomes parietal endoderm (PaE) (Fig. 4.1.1: A - D). We did not observe any opaqueness difference at E5.5 (Fig. 4.1.1: A). That the proximal edge of this opaqueness correlates with the proximal edge of exVE was confirmed using staining with DBA lectin (marker of the entire VE and PaE) (Fig. 4.1.1: E - H). Based on DBA positivity, the 'neck' region of exVE (rouphly concave region of proximal exVE up to the point where it begins to turn outwards) appeared shorter (along the P-D axis) in less advanced E6.5 embryos (Fig. 4.1.1: E –F and G – H).

Because the ExE-EPC boundary was suggested, but never tested directly, to be at the level of the point of insertion of RM into the egg cylinder, we aimed to identify this point and correlated it with the level of the proximal edge of the exVE 'neck' mentioned above. This insertion point is considered to be where the relatively thin basement membrane (BM) of exVE transitions into the thicker RM (Miner et al, 2004), using ColIV and BS-I lectin staining (both mark the RM and the BM of exVE, with BS-I lectin additionally staining exVE, PaE, as well as the cell surface of ExE and EPC cells). Immunofluorescence analysis of ColIV localization at early-streak

and mid-streak E6.5 stages and of BS-I at E5.5 revealed that the transition from BM to RM (that is, the point of insertion of RM) coincides with the proximal end of the neck region of exVE (Fig. 4.1.2: B, B' and C, C'; Fig. 4.1.2: A). Thus, our data lead us to conclude that the most proximal edge of exVE coincides with RM insertion point (this point can also be considered as the initiation of RM).

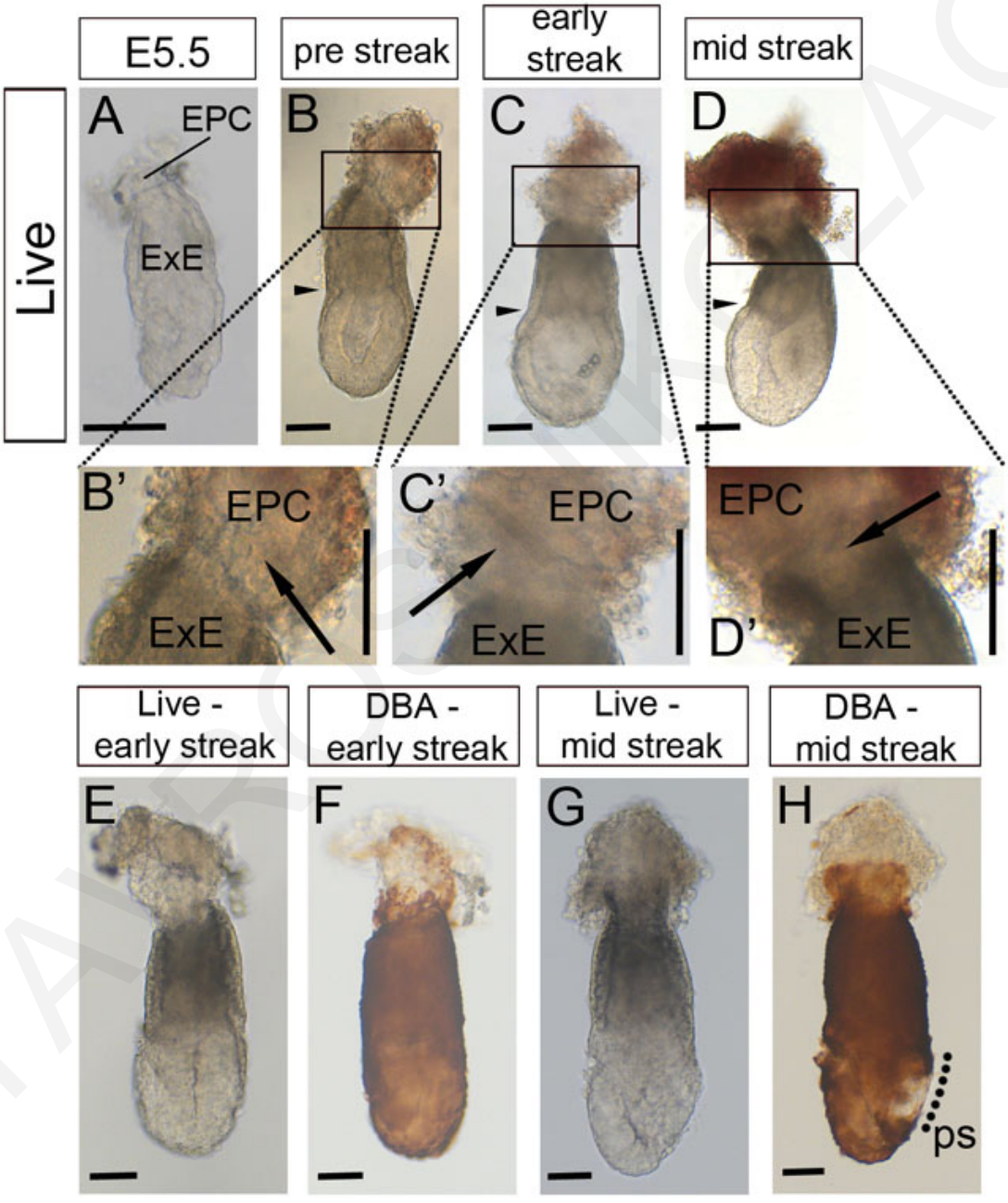

Figure 4.1.1: An opaque region of exVE nature characterizes the region of ExE – EPC junction in live embryos from the early to mid-streak stages in bright field microscopy. During the E5.5 stage, both ExE and EPC of live embryos are indistinguishable with regards to their color (A,

n=10/10) but live embryos at the pre-, early- and mid-streak stages are characterized by the presence of an opaque region initiating from the embryonic-extraembryonic junction (arrowheads in B, C, D, n=3/3 per developmental stage) and extending up to the region of assumed ExE-EPC junction (B, B', C, C', D. D'). In live pre-streak embryos, this opaque area stops abruptly (B', arrow shows the clear region - please notice the color difference between the opaque and the clear region) while in early- and mid-streak embryos the opaque area forms a neck-like formation (C', D', arrows show the neck region) (Ninomiya et al, 2005). Immunochemistry analysis for the localization of the VE-specific marker DBA lectin (Noguchi et al, 1982) demonstrates that the neck region has VE-origin (E – H, dotted line demarcates the absence of DBA lectin staining which occurs as a result of definitive endoderm cell engression into the emVE (Nowotschin and Hadjantonakis, 2010)). E – F and G – H show the same embryo alive (E and G) or after DBA staining in the same orientation (F, H), n=3/3 per developmental stage. ps: Primitive Streak, Scale bars indicate 100 μm.

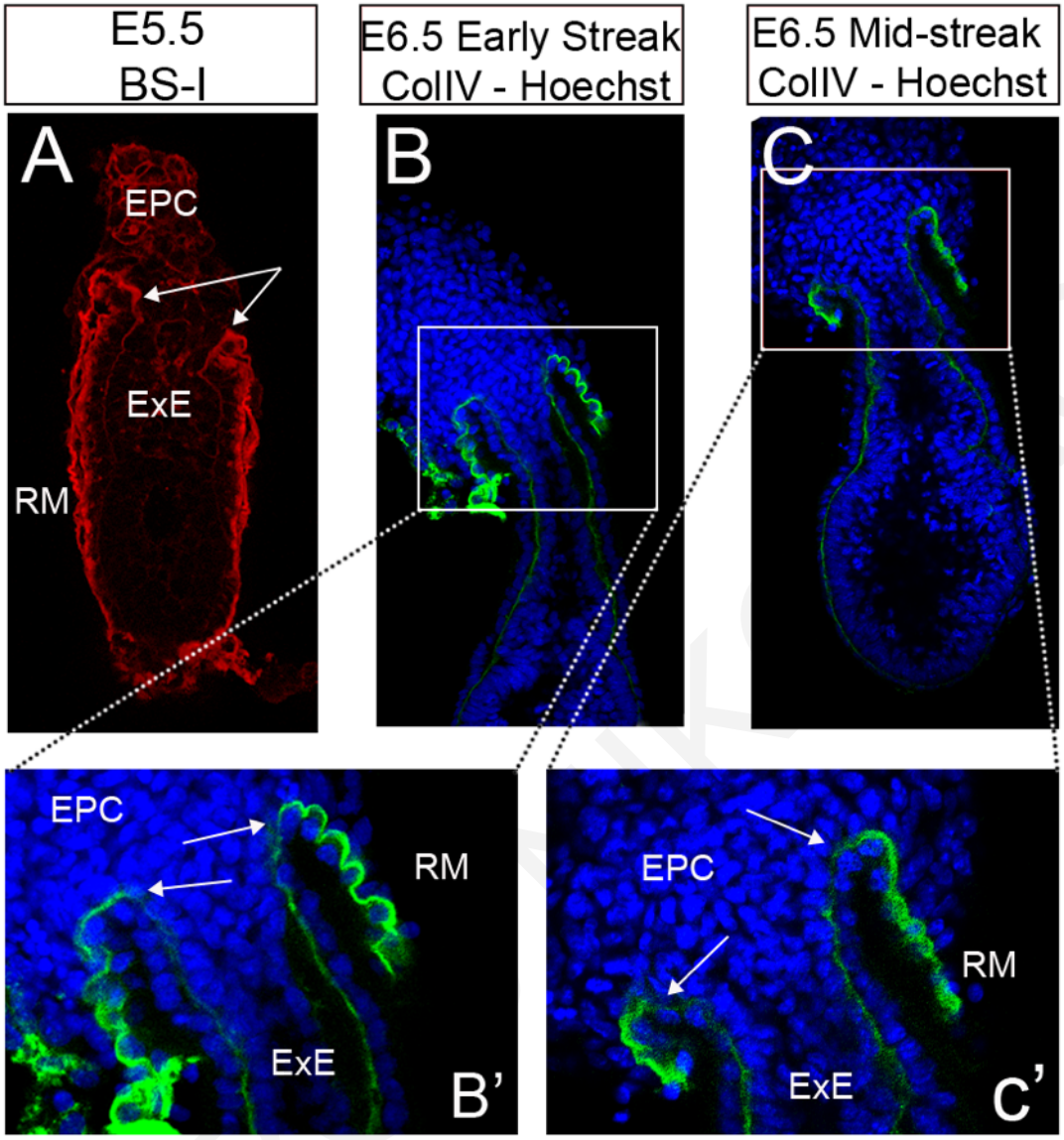

Figure 4.1.2: The most proximal region of exVE (i.e. before it turns distally to become PaE) coincides with an increase in the thickness of basement membrane, a characterization of RM. A) BS-I lectin staining on a E5.5 embryo dissected from the uterus but with its RM kept intact. Arrows indicate an increase in basement membrane thickness at the most proximal region of exVE, n=3/3, B and C) Immunofluorescence analysis of Collagen IV on an early streak and mid-streak embryo respectively. Arrows in B' and C' indicate an increase in basement membrane thickness at the most proximal region of exVE, n=3/3 per developmental stage. ExE: Extraembryonic ectoderm, EPC: Ectoplacental cone, RM: Reichert's membrane.

In order to test whether the level of insertion of RM/proximal edge of exVE coincide with the boundary between ExE and EPC trophoblast, the following experiments were carried out.

First, it was found here for the first time that the proximal limit of *Erf* expression (a gene previously reported to mark the ExE) and the distal limit of *Snail* expression (a gene previously reported to be a marker of the EPC) coincide with the most proximal edge of exVE, and hence with the point of insertion of the RM (Fig. 4.1.6: E – H, I – K).

Second, the presented data so far lead us to hypothesize that the trophoblast distally to the RM initiation point (referred to here as 'putative proximal ExE') should have ExE characteristics, whilst the trophoblast region proximal to this point (referred to here as 'putative core EPC') should have EPC characteristics. This hypothesis was tested in two different ways: 1) Putative proximal ExE (ppExE) and putative core EPC (pcEPC) explants were isolated from E6.5 embryos and cultured under conditions favoring ExE maintenance, that is, culture in the presence of Fgf2/Heparin and Activin proteins on matrigel-coated plates in a serum free medium (Kubaczka et al, 2015). Under these condtions, ExE tissue should be expected to remain ExE, whereas EPC tissue should differentiate into EPC derivatives, such as TGCs. This is because a defining difference between ExE and EPC is their different response to conditions that keep ExE undifferentiated: EPC, but not ExE, fails to respond to these conditions and as a result differentiates. 2) If *in vivo* developed ppExE and pcEPC are part of ExE and EPC respectively, they should display a different cell status because ExE is considered to be an epithelial tissue whereas EPC is not. To this end, the trophoblast of E5.5 and E6.5 embryos was examined using epithelial cell markers.

Regarding the first mode of testing for the ExE-EPC boundary, our microsurgery methodology allowed us to obtain sufficient numbers of isolated ppExE and pcEPC explants which were then cultured as mentioned above (Fig. 4.1.3). Culture of pcEPC under such conditions for 4 days (n=8/8) resulted in the appearance of cells migrating away of the initial explants. These cells had the classical appearance of TGCs, that is, cells with a relatively large cell size and perinuclear granules around some of their nuclei (Fig. 4.1.4: A, A'). In contrast, ppExE explants cultured in the same way (n=5/5) did not show the appearance of such cells (Fig. 4.1.4: B). The TGC status of the cells that migrated away from the pcEPC explants was confirmed by examining their DNA content (by definition, TGC cells are the only non-diploid trophoblast cell types and

have a high ploidy) in relation to that of diploid exVE cells that were cultured under the same conditions (Simmons et al, 2007). Specifically, the nuclei of these cells displayed a much higher and statistically significant DNA content than the diploid exVE cells. This was based on measuring nuclear fluorescence intensity after Hoechst treatment (Fig. 4.1.4: C – C' and D – D'; E – G).

These data strongly suggest that ppExE and pcEPC are indeed ExE and EPC tissues respectively and that the ExE-EPC boundary is within the trophoblast region that coincides with the level of insertion of RM.

To further support this conclusion ppExE and pcEPC explants were cultured under the above-mentioned conditons for 24h, followed by examination of the expression of *Snail* (EPC gene whose distal expression limit coincides with the RM insertion point – see our results above), *Erf* (ExE gene whose proximal expression limit coincides with the RM insertion point – see our results above), *Secretin* (marker of the EPC-derived cells located in the center of the E6.5 EPC) and *Pll* (marker of TGCs located in the periphery of E6.5 EPC). As expected, the EPC genes *Snail* (n=3/3) and *Secretin* (n=3/3) were robustly expressed only in pcEPC, but not in ppExE explants, whereas the ExE gene *Erf* (n=3/3) was only found to be expressed in ppExE explants (n=3/3) (Fig. 4.1.5 and 4.1.6). Interestingly, although pcEPC explants cultured for 4 days produce TGCs (see our results above), when these explants were cultured for only 24h, they rarely produce TGCs based on morphology and *Pll* expression (n=3/3) (Fig. 4.1.5: B). This can be explained by the fact that TGC differentiation in EPC explants *in vitro* first requires their migration away from the original explant (Gonçalves et al, 2003), an event that has barely started in our explants after only 24h of culture.

As a last way to verify the ExE identity of the trophoblast cells located just distal to the RM initiation point, we made use of the finding that from E5.5 onwards, ExE, but not EPC, is an epithelial tissue (Mehrotra, 1984; Bedzhov and Zernicka-Goetz 2014). We therefore hypothesized that if ppExE trophoblast cells are indeed ExE tissue, they should display epithelial characteristics. To investigate this, we first examined by immunofluorescence analysis the localization of the Par6B protein (apically localized in epithelial cells, but either localized in a non-polarized fashion or not present in non-

epithelial cells) in relation to the RM insertion point/proximal edge of exVE (assayed by BS-I binding distribution) at E5.5 and E6.5 (early- and mid-streak stages). Our results show for the first time that the distribution of Par6B within ExE is polarized up to the region that coincides with the proximal edge of exVE/RM insertion point at both E5.5 and E6.5 (n=3/3 for each stage) (Fig. 4.1.7: C_i and D_i).

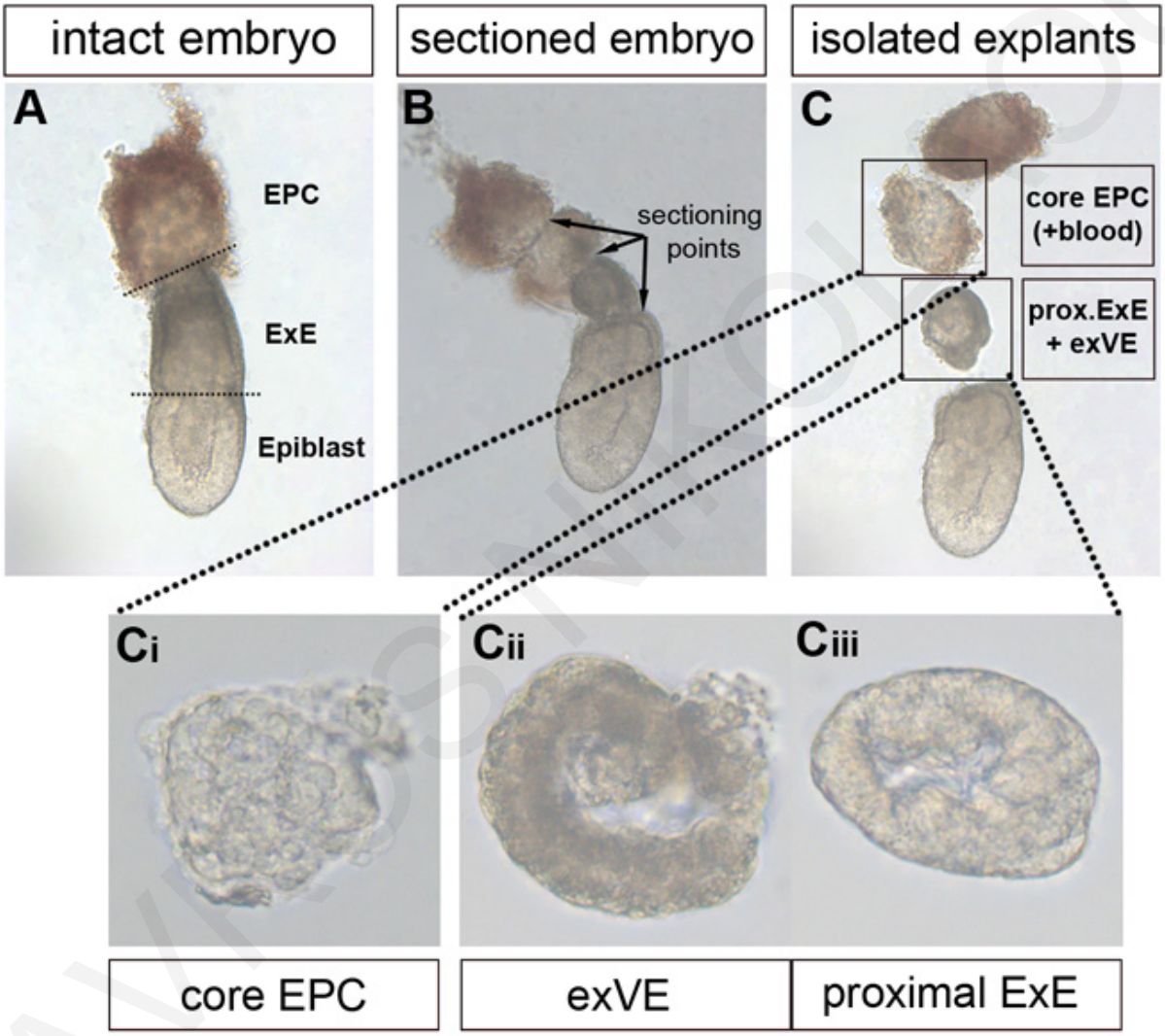

Figure 4.1.3: Microsurgery-based methodology for putative core EPC (pcEPC) and putative proximal ExE (ppExE) explant isolation from live embryos. A) intact E6.5 pre-streak embryo. B) three transverse cuts using custom-made glass needles where made at the region where the opaque color stops (i.e. the most proximal point of exVE) and proximally and distally to this (demarcated as "sectioning points"). C) This process allowed us to derive the proximal ExE enveloped into its surrounding exVE (prox. ExE + exVE) as well as the core EPC with maternal blood. C_i) maternal blood was mechanically removed from the core EPC, C_{ii} and C_{iii}) proximal ExE was released from the surrounding exVE by a brief exposure into an enzymatic digestion

followed mechanical separation of the two tissues. ExE: Extraembryonic ectoderm, EPC: Ectoplacental cone.

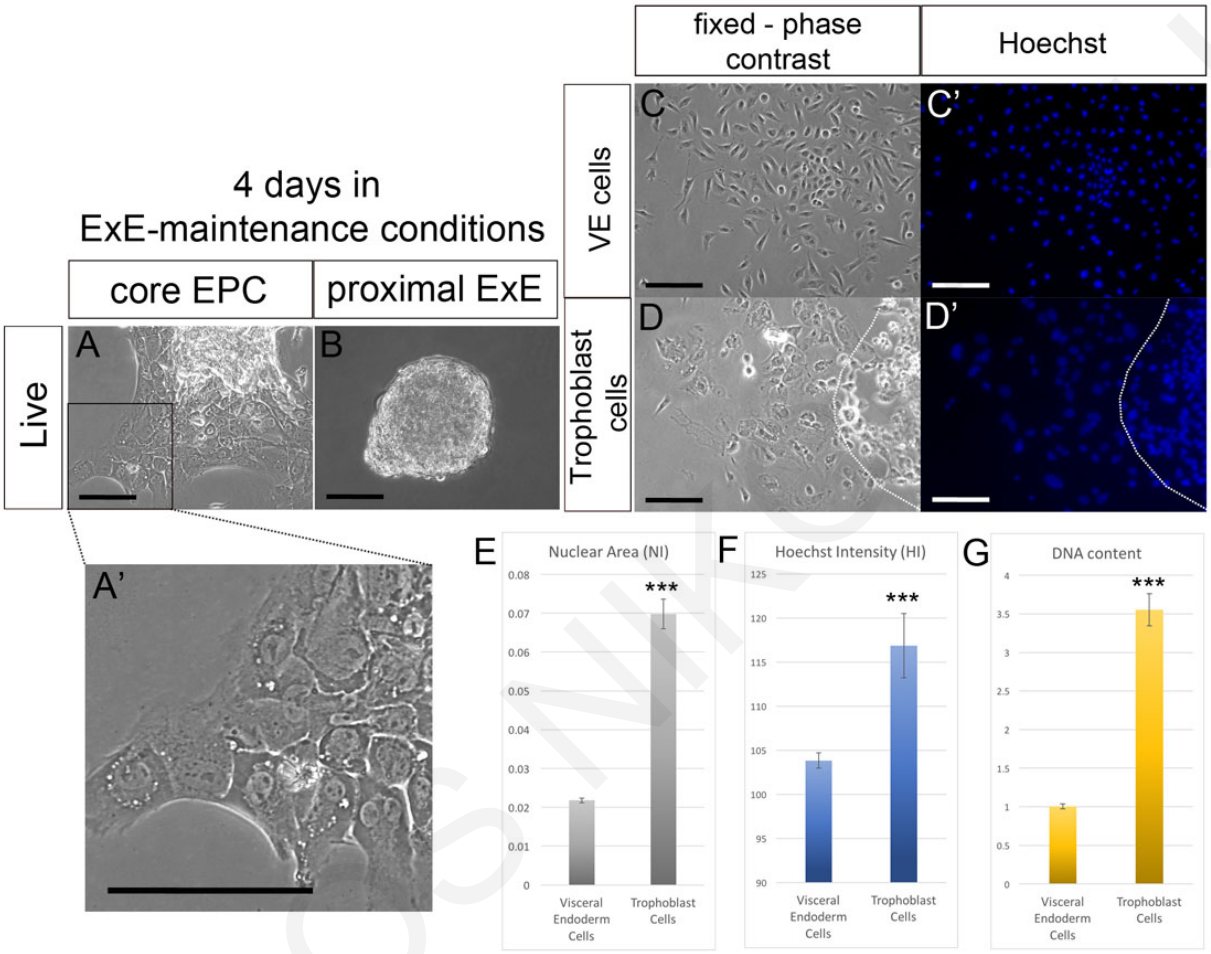

Figure 4.1.4: putative core EPC explants cultured under conditions maintaining ExE character, fail to maintain their own character and after four days in culture, they differentiate into morphologically distinct, trophoblast giant cells. A and B) phase contrast pictures of live explants cultured for four days on matrigel in the presence of Fgf2/Heparin and Activin (ExE maintenance conditions). Putative core EPC explants have morphologically giant cells (TGCs) spread around the initial explant in a cellular monolayer (A – A', n=8/8) while putative proximal ExE explants grow as a solid mass of cells (B, n=5/5). When compared to the diploid cell population of VE cells (C – C' and D – D'), TGCs from core EPCs, display an increased nuclear area (E), increased Hoechst Intensity (F) and an increase in their DNA content (G). Dotted line in D and D' indicate the contour of the initial explant. n=82, P<0.001, Student's *t*-test (independent). Scale bars: 100 μm.

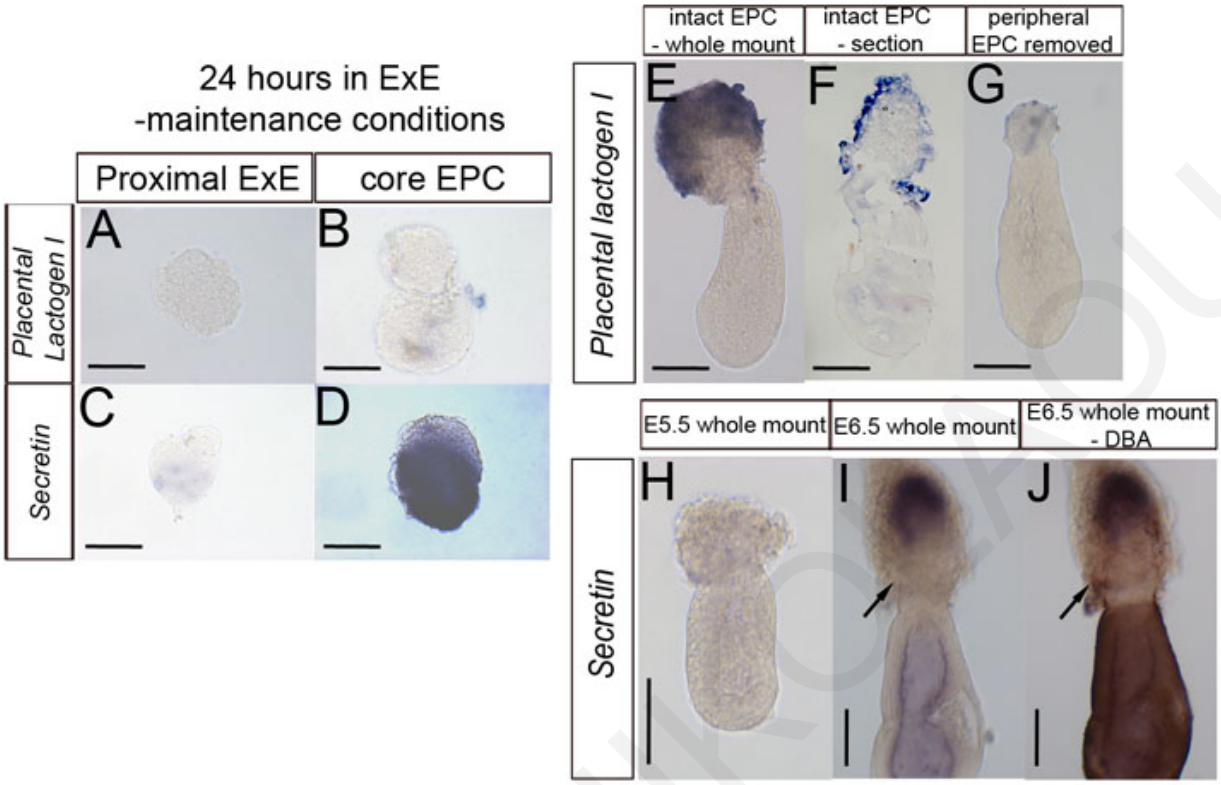

Figure 4.1.5: putative core EPC explants cultured under conditions maintaining ExE character, fail to maintain their own character and after 24 hours in culture, they differentiate into EPC derivative cell types. A and B) both types of explants fail to differentiate into the *Placental lactogen I* (*PlI*) expressing EPC-derivative cell types (E – G, n=2/2 for putative proximal ExE and n=3/3 for core EPC). This failure is not due to experimental reasons because embryo in (E) had served as an internal control for the reaction. F) section of a E6.5 embryo after *in situ* hybridization for *PlI* demonstrating presence of positive cells exclusively at the EPC periphery while if the periphery is mechanically removed, no *PlI* positive domain is seen. C and D) putative core EPC explants differentiate into *Secretin* positive EPC-derivative cells (n=3/3) while none of the putative proximal ExE explants behaves as such (n=3/3). (H, I, J). *Secretin* marks EPC derivative cells because neither the EPC at the E5.5 embryo (n=3/3) nor the core EPC at E6.5 (6/6) are positive for *Secretin* expression. *Secretin* positive cells appear at the proximal region of EPC by E6.5 (I, J, n=6/6). Scale bars: 100 μm.

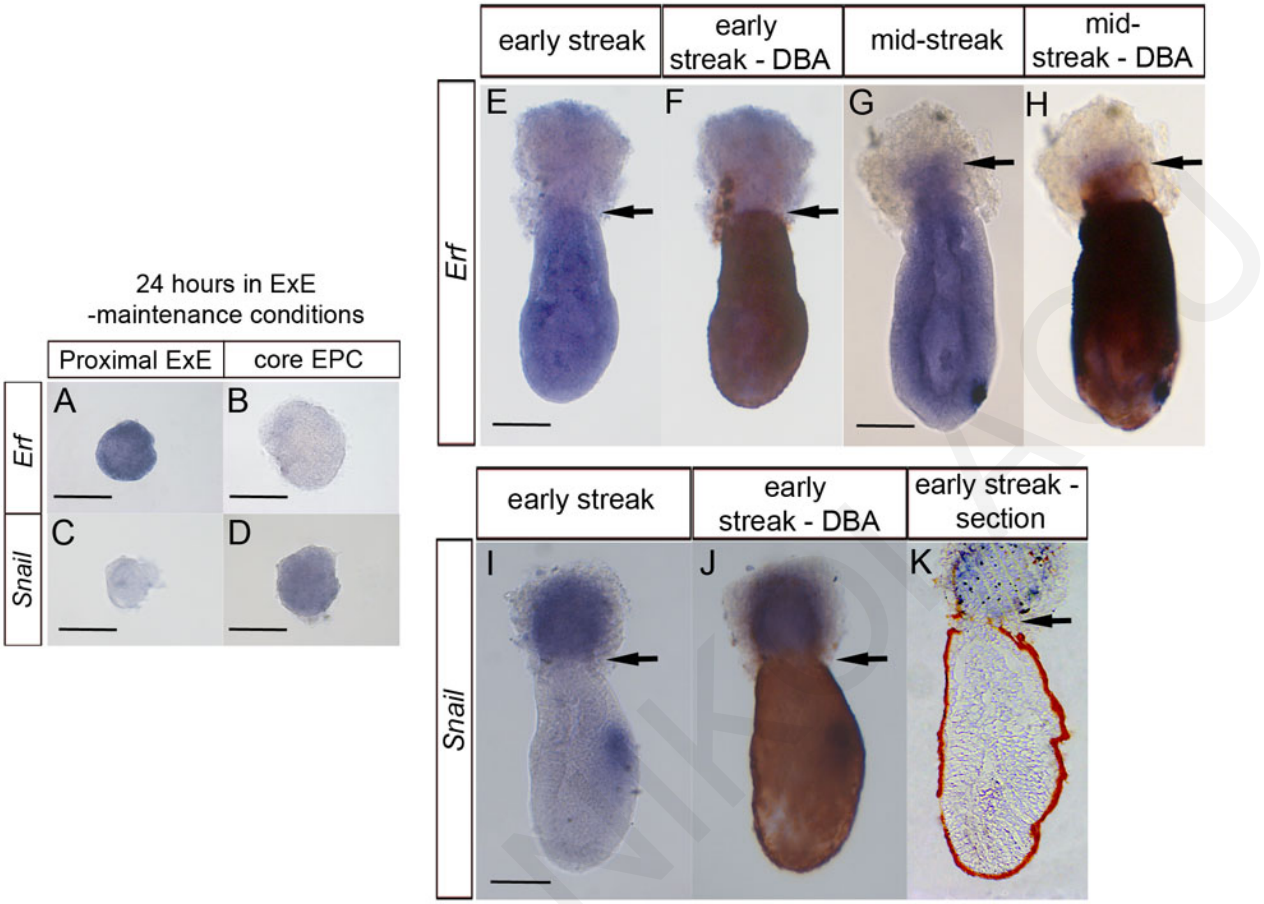

Figure 4.1.6: putative proximal ExE explants cultured for 24 hours under conditions maintaining ExE character, display ExE character. A and B) putative proximal ExE retains the expression of the ExE specific gene *Erf* (n=3/3) while core EPC is negative (n=3/3). *Snail* fails to get upregulated by proximal ExE explants cultured under such conditions (n=3/3) while core EPC retains its *Snail* expression (n=3/3). *Erf* expression during E6.5 respects the contour of Visceral Endoderm as its expression domain appears up to the most proximal point of DBA positivity (E – H, arrows indicate the most proximal point of *Erf* expression, n=3/3 for both developmental stages; The same embryo is displayed in E and F also the same is true for G and H). In agreement to the above, the most distal point of the expression domain of the EPC-specific gene *Snail* is also respecting the contour of Visceral Endoderm (I, J, K, arrows indicate the most distal point of *Snail* expression in relation to DBA lectin positivity; n=3/3). The embryo in I, J and K is the same embryo. Scale bar: 100 μm.

The proximal limit of trophoblast with epithelial characteristics was also examnined using the expression pattern of *Cldn4*, a component of tight junctions (one of the unique features of epithelial cells) that was shown previously to be expressed in the ExE-derived chorion at E7.5 (Günzel and Yu, 2013; Burtscher and Lickert, 2009). We show

here for the first time that the proximal limit of its expression coincides with the proximal edge of exVE (based on DBA lectin binding pattern) at E6.5 (Fig. 4.1.7: H – K) and at E5.5 (data not shown).

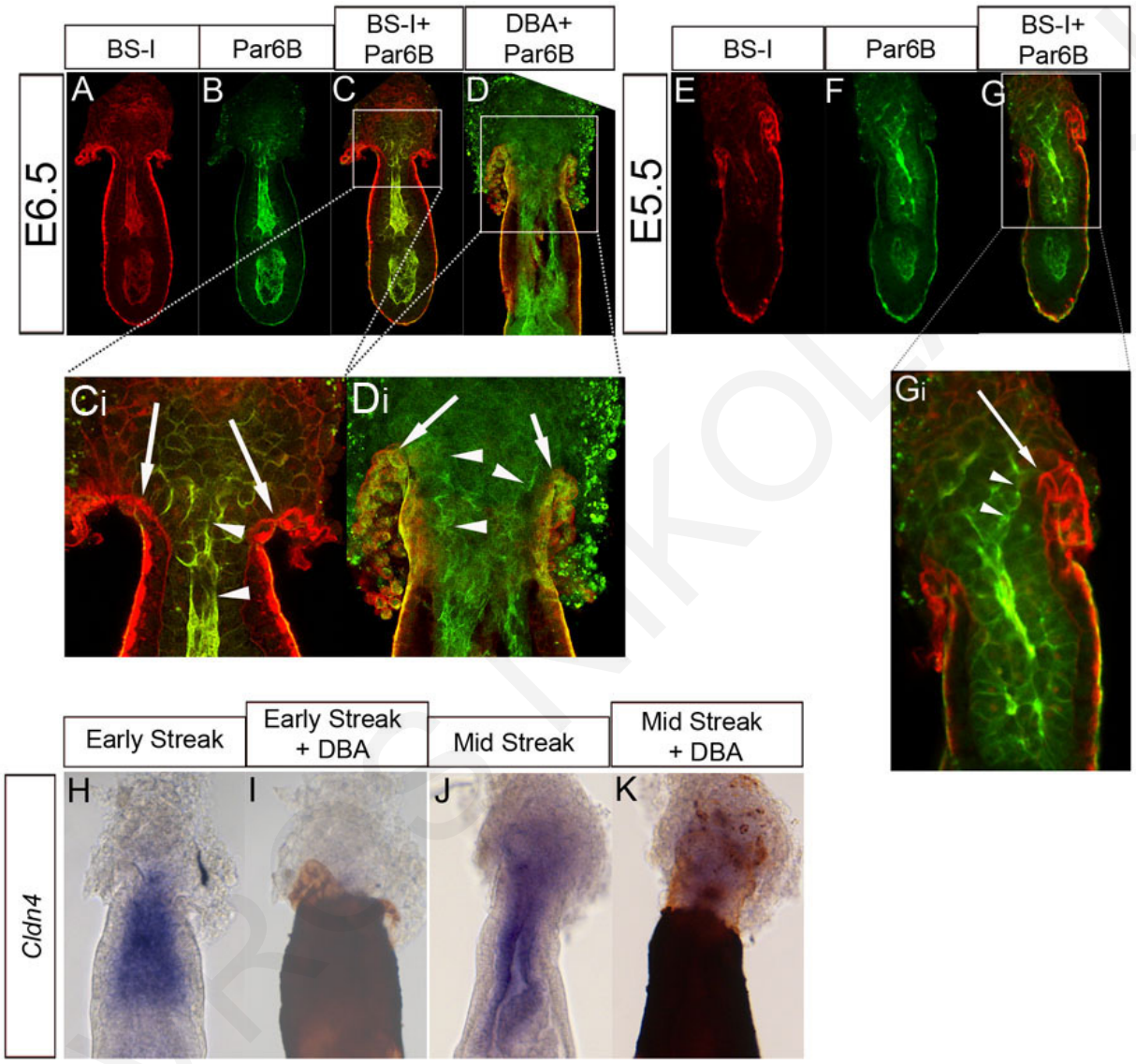

Figure 4.1.7: Trophoblast's epithelial polarity is associated with the presence of Visceral Endoderm at both E5.5 and E6.5. A, B, C, C_i) Epithelial polarity of ExE cells correlates with low thickness of the basement membrane as shown by the polarized localization of Par6B (arrowheads) up to the point of increased BS-I lectin-stained basement membrane, which is itself associated with the initiation of RM (C_i), n=3/3. The same is true also for mid streak embryos (D – D') as Par6B polarization (arrowheads) can be detected until the most proximal point of VE, here indicated by DBA lectin positivity (arrows) n=3/3. This association is also seen in E5.5 embryos (E – G_i; arrowheads indicate polarized Par6B, arrow shows RM initiation)

n=5/5. H – K) Expression of the epithelial marker gene *Cldn4* during early and mid-streak stages is strongly associated with DBA lectin positivity. n=3/3 for both developmental stages.

Taken together, the results presented here show for the first time that the ExE-EPC boundary coincides with the level where the RM inserts into the egg cylinder. Moreover, the expression of *Erf* and *Cldn4* can be used as a marker of the entire ExE, whereas *Snail* and *Secretin* are exclusively expressed in the EPC, with the distal boundary of the former coinciding with the ExE-EPC boundary.

4.2.1. Results for specific aim 1 of aim 2: To investigate whether there are more than two distinct regions within ExE along its PD axis using gene expression at E6.5 (a time when ExE is considered fully formed).

The existence of two regions within the E6.5 ExE has been suggested in the past by Donnison and coworkers, 2014, based on data obtained by whole mount *in situ* hybridization (Donnison et al, 2014). These workers took length measurements of the expression domain of several genes along the PD axis using as a starting point the embryonic-extraembryonic junction (that is, the boundary between distal ExE and epiblast). Although these data clearly demonstrated the existence of two transcriptionally distinct regions in the ExE (distal and proximal halves), our pilot experiments suggested that there are at least three regions (distal, intermediate and proximal ExE regions). Clarification of this is important for a more comprehensive understanding of ExE patterning.

We therefore readdressed this issue in the E6.5 ExE and EPC by performing single whole mount *in situ* hybridization for genes previously reported as distal ExE half markers (*Errb*, *Sox2*, *Bmp4*, *Eomes*, *Cdx2*; Fig. 4.2.1: A-E) and markers of proximal ExE and EPC (*Mash2*, *Ker8*; Fig. 4.2.1: F, G). We also compared these to the

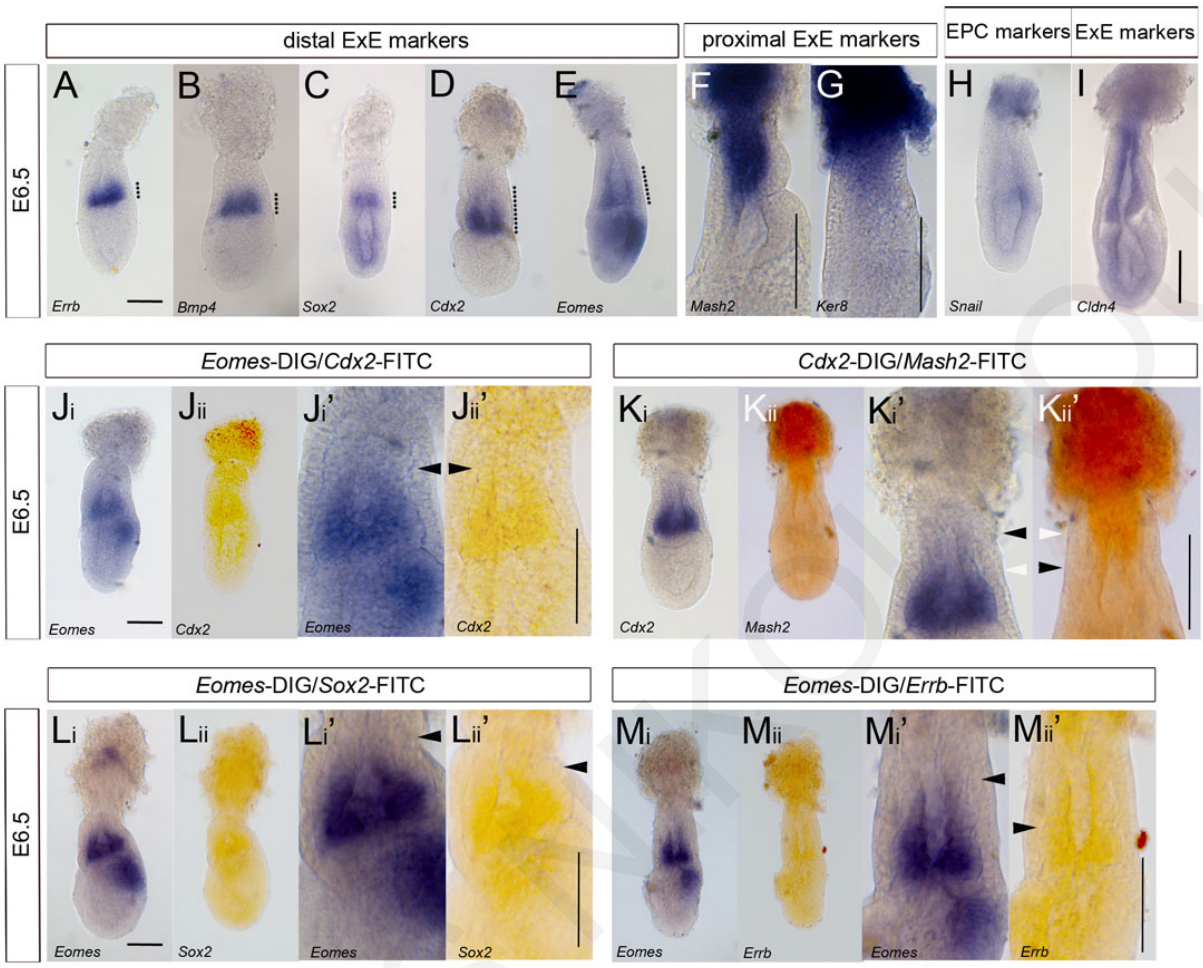

Figure 4.2.1: *In situ* hybridization analysis reveals that the E6.5 ExE is regionally divided into more than two regions. ExE at E6.5 displays distally localized expression of multipotency associated genes like *Errb* (A), *Bmp4* (B), *Sox2* (C), *Cdx2* (D) and *Eomes* (E) but the expression domain of *Cdx2* and *Eomes* is wider (dotted lines) and characterized by the existence of two subareas: a distally localized and strongly stained which is followed by a weakly stained subarea. Differentiation associated *Mash2* and *Ker8* display strong localization to the EPC and the proximal ExE but also display a region of weak staining distally to the proximal ExE (F and H). EPC and entire ExE can be distinguished by the expression of *Snail* (H) and *Cldn4* (I). Two color double *in situ* hybridization analysis reveals that although the expression domains of *Eomes* and *Cdx2* are largely overlapping (J_i – J_{ii}', black arrowheads indicate the edge of the expression domain), the expression domain of *Sox2* and *Errb* is more restricted than the one of *Eomes* (L_i – L_{ii}' and M_i – M_{ii}', black arrowheads indicate the edge of the expression domain). K_i - K_{ii}') Both *Cdx2* domain and *Mash2* domain are characterized by the existence of a strongly stained subarea (white arrowheads) and a weakly stained subarea (black arrowheads) which are largely overlapping. Gene expression positivity was verified in all samples examined (at least three embryos were used per experiment). Scale bars: 100 μm.

expression of validated EPC marker *Snail* (this work) (*Snail*; Fig. 4.2.1: H) and the validated marker of the entire ExE, *Cldn4* (this work) (*Cldn4*; Fig. 4.2.1: I**)**.

Our data show for the first time the existence of at least three, as opposed to two, regions within the ExE along its PD axis. This is based on the following. First, although some distal ExE marker genes like *Errb*, *Bmp4* and *Sox2* display a restricted and sharp expression domain (Fig. 4.2.1 A, B, C), the expression domains of *Cdx2* and *Eomes* appeared broader, suggesting that they extend more proximally (being stronger close to the epiblast and weaker proximally) than those of the former genes (Fig. 4.2.1 D, E, K_i, K'_i, L_i, L'_i). This suggestion was confirmed by two color (double) *in situ* hybridization analysis between *Eomes* - *Sox2* (Fig. 4.2.1: L_i, L_{ii}, L'_i, L'_{ii}) and *Eomes* – *Errb* (M_i, M_{ii}, M'_i, M'_{ii}) as in both cases, the expression domain of *Eomes* appears to extent further proximally than the expression domain of either *Sox2* or *Errb*. Importantly, using the same methodology, the expression domains of *Eomes* and *Cdx2* appear to coincide (Fig. 4.2.1: J_i, J_{ii}, J'_i, J'_{ii}). Furthermore, co-staining for *Cdx2* and *Mash2* indicated that the domains of these two genes overlap in the region of their weakest expression level (proximal end of *Cdx2* expression and distal end for *Mash2* expression) (Fig. 4.2.1: K_i, K_{ii}, K'_i, K'_{ii}). More extensive analysis using single color double *in situ* hybridization involving more combinations of genes, has revealed that the intermediate region is negative for *Bmp4* (Fig. 4.2.2: A and C), *Errb* (Fig. 4.2.2: D) and *Sox2* (Fig. 4.2.2: B) while it is weakly positive for *Ker8* (Fig. 4.2.2: A'), *Mash2* (Fig. 4.2.2: B', C', D') as well as for *Cdx2* and *Eomes* as this is verified by the undisturbed blue color presence across the entire ExE in double staining for *Mash2*-*Cdx2* and *Mash2*-*Eomes* (Fig. 4.2.3 A – A_{ib}' and B – B_{ib}').

Taken together, these data indicate for the first time that ExE can be subdivide into at least three regions along its PD axis, but not into two, as previously thought: distal ExE (marked by *Errb*, *Sox2*, *Bmp4*, strong *Cdx2* and strong *Eomes* expression levels), intermediate ExE (marked by weak *Cdx2, Eomes, Ker8* and *Mash2*) and proximal ExE (marked by strong *Ker8* and *Mash2* expression). This is summarized in the Table 4.1 shown below (this includes information about the EPC expression profile).

Table 4.1: List of genes and their expression domains in the E6.5 ExE and core EPC

	Errb	*Bmp4*	*Cdx2*	*Eomes*	*Cldn4*	*Mash2*	*Snail*
EPC	-	-	-	-	-	+	+
Proximal ExE	-	-	-	-	+	+	-
Intermediate ExE	-	-	+ (weak)	+ (weak)	+	+ (weak)	-
Distal ExE	+	+	+	+	+	-	-

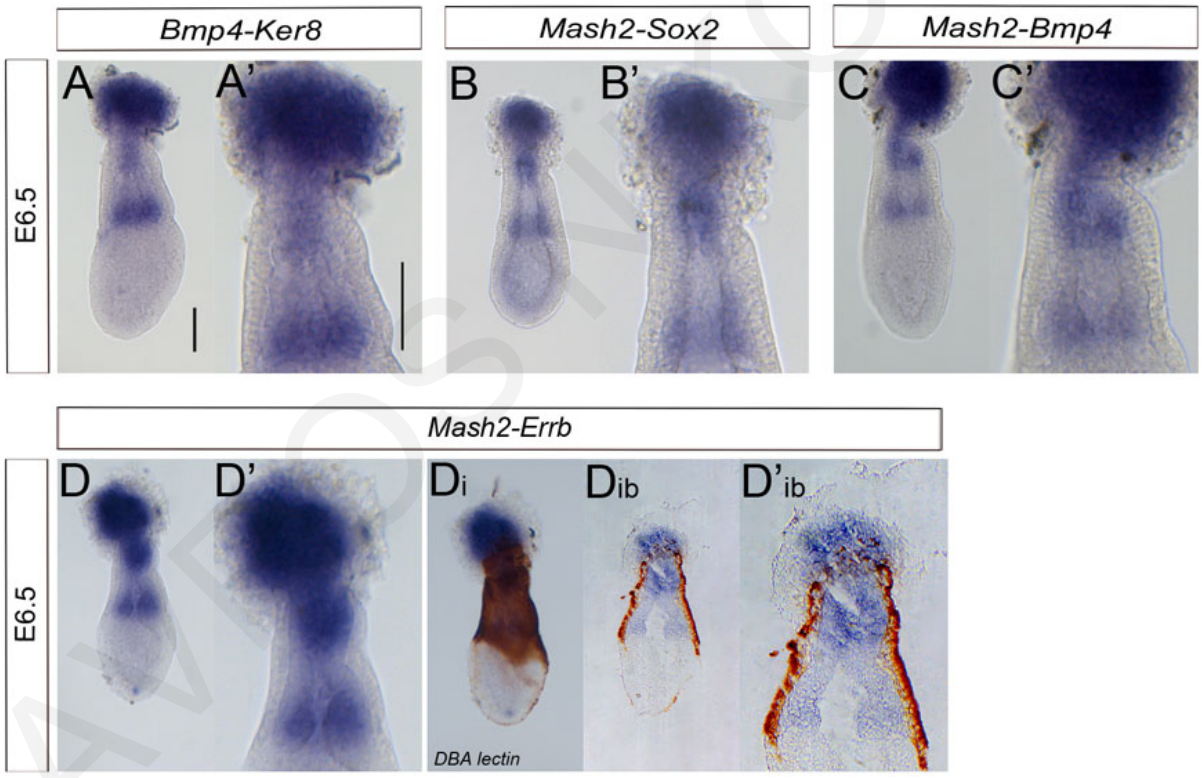

Figure 4.2.2: Existence of three transcriptionally distinct regions within the E6.5 ExE. A, A') single color double *in situ* hybridization analysis for *Bmp4* and *Ker8* has revealed the existence of a weakly stained, *Ker8* positive region in between the two strongly positive domains. B, B') The same approach was used to investigate the expression domains of *Mash2* and *Errb* with findings strongly suggesting the existence of a weakly *Mash2* stained region in between the two strongly positive domains. The same result was obtained when examining *Mash2* and *Bmp4* (C, C') as well as *Mash2* and *Errb* (D - D'$_{ib}$). n=3/3 per case. Scale bars: 100 μm.

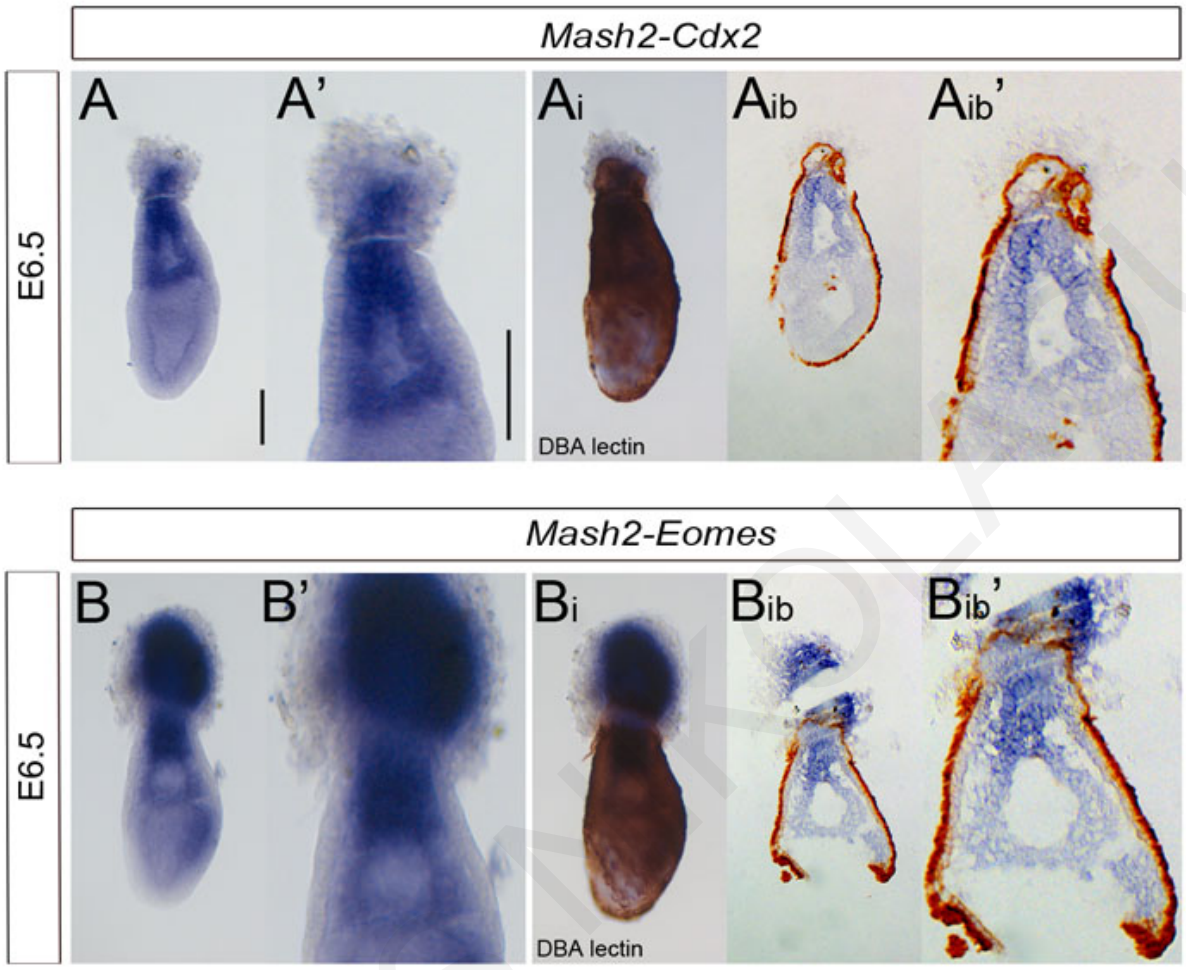

Figure 4.2.3: Intermediate ExE is characterized by *Cdx2* and *Eomes* positivity. Single color double *in situ* hybridization of either *Mash2* – *Cdx2* or *Mash2* – *Eomes* demonstrates the absence of a negatively stained area within the ExE (n=3/3 per case). Scale bars: 100 μm.

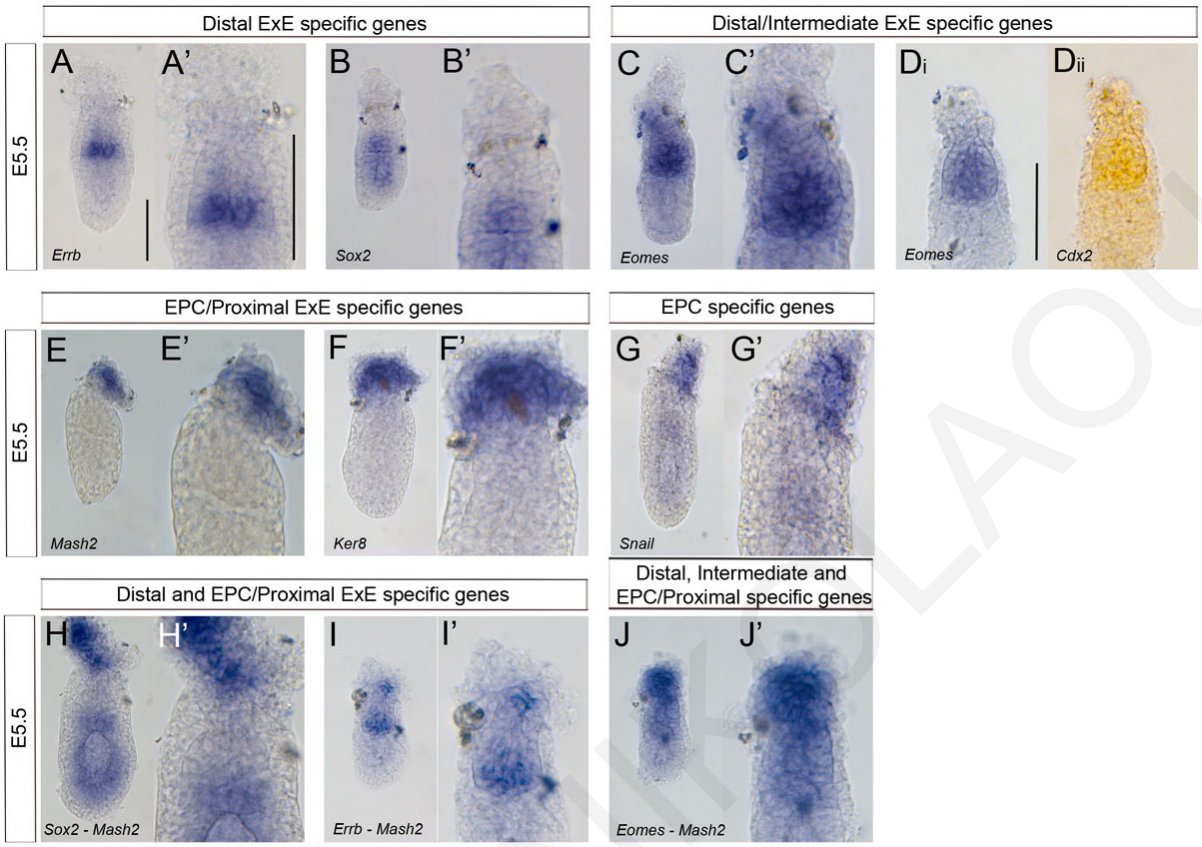

Figure 4.2.4: ExE at E5.5 is composed of two transcriptionally distinct regions. A and B) Distal half of ExE localization of *Errb* and *Sox2* at E5.5. C) Ubiquitous expression of *Eomes* in the E5.5 ExE. D_i, D_{ii}) The expression domain of *Eomes* mirrors the expression domain of *Cdx2* at the E5.5 ExE. *Mash2* (E) and *Ker8* (F) expression domain at E5.5 mirror the EPC-specific *Snail* domain (G). A region of ExE negative for *Sox2* (H) and *Errb* (I) but positive for *Eomes* (J) exists between the E5.5 ExE and EPC. n=3/3 per case except for *Eomes* - *Mash2* (n=4/4). Scale bars: 100 μm.

4.2.2. Results for specific aims 2 and 3 of aim 2: To investigate the sequence of appearance of distal, intermediate and proximal ExE regions (based on gene expression profiles shown in the previous section) and relate it to the timing of EPC formation. This was examined at E5.0 (a time before EPC formation), E5.25 (a time coinciding with the appearance of the EPC) and E5.5 (just after the EPC has formed).

First, we provide evidence that at E5.5, all trophoblast regions are present except proximal ExE. This because although *Errb* and *Sox2* are marking the distal half of E5.5 ExE, *Eomes* and *Cdx2* are expressed along the entire ExE, while both *Mash2* and *Ker8* are intensively expressed only in the EPC which is also *Snail* positive (Fig. 4.2.4: A -

F). Double *in situ* hybridization analysis suggests that there is a gap in the expression domains of *Sox2-Mash2* and *Errb-Mash2* (Fig. 4.2.4: H' and I'), however this gap is absent when we stain for *Eomes-Mash2* (Fig. 4.2.4: J'). Collectively, the data suggest that by E5.5, ExE is composed of two regions with transcriptional profiles of distal and intermediate ExE.

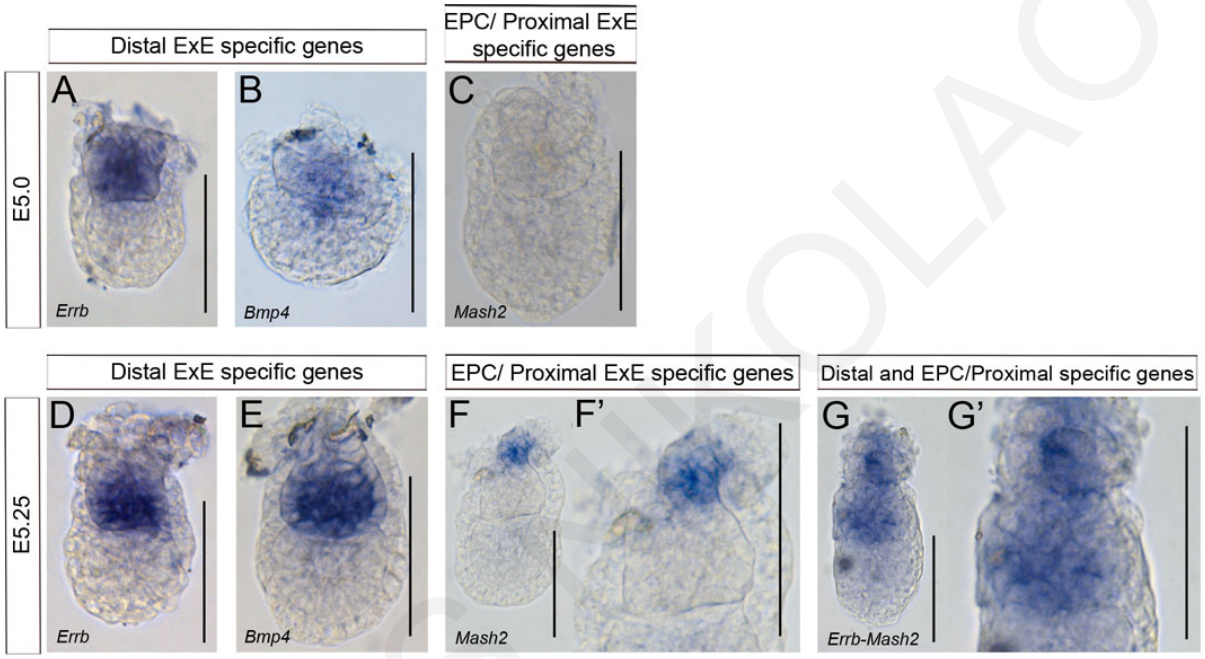

Figure 4.2.5: Early ExE is ubiquitously positive for distal ExE marker genes and is the source of EPC. A and B) Expression of *Errb* and *Bmp4* demarcates the entire ExE at E5.0. C) Absence of expression of the Proximal ExE-EPC marker gene *Mash2* at E5.0. D and E) Early EPC is negative for *Errb* and *Bmp4* but positive for *Mash2* (F, F'). G, G') The *Errb* demarcated early ExE is contiguous with the *Mash2* demarcated early EPC without any negative area in between the two tissues. n=3/3 except for E5.0 and E5.25 *Errb* (n=4/4 per case). Scale bars: 100 μm.

Second, our data support the notion that at E5.0, the entire trophoblast compartment consists of distal ExE character. This is because all trophoblast was positive for the distal ExE markers *Errb* and *Bmp4* (Fig. 4.2.5; A and B), but completely negative for the proximal and intermediate marker *Mash2* (Fig. 4.2.5; C). As expected, no morphological EPC was visible at this stage.

Third, since EPC froms from proliferation of the proximal edge of the first-formed ExE, our data obtained at E5.5 and E5.0 suggest that the EPC could be derived from ExE

with either distal or intermediate character. In order to address this, we performed single and double *in situ* hybridization at E5.25, the developmental stage when the EPC is forming from the proximal edge of the first-formed ExE (Robertson, 1942). Our results suggest that at E5.25, the entire ExE is positive for the distal ExE markers *Errb* and *Bmp4* (Fig. 4.2.5: D and E) and the EPC is strongly positive for *Mash2* (Fig. 4.2.5: F, F'). Double staining with *Errb* and *Mash2* probes revealed the absence of a gap between their expression domains, suggesting that the *Mash2*$^{+}$ EPC cells derive directly from *Errb*$^{+}$ distal ExE cells (Fig. 4.2.5; G, G').

4.2.3. **Results for specific aim 4 of aim 2:** To correlate the localization of Fgf and Activin/Nodal signaling in relation to our newly discovered ExE PD pattern (proximal, intermediate and distal ExE).

In order to correlate Fgf and Activin/Nodal signaling-responsive regions in the ExE with the corresponding ExE regions, we first needed to verify that the probes used were valid markers of their respective signaling pathways and if yes, we aimed to identify which of the trophoblast regions they are found.

Regarding the Fgf pathway, we cultured E6.5 embryos in serum free conditions (Drakou and Georgiades, 2015) for 8 hours in the absence (mock) or presence of 40uM of the FGFR inhibitor SU-5402 (Corson et al, 2004). Similar results were obtained with PD161570, another Fgf inhibitor (data not shown). The expression of the Fgf-responsive gene *Spry4* is normally localized to the epiblast and the ExE region closest to the epiblast (Fig. 4.2.6: A and Donnison et al, 2015). Under mock culture conditions, *Spry4* expression (using RNA *in situ* hybridization) appears to be unaffected (compare Fig. 4.2.6: A and B), whereas in the presence of inhibitor its expression is eliminated from the entire embryo (Fig. 4.2.6: C). Inhibitor treatment appears to be highly efficient as verified by Real Time PCR quantification of *Spry4* expression levels (Fig. 4.2.6: D). Similar findings were obtained in whole-mount immunofluorescence analysis, using the phosphorylated Erk (pErk), another indicator of Fgf signalling (Corson et al, 2004). It was found that Erk is phosphorylated in the ExE region closest to the epiblast, in the

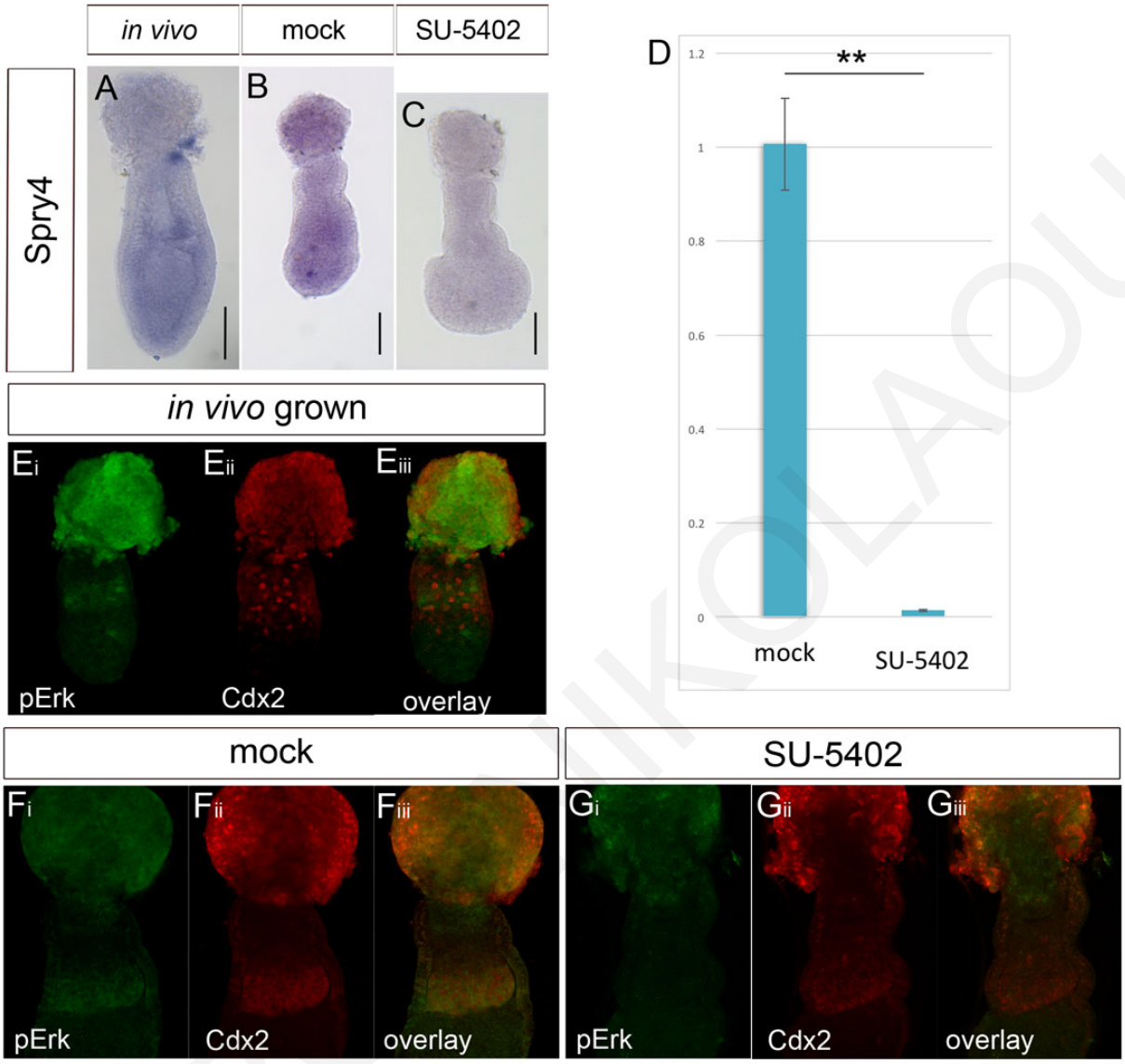

Figure 4.2.6: *Spry4* expression demarcates Fgf-responsive regions in the E6.5 embryo. A) *in vivo* grown E6.5 embryo displaying *Spry4* positivity in the epiblast and the ExE close to the epiblast (n=3/3). In the presence of 40 uM of the FGFR inhibitor SU-5402 in serum-free culture conditions for 8 hours, *Spry4* expression is completely abolished from all positive domains (B and C, n=2/2 per experiment). D) Quantification of *Spry4* with Real Time PCR verifies that *Spry4* expression is eliminated. Three samples of 4 pooled embryos per sample were used for this experiment, each sample was measured twice; data were normalized to *Gapdh* level. P<0.01. Scale bars: 100 μm. E_i) phosphorylated Erk marks the epiblast, the region of the ExE close to the epiblast as well as the entire EPC. The ExE-located pErk domain is more restricted than Cdx2 domain (E_{ii}, E_{iii}) n=3/3. The EPC-located pErk domain is independent of Fgf signaling and upon *in vitro* culture it seems to expand within the ExE region independently of the

presence of SU-5402. Cdx2 remains in the ExE after Fgf inhibition albeit at reduced level (F_i, F_{ii}, F_{iii} and G_i, G_{ii}, G_{iii}, n=3/3).

epiblast itself as well as in the EPC, consistent with previous reposrts (Fig. 4.2.6: E_i, Corson et al, 2004). In *in vivo* grown embryos, the localization of pErk within ExE appears to extend more distally than that of Cdx2 (Fig. 4.2.6: E_{ii}, E_{iii}). This pattern is also maintained after culture with the only difference being the expansion of the EPC-specific pErk region into the ExE (Fig. 4.2.6: F_i, F_{iii}). In the presence of SU-5402 however, the entire pErk positive region is eliminated except for the EPC-specific (including its expansion into the ExE) region which retains its pErk positivity (Fig. 4.2.6: G_i, G_{iii}). Our data are in agreement with those of other researchers (Corson et al, 2004) and strongly suggest that Erk phosphorylation in the EPC is independent of Fgf signaling. The reason for pErk expansion into the ExE is currently unknown, however it could be a side effect of the *ex vivo* culture because a similar finding was previously reported (Shimokawa et al, 2011). Interestingly, the Cdx2 positive domain is retained after inhibition, although signal intensity is weaker than the mock (Fig. 4.2.6: F_{ii}, F_{iii}, G_{ii}, G_{iii}).

Regarding the Nodal/Activin signaling, we used *Smad7* expression, which was previously shown to be an indicator of this signalling in TS cells (Erlebacher et al, 2004). Surprisingly however the *Smad7* expression has not been described in the ExE/EPC (Zwijsen et al, 2000). Our data show that *in vivo*, *Smad7* is ubiquitously expressed, displaying an intensively stained area in the ExE closer to the epiblast (Fig. 4.2.7: C). Upon DBA lectin staining, wax embedding and sectioning, a second, moderately stained area is uncovered at the periphery of EPC (Fig. 4.2.7: C_i and C_i'). In order to identify the Nodal/Activin responsive regions demarcated by *Smad7* expression, we cultured E6.5 embryos for 8 hours in serum-free culture medium, either in mock conditions or in the presence of 20uM of the ALK4/ALK7 inhibitor A83-01. *Smad7* expression in the mock embryos shows the same pattern of expression as in the *in vivo* grown embryos with the only difference being the enhanced ectopic expression of *Smad7* at the region of ExE closer to the EPC (Fig. 4.2.7: A, A_i, A_i').

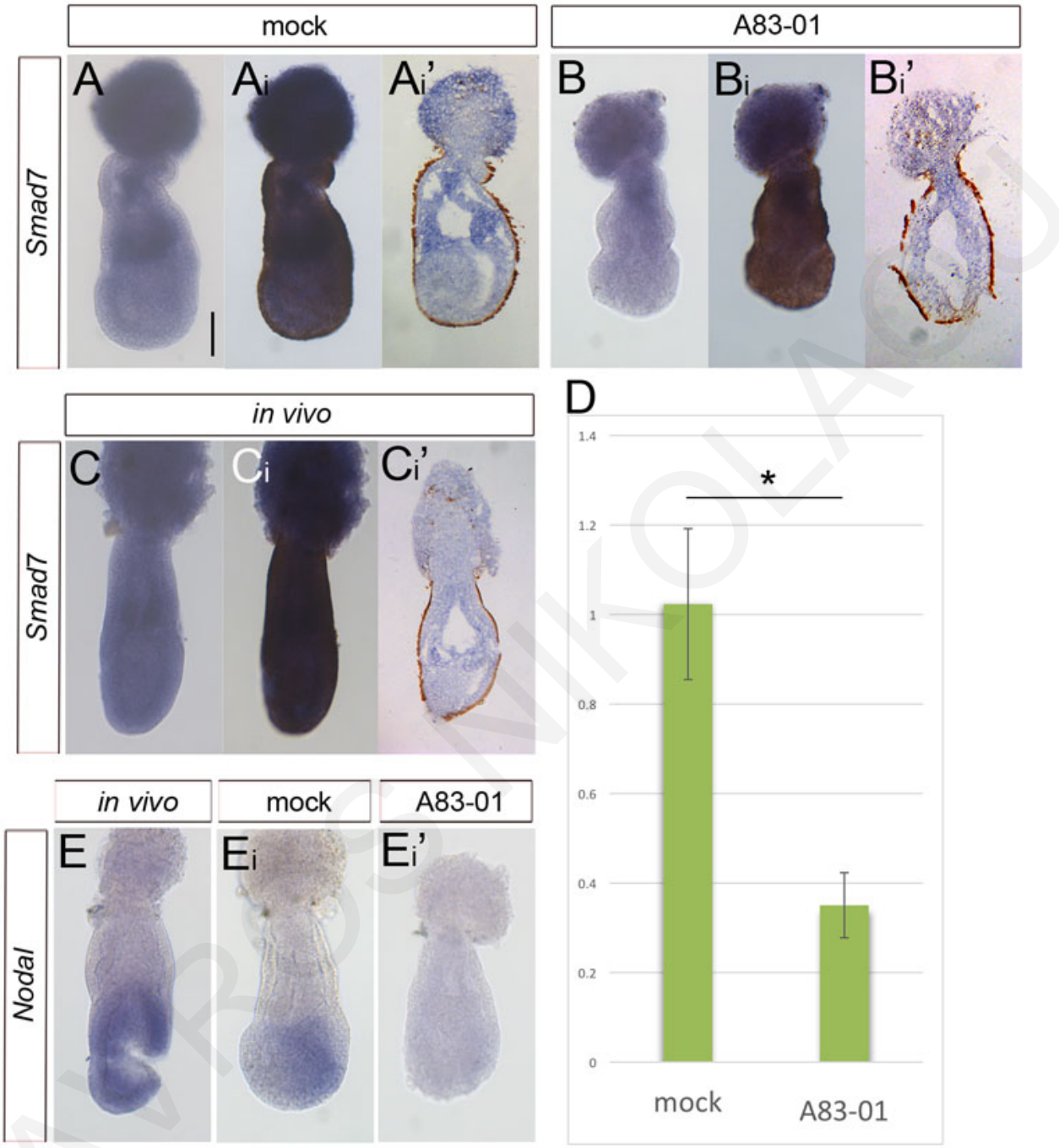

Figure 4.2.7: *Smad7* is a Nodal/Activin responsive gene. ExE and peripheral EPC but not core EPC respond to this signaling pathway. *Smad7* expression is ubiquitous along the entire E6.5 embryo with stronger expression in the region of ExE closer to the epiblast and the peripheral EPC (C, C_i, C_i', n=3/3). In order to identify the Nodal/Activin responsive domains of *Smad7* positivity, E6.5 embryos were cultured for 8 hours in serum-free mock conditions (A, A_i, A_i', n=2/2) or in the presence of 20uM of the Nodal/Activin inhibitor A83-01 (B, B_i, B_i' n=3/3). Embryos cultured in mock conditions display a similar expression pattern of *Smad7* except for the appearance of a strongly positive region of *Smad7* at the region of ExE in close contact

with the EPC. Expression in this region as well as in the core EPC remains unaffected in the presence of A83-01 but *Smad7* expression in the ExE, the peripheral EPC and the epiblast is attenuated. Real Time PCR supports these observations (D). The functionality of the inhibitor is further supported by a separate culture experiment demonstrating eliminated *Nodal* expression (an established Nodal/Activin responsive gene – Arnold and Robertson, 2009) in the presence of this compound (E, E_i, E_i', n=2/2 per case). Scale bar: 100 μm. For *in situ* hybridization experiments, three embryos were used per experiment. For Real Time PCR, three samples of four pooled embryos per sample were used, each sample measured in duplicate. Data were normalized to *Gapdh* level. $P<0.05$.

We assume that the reason for this discrepancy must the same as for the Erk ectopic phosphorylation under culture conditions. In the presence of A83-01 (Nodal/Activin signalling inhibitor), *Smad7* expression was highly diminished from the ExE and the peripheral EPC but persists in the core EPC and the region of ExE associated with this (Fig. 4.2.7: B, B_i, B_i'). The downregulation of *Smad7* expression levels in the presence of A83-01 was confirmed by Real-Time PCR and was found to be statistically significant (Fig. 4.2.7: D). As a second means of verifying the activity of the Nodal/Activin pathway in the ExE, we repeated the inhibitor treatment but performed whole-mount immunofluorescence analysis of pSmad2/3. We didn't observe any difference in the intensity or localization of the signal between mock and treated embryos (data not shown) and therefore did not pursue this further. Moreover, in order to use a second way to verify our data, the expression of the Activin/Nodal-responsive gene *Nodal* was assayed to verify the efficiency of the A83-01 inhibitor. It was found that indeed *Nodal* expression is eliminated in the treated embryos (Fig. 4.2.7 E, E_I, E_I').

The conclusion from the above set of experiments is that both Fgf and Nodal/Activin signaling are active in the ExE: the Fgf is exclusively restricted to the distal region of ExE while Nodal/Activin responsive area is broader and involves the entire ExE. In

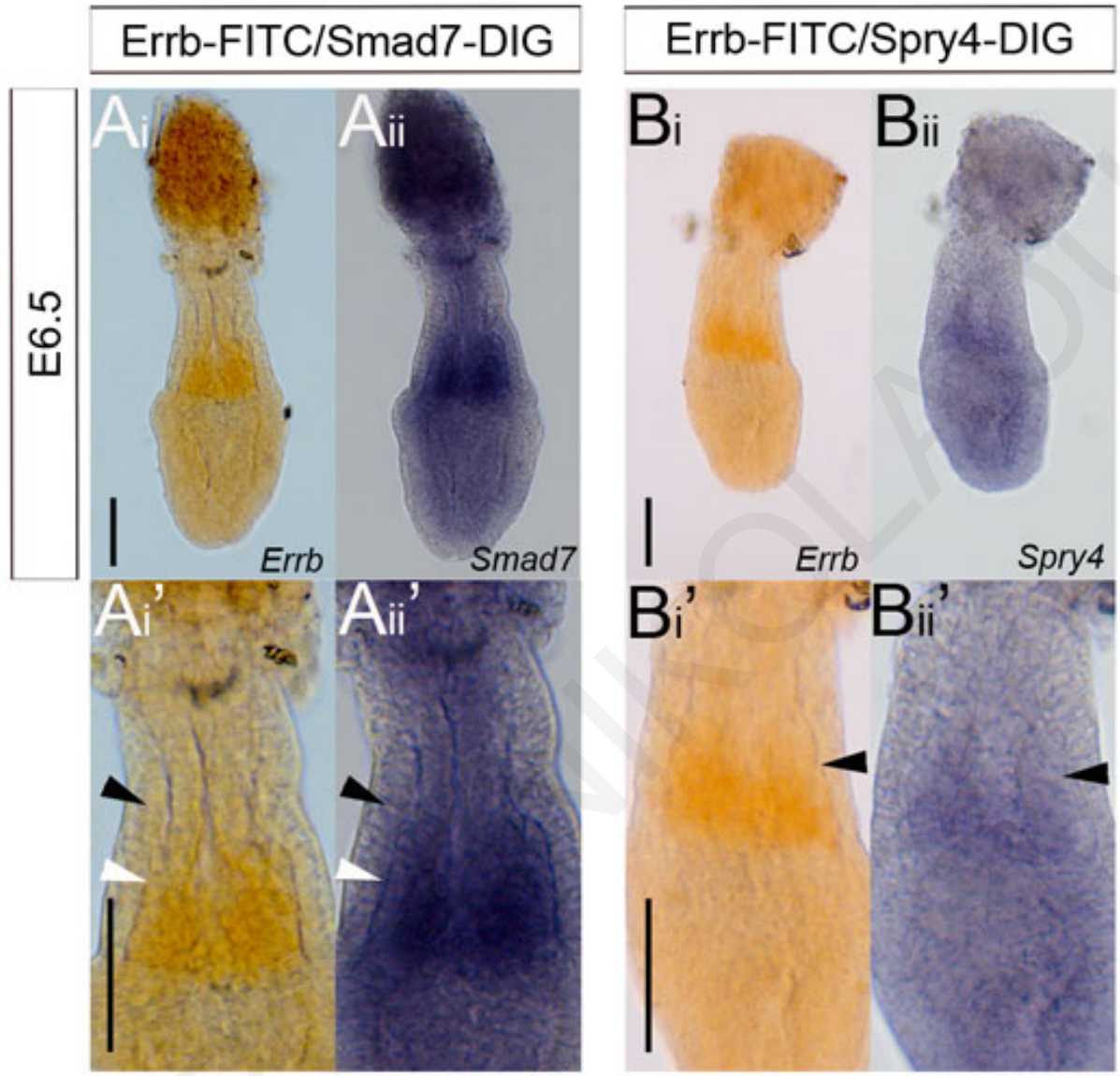

Figure 4.2.8: Distal ExE is strongly responsive to Fgf and Nodal/Activin while intermediate and proximal ExE respond only to Activin. Double color whole mount *in situ* hybridization for the Nodal/Activin responsive gene *Smad7* and the distal ExE marker *Errb* (A_i' and A_{ii}') shows colocalization of *Errb* and strong *Smad7* (white arrowheads). *Smad7* expression continues through the intermediate region of ExE albeit slightly reduced (black arrowheads) and even more reduced in the proximal ExE. In constrast, *Spry4* expression coincides with *Errb*. n=3/3 per case. Scale bars: 100 µm.

order to better describe this pattern, we sought to correlate this signaling responsiveness to our newly identified ExE regions (distal, intermediate and proximal). To this end, we performed double color whole mount *in situ* hybridization analysis for *Errb* – *Smad7* or *Errb* – *Spry4*. Our findings indicate that the *Errb*-positive distal ExE region is highly responsive to both Fgf and Nodal/Activin signaling (Fig. 4.2.8: A_i', A_{ii}', B_i', B_{ii}'). However, in contrast to the sharp disappearance of expression observed in *Spry4* proximal to distal ExE region, *Smad7* expression displays a gradual drop in expression, first to a less intensively stained ExE region which is followed by a weakly stained region. Collectively the data support a model where the distal ExE is highly responding to both Fgf and Nodal/Activin, while the rest of ExE is only responding to Activin with gradual drop in its responsiveness at its proximal region. EPC is not responding to either Activin or Fgf, except for its peripheral cells.

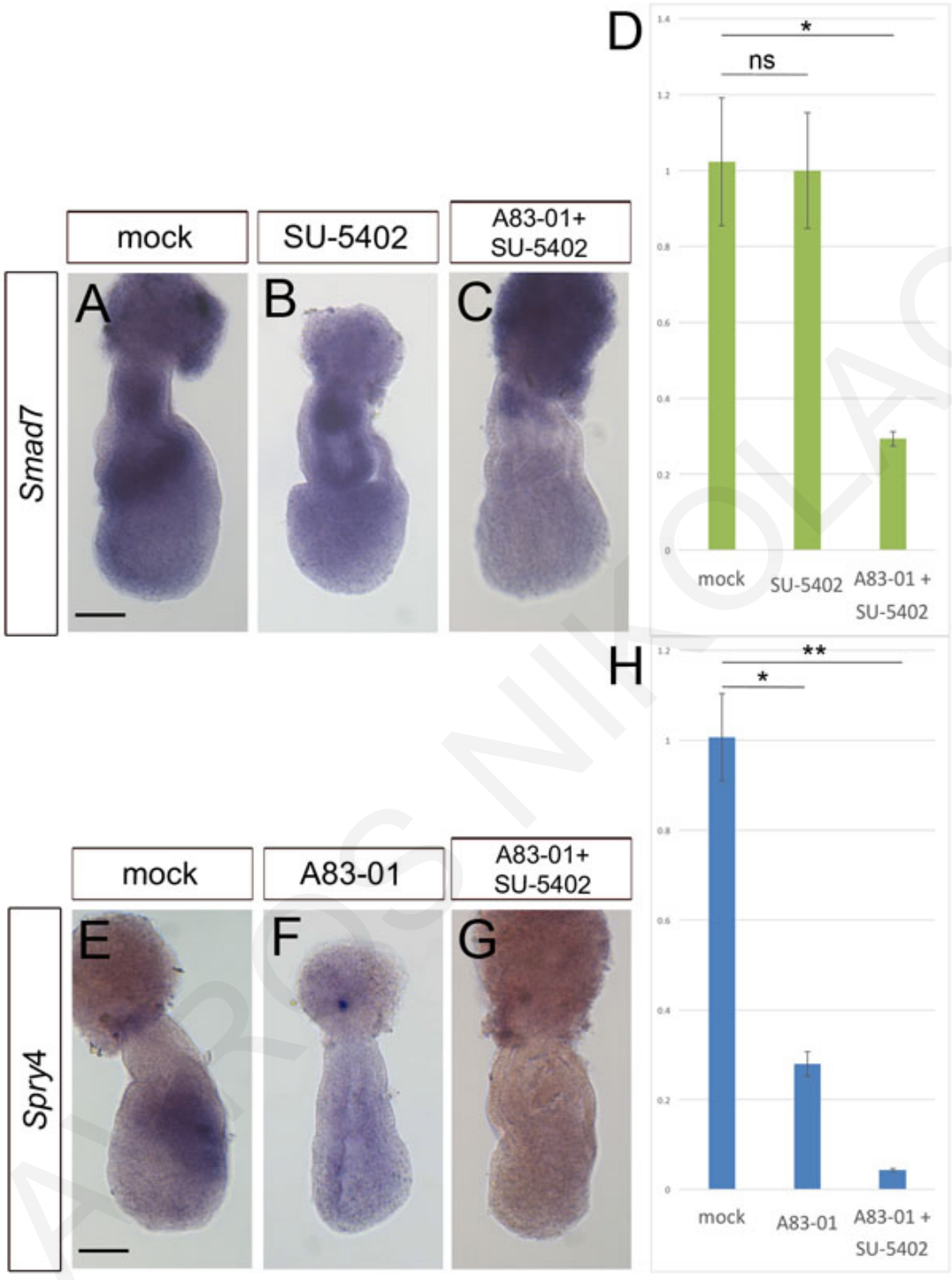

Figure 4.2.9: Fgf signaling attenuation does not affect Nodal/Activin responsiveness in the embryo but Activin signaling is necessary for embryo's responsiveness to Fgf. E6.5 embryos cultured for 8 hours in serum free culture medium in mock conditions (A and E) respond properly to both Nodal/Activin or Fgf signaling as verified by *Smad7* and *Spry4* expression (n=2/2 per case). The presence of 40uM of the Fgf inhibitor SU-5402 is not capable to affect Nodal/Activin responsiveness as *Smad7* expression level is unaffected (B and D, n=2/2). In

contrast, in the presence of 20uM of A83-01 (Nodal/Activin inhibitor), Fgf signaling is attenuated albeit not completely since there is detectable *Spry4* expression by both whole-mount *in situ* hybridization (n=2/2) and Real Time PCR (F and H). In the simultaneous presence of both inhibitors, both Activin and Fgf signaling pathways are eliminated (C, D and G, H, n=2/2). Scale bars: 100 μm. For Real Time PCR, three samples of four pooled embryos per sample were used, each sample measured in duplicate. Data were normalized to *Gapdh* level. Single star: P<0.05, double star: P<0.01, ns: not statistically significant.

4.2.4. **Results for specific aim 5 of aim 2:** To investigate the role of Fgf and Activin/Nodal signaling in the maintainance of ExE PD patterning.

Prior to investigating the effect of each these signalling pathways on ExE's pattern maintenance, it was necessary to investigate what occurs to each pathway when the other pathway is inhibited. By this we sought to investigate whether the two pathways are independently activated or they depend on each other for their activation. *In vivo* and *ex vivo* data using *Nodal* knockout embryos and explant cultures suggest that *Fgf4* expression is induced by *Nodal* (Guzman-Ayala et al, 2004). However, in the *in vivo* conditions, maternally supplied Activin or other factors could be masking the results while in the *ex vivo* conditions, unidentified and variable serum derived factors could lead to biases in findings (Uehara et al, 2009; Drakou and Georgiades, 2015). Hence, we reassessed the effect of the absence of one signaling pathway to the other one by using the FGFR inhibitor SU-5402 and the ALK4/ALK7 inhibitor A83-01. In addition, we sought to verify that when both inhibitors are administered simultaneously, both pathways are silenced. Interestingly, our data clearly demonstrate that after culturing embryos in the presence of SU-5402 for 8 hours, *Smad7* expression remains essentially undisturbed while in the presence of both inhibitors, as expected, *Smad7* expression levels drop significantly (Fig. 4.2.9: A, B, C and D). In contrast, exposure of embryos on A-8301 for the same time resulted to a significant drop to *Spry4* expression, indicating the presence albeit reduced of Fgf responsiveness (Fig. 4.2.9: E, F, H). As expected, in the simultaneous presence of both inhibitors, *Spry4* expression is eliminated (Fig. 4.2.9: E, G, H). Thus, it turns out that the elimination of Fgf pathway does not affect the Nodal/Activin pathway while the elimination of

Nodal/Activin reduces but does not totally eliminate Fgf pathway. In the simultaneous presence of both inhibitors, both pathways are simultaneously silenced. Importantly, the presence of any inhibitor, alone or in combination, did not show toxic effects because in a separate culture, embryos were left to grow in the presence of inhibitors for 24 hours without any signs of death (data not shown).

In order to investigate the effect of these signaling pathways on ExE's pattern maintenance, we cultured embryos for 12 hours in mock conditions, in the presence of A83-01, in the presence of SU-5402 or in the simultaneous presence of both inhibitors. Patterning defects were examined by whole-mount *in situ* hybridization for the distal ExE marker, *Errb*; the distal/intermediate ExE marker, *Cdx2*; the whole ExE marker *Cldn4*; the proximal ExE/EPC marker, *Mash2*; and for the EPC marker, *Snail*. The mock embryos displayed the wild type pattern with distally localized *Errb*, a bi-regional *Cdx2* with a strong and weak domain, an ExE-specific *Cldn4*, and *Mash2* expressed in both proximal ExE and EPC. *Snail* was also marking the EPC, albeit in most cases (3/4 embryos) it appears to expand within the ExE, as is the case for pErk and *Smad7* (Fig. 4.2.10: A - E). In addition, the ExE appeared to retain its polarized appearance until the area below the EPC (presumably a *Snail*$^{+}$ region) as shown by the polarized localization of Par6B (Fig. 4.2.11: A – D). In the presence of A83-01, our hypothesis was that since Nodal/Activin signaling is required along with Fgf signaling for the maintenance of the distal ExE character (Guzman-Ayala et al, 2004), in its absence, the distal ExE marker genes should be eliminated, and ExE would be differentiated. Our hypothesis was true because in the presence of A83-01, *Errb* expression was absent and *Cdx2* retained an expanded albeit weakly positive domain (Fig. 4.2.10: F, G). The undisturbed presence of *Cldn4* and *Snail* indicates that ExE retains its character and has not differentiated towards EPC phenotype (Fig. 4.2.10: H, J). In contrast, the weak *Mash2* domain has expanded towards the embryonic-extraembryonic junction (Fig. 4.2.10: I). These data strongly suggest that in the absence of Nodal/Activin signaling, ExE pattern is not maintained and distal ExE differentiates towards intermediate ExE while the other two ExE regions and the EPC remain undisturbed. This is in agreement to the polarized localization of Par6B observed under these conditions (Fig. 4.2.11: E – H). Strikingly, the same phenotype is seen when Fgf pathway is inhibited with SU-5402 (Fig. 4.2.10: K, O) and (Fig. 4.2.11: I – L). The combined data strongly suggest that both Fgf and Activin are required to be simultaneously active to the distal ExE in order to prevent it

from differentiating towards an intermediate ExE. In constrast, when both signaling pathways are inhibited, the entire domains of *Errb* and *Cdx2* disappear while the expanded *Mash2* is strongly expressed along the entire ExE. The expansion of *Snail* towards the entire ExE as well as the persistence of *Cldn4* in the ExE strongly suggests that in the absence of both signaling pathways, the entire ExE differentiates towards a core EPC phenotype. This is in agreement to the finding that under such conditions, ExE cells lose their polarized appearance and become apolar, as is indicated by Par6B localization (Fig. 4.2.11: M – P)

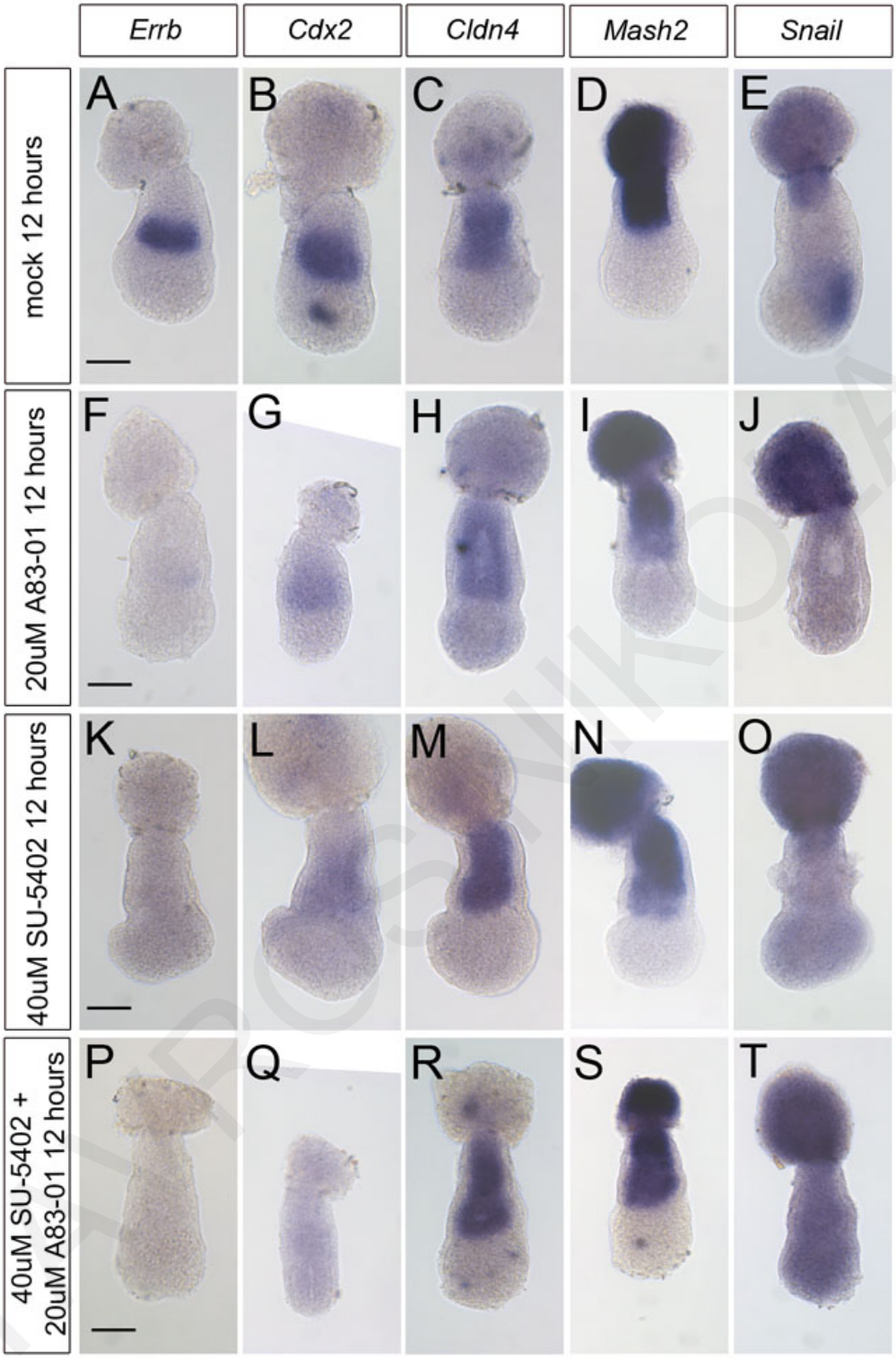

Figure 4.2.10: Simultaneous inhibition of both Fgf and Nodal/Activin signaling pathways is necessary for the entire ExE to differentiate towards core EPC. A – E) E6.5 embryos cultured in serum-free mock conditions for 12 hours retain their gene expression pattern, across the entire ExE and EPC except the ExE region close to the EPC which is positive for the EPC-specific *Snail*. In the absence of either Nodal/Activin (F - J) or Fgf (K - O) signaling pathways,

the distal ExE-specific *Errb* and strong *Cdx2* disappears while and expanded weak region of *Cdx2* (G, L) is obvious, along with an expanded weak *Mash2* (I, N) and absence of *Snail* (J, O). In the simultaneous absence of both signaling pathways, the entire ExE adopts a core EPC transcriptional profile as shown by the *Snail*, strong *Mash2* over the entire ExE and *Cldn4* positivity (T, S, R). n=3/3 per case. Scale bars: 100 μm.

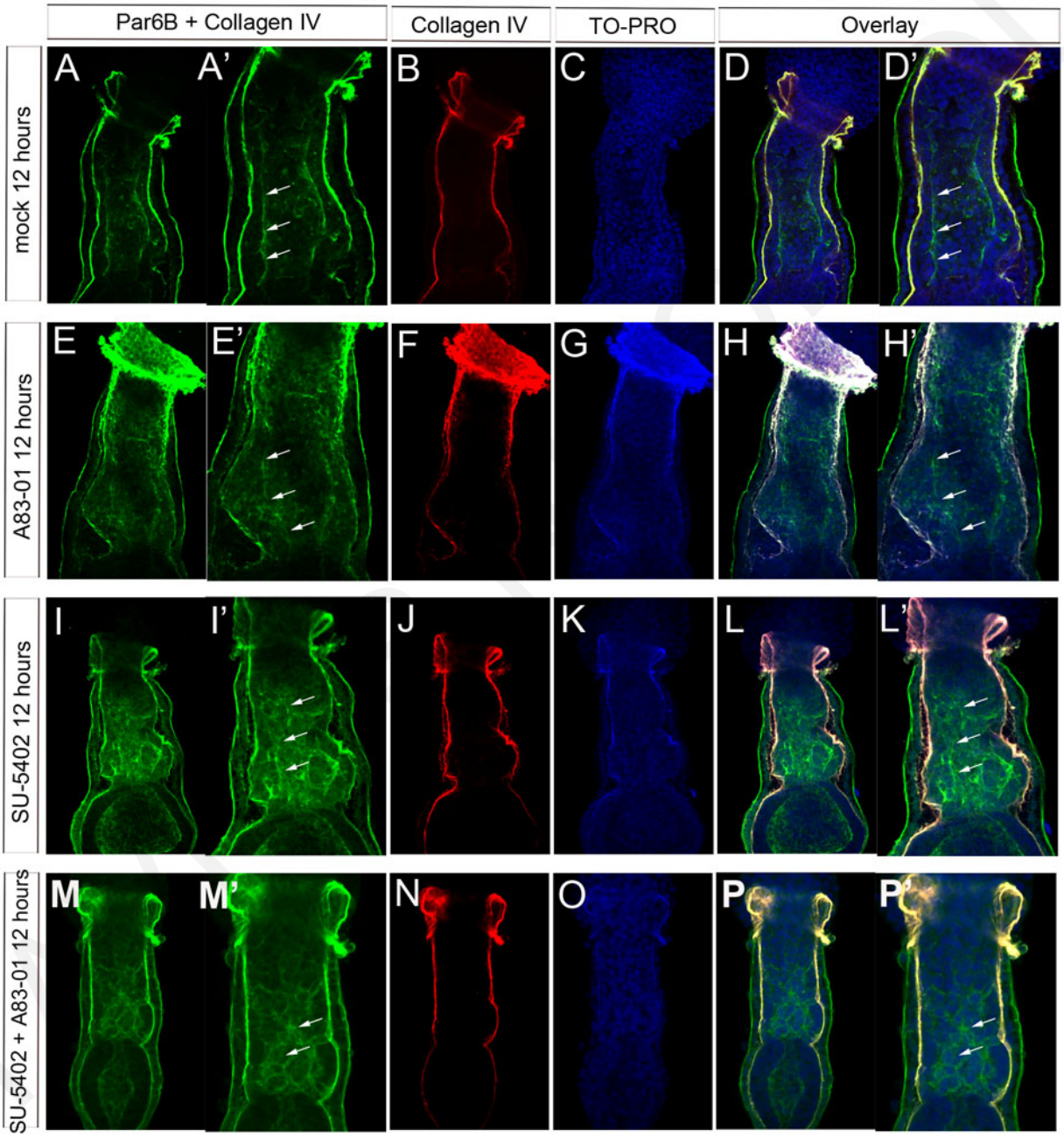

Figure 4.2.11: Simultaneous inhibition of both Fgf and Nodal/Activin signaling pathways is necessary for the entire ExE to lose its epithelial polarity. A – D) E6.5 embryos cultured in serum-free mock conditions for 12 hours retain their epithelial polarity, across the entire ExE except the ExE region close to the EPC. Arrows indicate the polarized distribution of Par6B at

the apical membrane of ExE cells. Epithelial polarity is maintained when either Nodal/Activin signaling (E - H) or Fgf signaling (I - L) is inhibited for 12 hours. Arrows indicate the polarized distribution of Par6B at the apical membrane of ExE cells. (M – P) Epithelial polarity of ExE cells is disrupted when both signaling pathways are inhibited for 12 hours. Arrows indicate the disrupted polarization of ExE cells as shown by the pericellular distribution of Par6B. n=3/3 per case.

4.2.5. Results for specific aim 6 of aim 2: To investigate the role of Fgf and Activin/Nodal signaling on the ability of distal ExE (the earliest ExE region to appear) to generate the other ExE regions as well as EPC.

Although it is known that both Fgf4 and Nodal/Activin are required for the maintenance of the distal ExE identity (see results in previous section), it is currently unknown how these pathways regulate the differentiation of distal ExE. Data obtained from this Thesis, suggest that distal ExE can give rice to EPC, intermediate ExE and proximal ExE. In addition, our data suggest that while distal ExE responds to both signaling pathways, EPC does not respond to any one and intermediate ExE/proximal ExE only respond to activin. This let us to hypothesize that in the absence of both signaling pathways, distal ExE will differentiate towards an EPC phenotype while in the presence of exogenously supplied Activin, distal ExE wil differentiate towards a proximal ExE phenotype. Although this hypothesis is supported by findings in trophoblast stem cells (Latos and Hemberger, 2016; Tanaka et al, 1998), other investigators have, in the past, examined the effect of Fgf and Nodal/Activin on the distal ExE (Guzman-Ayala et al, 2004) using explant cultures and found that both factors are necessary to simultaneously act on distal ExE in order to maintain its identity. In addition to this, they suggest that the presence of exogenously supplied Nodal in the culture medium has not any effect while the presence of Fgf alone is sufficient to prevent differentiation towards and EPC phenotype. However, their approach has several weaknesses. For example, these authors did not use a sufficient set of probes to correctly identify the existence of the several trophoblast regions, but instead used the proximal ExE/EPC marker gene *Mash2* as an exclusively EPC marker. In addition, during explant preparation, they left the VE attached on the explant, thus the possibility of VE-derived effect on the phenotype cannot be excluded. Importantly, since their culture medium

contained serum, the unwanted effect of a serum-derived factor on the observed phenotype, remains a serious possibility. In order to better address this question, we took advantage of the complete set of marker genes we have previously described in this Thesis and of the serum free culture conditions recently described for trophoblast stem cells (Kubaczka et al, 2014) as well as we enzymatically and mechanically removed the VE from all ExE explants prior seeding on matrigel-coated dishes (Fig. 4.2.12).

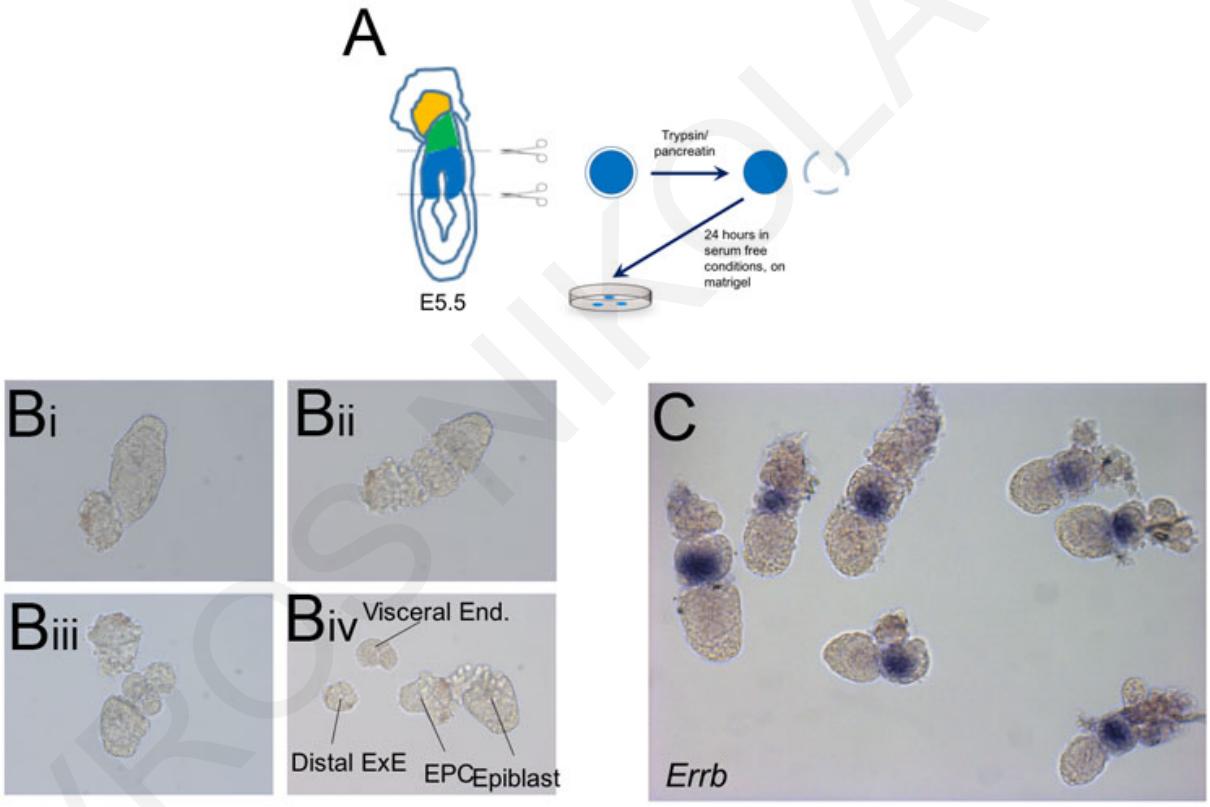

Figure 4.2.12: Microsurgery-based methodology for distal ExE explant derivation from E5.5 embryos. A) diagram depicting the followed methodology. B) series of pictures of the same embryo during the process of explant derivation. C) whole mount *in situ* hybridization for *Errb* on embryos stopped at step B_{ii}. In order to make sure that only uniformly *Errb*$^{+}$ explants were used, only smaller embryos were used for explant derivation.

Thus, the presence of exogenously supplied Fgf2 and Activin A for 24 hours was capable of maintaining the expression of multipotency associated genes like *Errb*, *Cdx2* and *Eomes*, the distal ExE marker gene *Bmp4* and the whole ExE marker *Cldn4* (Fig.

4.2.13: A - E) at the expense of *Mash2* and *Snail* (Fig. 4.2.13: F - G). In contrast, culture in the absence of both factors for 24 hours, resulted to differentiation towards an EPC-like phenotype as verified by the expression of *Snail*, *Mash2* and weak *Cldn4* (Fig. 4.2.13: L - N) and silencing of pluripotency associated genes (Fig. 4.2.13: H - K). The specification towards EPC differentiation appears to be a single step process and to occur early after the induction of differentiation because we could observe the same phenotype after culturing the explants for only 6 hours instead of 24 (Fig. 4.2.13: O - S). In contrast, when the explants were cultured in the absence of Fgf2 but presence of Activin, they were differentiated towards a proximal ExE phenotype because only *Cldn4* and *Mash2* were expressed, while *Snail* and multipotency associated genes were silent. The specification towards proximal ExE phenotype appears to be a two-step process as it involves a first step of differentiation towards an intermediate ExE followed by a second step of differentiating to the proximal ExE because explants cultured in the presence of Activin for only 6 hours, display an intermediate ExE-specific transcriptional profile (Fig. 4.2.13: AA - AF). Explants cultured in the presence of exogenous Fgf2 but not Activin for 24 hours, display differentiation towards EPC, which is the same case as in the absence of both factors. This discrepancy can be explained by the finding that Nodal/Activin signaling is required to maintain Fgf-responsiveness in the ExE and therefore the prolonged absence of Nodal/Activin rendered explants unable to respond to Fgf2 thus differentiating towards EPC. Indeed, *in vitro* data from TS cultures suggest that in the absence of Activin, *Fgfr2* expression drops 10-fold within 24 hours (Erlebacher et al, 2004)

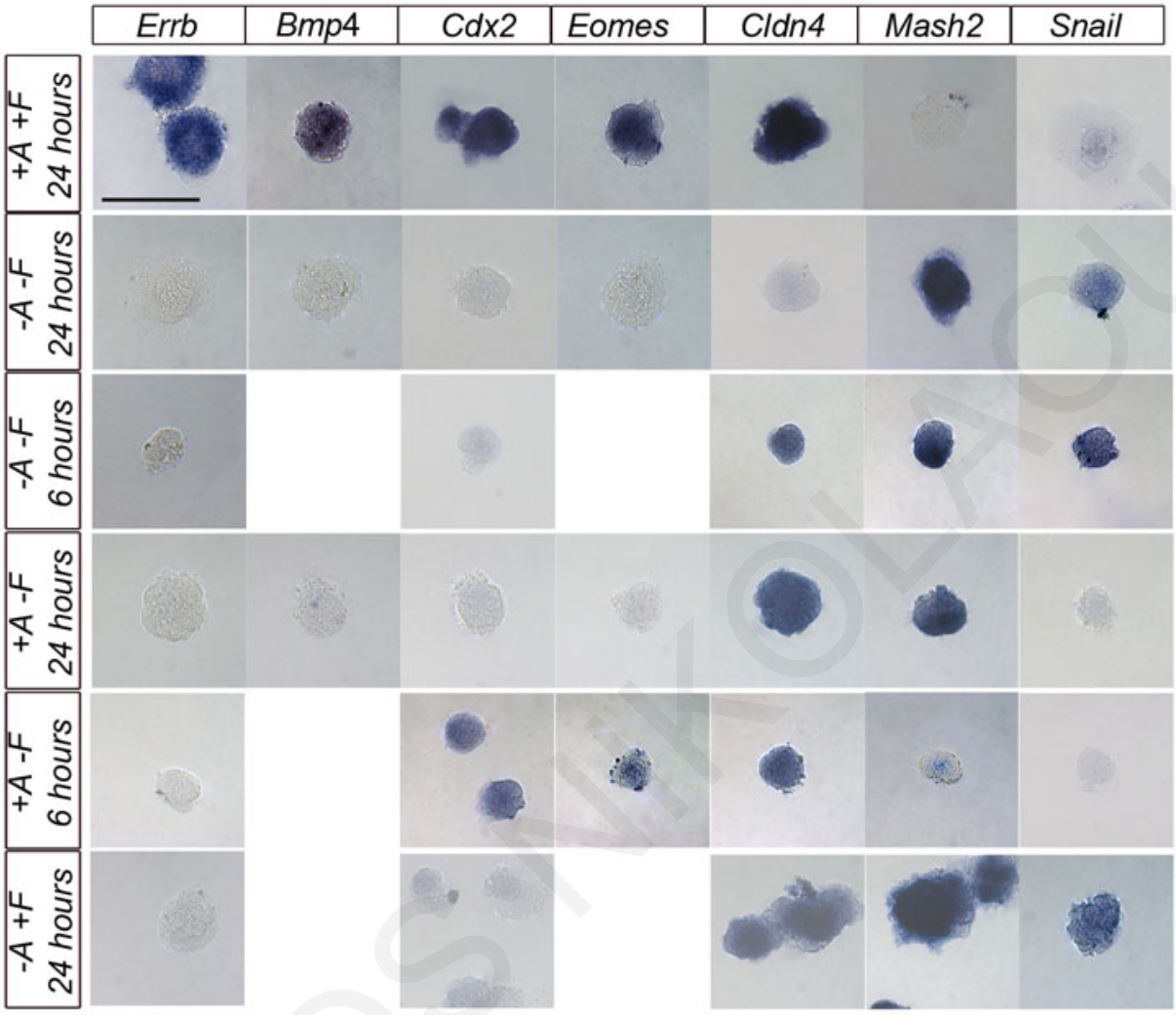

Figure 4.2.13: Distal ExE differentiates into core EPC in the absence of growth factors or into proximal ExE through intermediate ExE in the presence of Activin. A – G) distal ExE maintains the expression of the multipotency associated factors *Errb*, *Bmp4*, *Cdx2* and *Eomes* as well as the ExE-specific marker *Cldn4* in the presence of Fgf2 and Activin, while the expression of differentiation associated *Mash2* and *Snail* is silenced. H – N) In the absence of growth factors for 24 hours, or for only 6 hours (O - S) distal ExE differentiates into core EPC because it expresses *Mash2* and *Snail* but not *Cldn4*. (T - Z) In the presence of Activin for 24 hours distal ExE explants differentiate into upper ExE as shown by the expression of *Cldn4* and *Mash2* but absence of expression of *Snail* and multipotency associated genes. (AA – AF) The differentiation of distal ExE to proximal ExE involves a first differentiation step through an intermediate ExE as shown by the weak expression of Cdx2, Eomes and Mash2, strong expression of Cldn4 and absence of expression of *Errb* and *Snail*. (AG – AK) Presence of Fgf2 for 24 hours mirrors the culture conditions without growth factors. At least three distal ExE explants were seeded per well and all explants were hybridized with the same concentration of

probe and allowed the same time for color development (n=3/3 explants per case). Scale bar: 100 μm.

4.3.1. Results for specific aim 1 of aim 3: To use a lentivirus-based approach to develop a TS cell line that simultaneously expresses Ruby-fused F-actin (fluorescing at the red spectrum) and GFP-fused Histone H2B (fluorescing at the green spectrum).

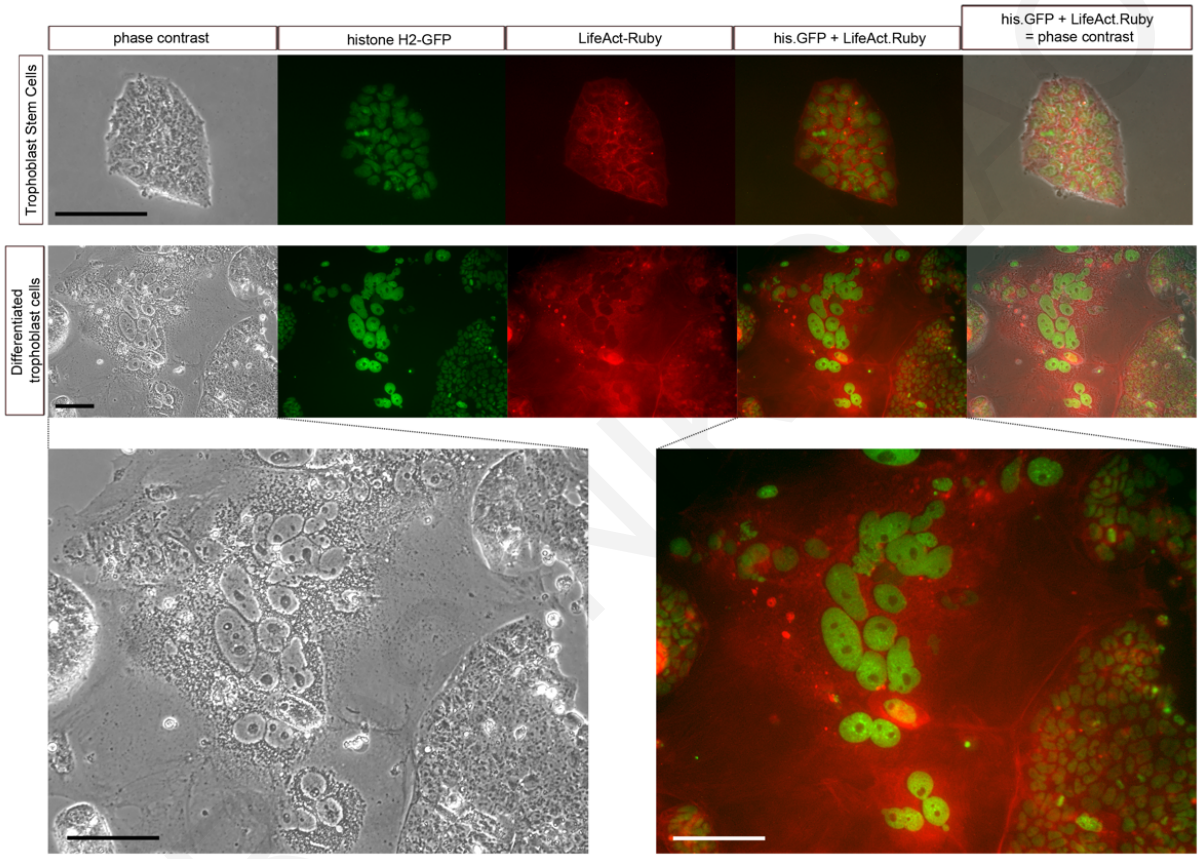

Figure 4.3.1: Double lentivirus-mediated transduction of TS cells for live cell morphology tracking. A - E) TS cells were transduced with lentivirus FG12.hisGFP followed by clonal selection and expansion. Then a second transduction step was followed with lentivirus PGK.LifeAct-Ruby.W (addgene #51009) followed by a second clonal selection and expansion. F – J) GFP and Ruby fluorescence are obvious at differentiated trophoblast cell types. F' and I' are high magnifications of F and I. Arrows show fibrillar Actin separating a syncytial cell from its neighbors. Scale bars indicate 50 μm.

TS cells represent a great tool for *in vitro* studies of trophoblast specification (review of Latos and Hemberger, 2016). The current approaches however involve gene expression studies requiring the biochemical extraction of the desired type of molecule,

and therefore sample destruction, accompanied by immunofluorescence studies on a different sample requiring fixation and sample preparation (Murray et al, 2016; Simmons et al, 2007). This approach however, lacks the ability to track dynamic processes like cell and nuclear shape/size change as well as chromatin increase as they happen. Moreover, although the scientific community currently enjoys a wealth of information regarding the transcriptional profile characterizing different trophoblast cell types, we know surprisingly little about their live morphology and, unfortunately, even less regarding their precursor cell types. In order to approach this challenge, we sequentially transduced TS cells with two lentivectors, capable of overexpressing a histone H2B-fused GFP (FG12.hisGFP – constructed by the writer during his M.Sc. Thesis, Kanda et al, 1998) and the small peptide lifeAct fused to the red fluorescing protein Ruby (PGK.LifeAct-Ruby.W - addgene #51009, Riedl et al, 2008; Kredel et al, 2009) respectively. Upon clonal selection and expansion, we were capable to derive a homogenous cell population of TS cells presenting a nuclear localized GFP with red fluorescence around their cellular periphery (Fig. 4.3.1: A - E). The expression and subcellular localization of both transgenes was maintained even in differentiated derivatives spontaneously appearing into the culture (Fig. 4.3.1: F - J).

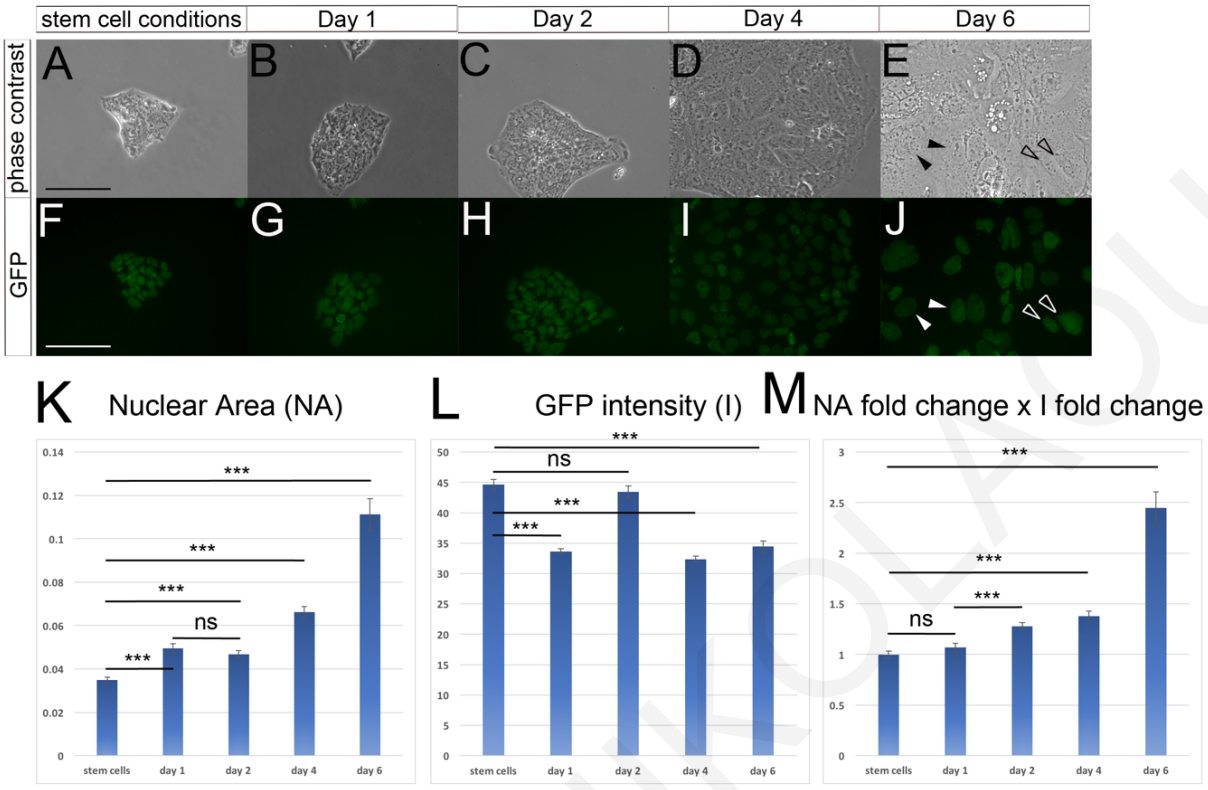

Figure 4.3.2: Morphological changes occurring during TS cell differentiation. A – E) phase contrast microscopy of random live TS cell colonies during differentiation, documented at the corresponding day. Filled and empty arrowheads correspond to the filled and empty arrowheads shown in J. F – J) nuclear GFP fluorescence of the corresponding cells shown in A – E, documented by exposing them under the same exposure (13.99 ms). Filled arrowheads in J show two nuclei of a similar size but different GFP intensity, empty arrowheads in J show two nuclei of different size but of similar GFP intensity. Scale bars indicate 50 μm. K) Nuclear area (NA) and L) mean GFP intensity (I) for each day of differentiation was measured using ImageJ. Mean nuclear area increases with advanced differentiation time while mean GFP intensity varies. However, during the second day of differentiation, nuclear size does not change significantly. M) Chromatin content increases with advanced differentiation but during the first day of differentiation it remains essentially the same as in control stem cells. n=253, ns=not statistically significant, P<0.001; Student's *t*-test (independent).

In order to examine the ability of this system to recapitulate the published behavior occurring during TS cell differentiation (i.e. giant cell formation characterized by gigantic cell size, expanded nucleus and increased chromatin content - Tanaka et al, 1998; Simmons et al, 2007), we induced the cells to differentiate by switching their culture

medium into a culture medium devoid of Fgf2 and Activin for 6 days, each time documenting random fields of view and returning the cells back to the culture incubator. Unfortunately, Ruby-stemmed fluorescence appeared extremely faint to be documented so we focused our efforts on the nuclear part of our study. As shown in figure 4.3.2, TS live morphology is altered during differentiation (Fig. 4.3.2: A and E). In addition, although TS nuclear size and fluorescence intensity varies by day 6 of differentiation (Fig. 4.3.2: F and J), overall, the nuclear size and chromatin content (measured as the product of nuclear fold change and intensity fold change) increases, thus our data are in agreement to published data (Fig. 4.3.2: K - M). Surprisingly, the granular morphology of TS colonies is maintained until day 2 of differentiation with a variability of morphological changes occurring after this day (Fig. 4.3.2: A, B, C and D, E). In addition, we observed a statistically significant expansion in nuclear size during the first day of differentiation which was not accompanied by a subsequent increase in chromatin content (which remained essentially the same as in control stem cells – Fig. 4.3.2: K - M). In contrast, nuclear size remains constant during the transition from day 1 to day 2 of differentiation but at the same time the chromatin content increases (Fig. 4.3.2: K - M).

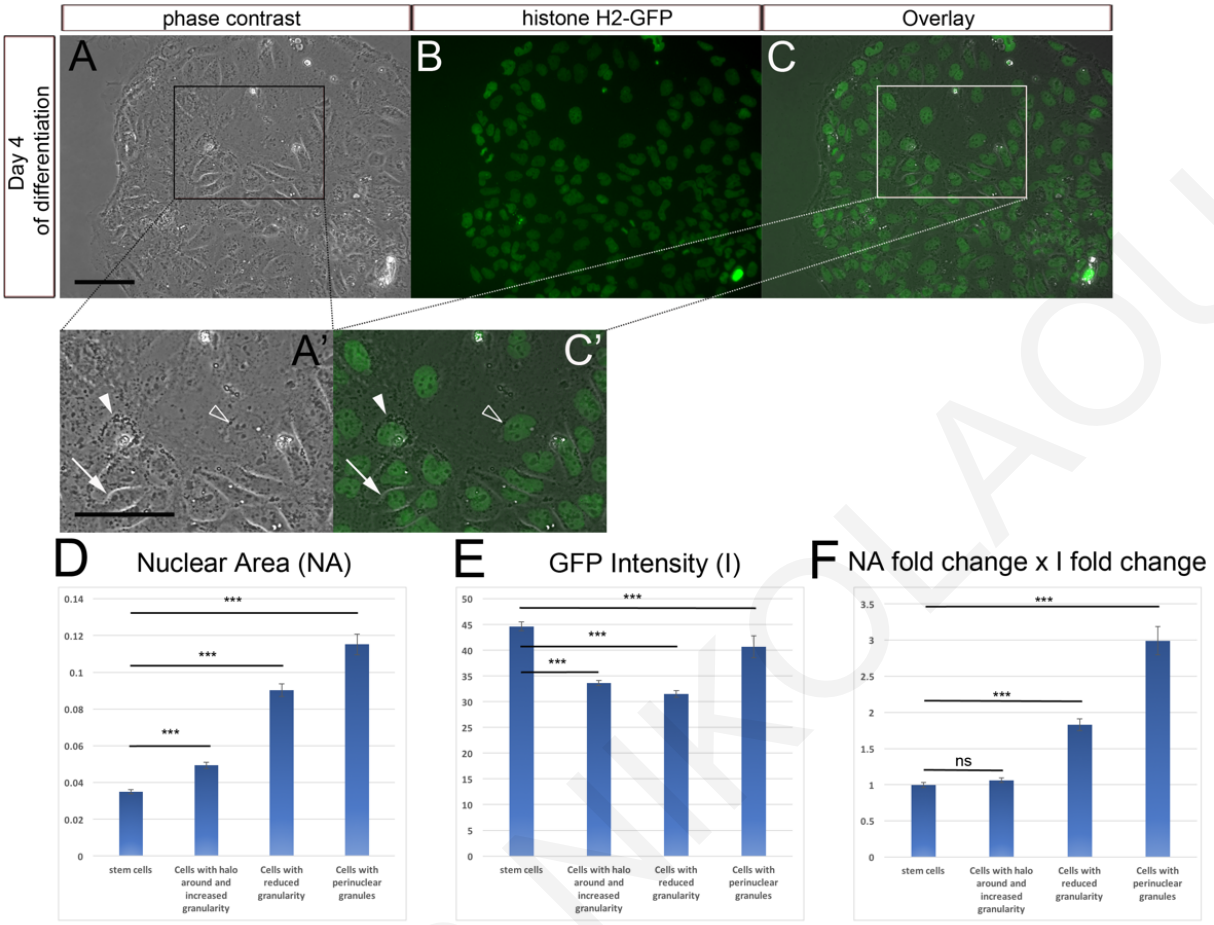

Figure 4.3.3: Different trophoblast cell types are obvious after four days in differentiation conditions. A) Phase contrast, live cell morphology of TS cells grown under differentiation conditions for 4 days. B) Nuclear GFP fluorescence of cells in A. C) Overlay of A and B. A' and C)' high magnification of the corresponding picture. Arrow depicts a granular cell with small nucleus and peripheral halo, empty arrowhead depicts a cell with big nucleus and reduced perinuclear granularity, filled arrowhead depicts a cell with big nucleus and increased perinuclear granularity. Scale bars indicate 100 μm. D) Nuclear area (NA) and E) mean GFP intensity (I) for each cellular morphology was measured using ImageJ. F) Cells with halo around their periphery have the same chromatin content as stem cells while the other two cell types display significantly increased chromatin content. n=33, ns=not statistically significant, P<0.001; Student's *t*-test (independent).

4.3.2. Results for specific aim 2 of aim 3: To use TS cells expressing GFP-fused Histone H2B to correlate changes in their nuclear size and chromatin content with live cell morphology, during their differentiation.

The variable morphological differences as well as the variability in nuclear sizes and GFP intensities, indicates the co-existence of different cell types after 4 days into the culture. Simmons and co-workers, 2007, have verified the existence of several trophoblast giant cell types in cultures of differentiated TS cells. Data obtained from immunofluorescence on histological sections have revealed that the several giant cell types differ not only in their transcriptional profile but also in their nuclear size and their chromatin content, with P-TGCs having the larger nuclei with the most chromatin content (Simmons et al, 2007). In addition, the commonly reported expression of *TpbpA* in differentiated cultures of TS cells strongly suggests the co-existence of SpT and/or GlyT cells (Tanaka et al, 1998, Donnison et al, 2015) which are diploid and proliferating (Mould et al, 2012). By day 4 of differentiation, we could identify three different morphologically distinguishable cell types: (i) granular cells with small nuclei and halo demarcating their cellular periphery, (ii) cells with big nuclei but reduced perinuclear granularity and (iii) cells with big nuclei and increased perinuclear granularity (Fig. 4.3.3: A - C). In all cases, their nuclear size was increased relative to the control stem cells (Fig. 4.3.3: D), however the chromatin content of the granular cells with halo appeared to be essentially the same as in control stem cells (Fig. 4.3.3: F). Because the other two groups of cells display enlarged nuclei and increased chromatin content, they must represent different types of giant cells. This is in agreement to the finding that cells with reduced granularity and big nuclei have less chromatin content than the cells with increased perinuclear granules (Fig. 4.3.3: F). Therefore, our findings, although preliminary, indicate that during early differentiation (one day in differentiation conditions) the nuclear area increases without concomitant increase in chromatin amount. Additionally, after 4 days in differentiation conditions, TS cells can be differentiated in at least 3 different cell types, based on live morphology and chromatin content.

CHAPTER 5:

DISCUSSION

5. Discussion

The data of this work are expected to make a significant contribution to the understanding of early trophoblast patterning, the ill-defined, but clinically significant initial phase of placenta formation using the mouse as a model. Specifically, we identified for the first time the boundary between ExE and EPC, the first two trophoblast compartments from which the entire trophoblast population of the mature placenta arises. This is an important prerequisite to the elucidation of the mechanisms of early trophoblast patterning, mainly because it allows the use of validated gene expression markers that define either the entire ExE or the core EPC. This study also shed new light on the patterning within ExE trophoblast with our discovery of at least three ExE regions at E6.5 (distal, intermediate and proximal), as opposed to the only two, as previously thought. Importantly, the data presented here support the notion that the first-formed ExE (E5.0) has a distal ExE character, which displays active FGF and Nodal/Activin signalling, and upon the removal of both of these signalings, this ExE region forms the EPC. In contrast, distal ExE forms proximal ExE (region with only Nodal/Activin signalling) through the transient formation of intermediate ExE, when only Nodal/Activin signalling is present.

Our findings allowed us to locate the boundary between ExE and EPC at the most proximal point of exVE cells, which coincides with the point where the RM inserts into the egg cylinder. This region was arbitrarily considered by some researchers to be the boundary between ExE and EPC (Rossant and Ofer, 1977), while some others used an ill-defined and untested morphological ‘constriction’ reported to exist between ExE and EPC as this boundary (Donnison et al, 2015).

The origin of the opaque nature characterizing the exVE after the E5.5 is not clear. It could be due to morphological alterations occurring in the exVE. The exVE cells are tall columnar epithelial cells containing several microvilli, in contrast to emVE cells (Kawamura et al, 2012). In addition to this, exVE, in contrast to emVE cells display localization of several molecules like F-actin in an apical shroud (Trichas et al, 2011). Unfortunately, it is currently unknown whether exVE already has microvilli and a shroud of apical F-actin already from the E5.5 stage or it adopts that at some later point.

The presence of a 'neck' region in the exVE has been identified by Ninomiya and coworkers in the past (Ninomiya et al, 2005). These researchers have found that the VE at the neck region is positive for *Sparc* expression, a gene encoding for a major constituent of the RM. However, these authors did not examine the relationship between the level of insertion of RM and the proximal edge of this 'neck', as we have done in this study (Inoue et al, 1983; Miner et al, 2004).

Our explant cultures strongly suggest that we have correctly localized the exact boundary between ExE and EPC since in the presence of culture conditions that are expected to maintaine ExE, but not EPC, character, the latter differentiates into its derivative tissues while the former retains its initial character (Rossant and Ofer, 1977). Known EPC derivative tissues are the trophoblast giant cells (TGCs), demarcated by *Pll* expression. The absence of *Pll* in our explant after 24h, but not after 4 days, culture is likely to be due to the insufficient time of culture under these conditions. This is because when the explants were cultured for longer time, morphologically giant cells had appeared. This finding is in agreement with the behavior of TS cells during differentiation where the *Pll* induction is a late event (Tanaka et al, 1998). In addition to *Pll* we show for a first time that *Secretin*, a gene previously reported to be a marker of the entire EPC (Pearton et al, 2014), is actually a central EPC derivative. This is because its expression appears in the E6.5, but not the E5.5 EPC and only in a subregion (central area) of the latter. Importantly, although this is the first time ExE explants are used in the presence of matrigel in chemically defined conditions, these conditions were sufficient to maintain ExE character as verified by the presence of *Erf* and absence of *Snail*. This was expected, since the same conditions were used for the maintenance of TS cells (Kubaczka et al, 2014). *Erf* and *Snail* gene expression is a valid marker of ExE and EPC respectively, since their expression domains were shown here to respect the point of RM insertion.

In addition to marker gene expression studies, we verified that apico-basally polarized trophoblast cells (an ExE characteristic) exist up to the RM insertion point. Proximally to this point, trophoblast cells appear to be non-polar (an EPC characteristic). Although our functional studies were focused on the E6.5 stage, our data are also applicable to

the E5.5 stage, as the point of RM insertion was found here to also coincide with the proximal limit of polarized ExE cells at E5.5.

Patterning in the ExE has been studied in the past by other workers which concluded that ExE is composed of only two regions, proximal and distal halves (Donnison et al, 2015). These authors used the distance of the embryonic-extraembryonic junction as a measure of the PD extent of ExE expression domains of several genes. However, this approach may not be reliable because the overall PD length of ExE varies between littermate embryos or between embryos of different developmental stage. Our data extend their findings in that we have identified a third region between the two previously known distal and proximal ExE halves. There were several indications for the existence of that region coming from *in vivo* and *in vitro* data: In embryos, the expression domain of either *Eomes* or *Cdx2* was longer than the domain of *Sox2* (Adachi et al, 2013; Donnison et al, 2015) while in differentiating TS cells, *Cdx2* and *Eomes* present a milder drop of their expression levels than *Errb* and *Sox2* (Donnison et al, 2015; Latos et al, 2015). Specifically, within 12 hours of differentiation induction in TS cells, the expression levels of *Cdx2* and *Eomes* appear to drop at ~50% of their initial levels while the expression of *Sox2* is diminished. Importantly, at the same time, the expression of *Mash2* appears to be at ~50% of its maximum. Our *in vivo* data strongly agree with these because *Errb*, *Sox2* and *Bmp4* present an abrupt expression domain while *Cdx2* and *Eomes* show a region of weak expression proximally to a region of strong expression. In addition, this region is also positive for weak *Mash2* staining.

The appearance of these regions during embryogenesis appears to follow a stepwise model with the distal region being the first to appear, followed by the intermediate and lastly by the proximal region. Furthermore, the distal region is the source of the early EPC tissue. Evidence coming from *in vitro* data supports this finding: when TS cells (whose transcriptional profile appears to mimic that of distal ExE) are induced to differentiate, they are preferentially differentiating towards the EPC pathway (Latos and Hemberger, 2016).

In order to investigate the Nodal/Activin and FGF signaling pathways regulating early trophoblast patterning along its PD axis, we first had to associate the responsiveness

to these pathways in relation to the three ExE regions. Although the Fgf responsiveness has been investigated in the past and found to be at the region of ExE close to the epiblast, whether both distal and intermediate or only distal ExE responding to it was unknown before this work (Donnison et al, 2015; Shimokawa et al, 2011). In addition to this, information regarding the Nodal/Activin responsiveness was largely unexplored. Our use of *Smad7* expression as a marker for this signaling pathway was useful since it was previously used in trophoblast stem (TS) cells to indicate Nodal/Activin signaling (Erlebacher et al, 2002). Our findings show that the distal ExE is strongly responsive to both Fgf and Nodal/Activin pathways, intermediate and proximal ExE respond to Activin but not to Fgf and EPC does not respond to any of the two pathways. In addition to this, we found that Fgf responsiveness was positively regulated by Nodal/Activin signaling. Whether this is via regulating ligand or receptor expression/availability or both, is currently unknown but data from others indicate that both scenarios might be true. For example, Guzman-Ayala and coworkers, 2004, had found that Nodal induces the expression of *Fgf4* in the epiblast while at the same period Erlebacher and coworkers suggested that Activin induces the expression of *Fgfr2* in trophoblast stem cells (Guzman-Ayala et al, 2004; Erlebacher et al, 2004). However, our findings show that at least for a period of 8 hours post Nodal/Activin inhibition, *Spry4* is still expressed in the ExE, albeit at low levels; in order to totally eliminate both pathways is required to inhibit both of them simultaneously.

The effect of Fgf signaling on the maintenance of ExE patterning has never been tested mainly because *Fgf4* knockout embryos die around postimplantation (Feldman et al, 1995). In contrast, *Nodal* knockout embryos examined at E6.5 lack *Bmp4* expression and have their entire ExE being *Mash2* positive (Brennan et al, 2001; Guzman-Ayala et al, 2004). Based on that, these authors had concluded that in the absence of Nodal, ExE differentiates into EPC; this however might not be true because (i) since *Mash2* positivity marks intermediate (weakly) and proximal ExE in addition to EPC, they didn't use a sufficient number of marker genes to better investigate this defect, (ii) although unlikely, it is possible that traces of Fgf responsiveness might had remained in the ExE due to incomplete silencing of *Fgf4* in the epiblast and (iii) it is possible that maternally derived Activin had masked the *Nodal* knockout phenotype. The use of the chemically defined *in vitro* culture system recently described by Drakou and Georgiades, allowed

us to overcome these limitations (Drakou and Georgiades, 2015). Hence, we concluded that both Fgf and Nodal/Activin signalling pathways are required for the maintenance of ExE's pattern, as in the absence of one of the two, the distal ExE becomes intermediate ExE while proximal ExE remained unaffected. The differentiation of ExE towards EPC required the simultaneous absence of both pathways.

Having verified the necessity of both signaling pathways for the maintenance of ExE pattern, we sought to investigate their effect on the behaviour od distal ExE iteslf. Other researchers had addressed this question in the past by using ExE explants cultured in the presence or absence of Fgf and Nodal/Activin (Guzman-Ayala et al, 2004). However, their explants were not purely composed of ExE cells since they were not denuded from their surrounding exVE layer. Furthermore, they were cultured in serum containing medium, thus making the masking of their results by unknown serum factors a possible scenario. In order to avoid these limitations, we used distal ExE explants denuded from their surrounding exVE layer and cultured under chemically defined conditions in the presence of matrigel (Kubaczka et al, 2014), as we did for proximal ExE explants. Our findings suggest that distal ExE cells differentiate into EPC cells quickly in the absence both Fgf2 and Activin proteins, while in the presence of Activin and absence of Fgf2, they differentiate towards proximal ExE via intermediate ExE. In the presence of Fgf2 and absence of Activin, unexpectectly, our explants seem to behave like in the absence of both factors and they differentiate towards EPC. Although this unexpected phenotype needs more investigation, one possible scenario could be that in the absence of Activin, distal ExE explants fail to respond to Fgf signaling thus behaving as in the absence of both. Our findings are in contrast to the findings of Guzman-Ayala and coworkers. For example, these authors had found that the presence of Fgf4 alone, was sufficient to prevent the expression of *Mash2* while in our hands this was never true. Furthermore, they found that in the presence of Activin alone, explants were behaving like in the absence of both factors (Guzman-Ayala et al, 2004). These discrepancies might stem from the incomplete set of marker genes they had used (for example in the case of Activin, they should also investigate the expression of *Snail* and *Cldn4*) and the presence of exVE and serum in the culture medium. Our data are in agreement to data obtained from *in vitro* studies because in the absence of both pathways TS cells differentiate into EPC derivatives while in the

presence of Activin, they differentiate into chorion, the derivative of proximal ExE (Latos and Hemberger, 2016). Taken together our data, we were able to derive a new model for trophoblast development during early embryogenesis and a model of the molecular mechanisms regulating this (Fig. 5.1)

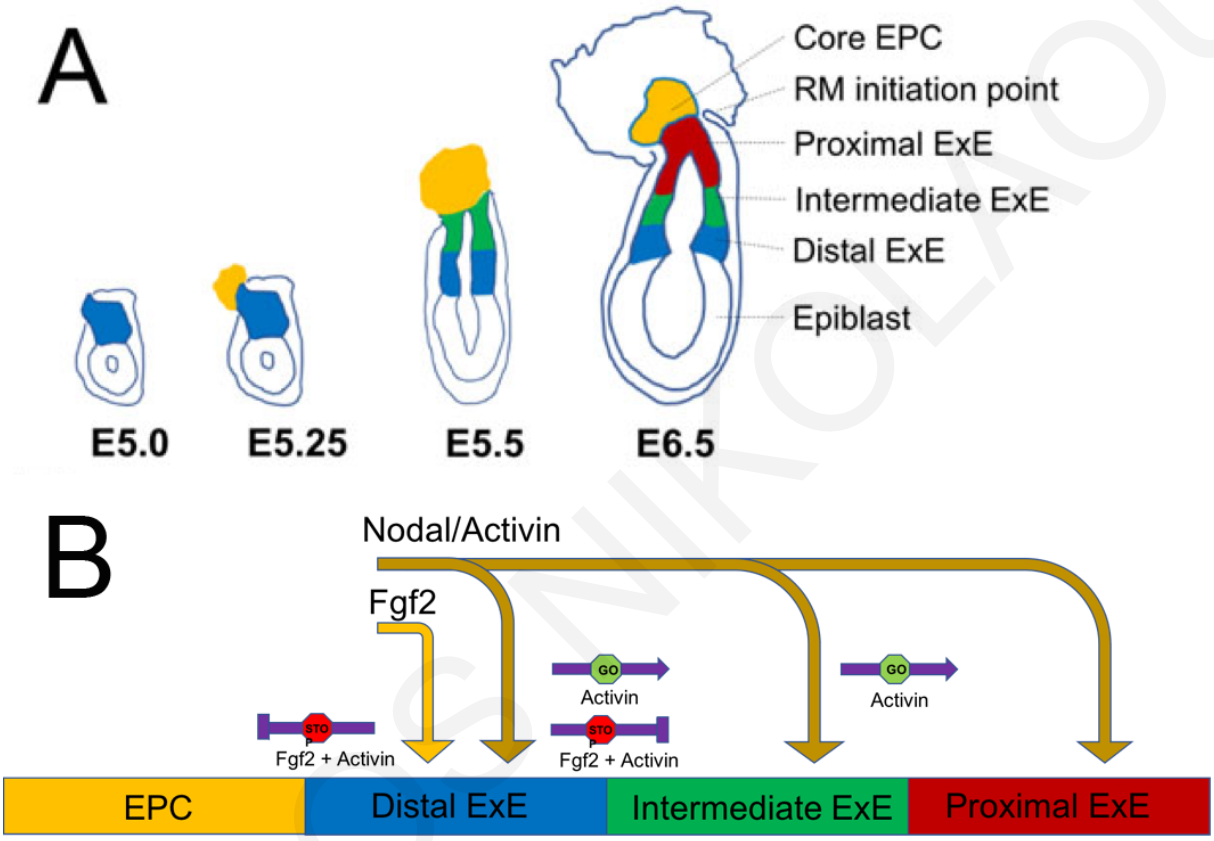

Figure 5.1: Novel model of early trophoblast development and the signaling pathways regulating it. A) Soon after implantation (E5.0), the trophoblast is entirely composed of a transcriptionally uniform epithelial tissue, the distal ExE. A few hours later (E5.25), distal ExE gives rise to the core EPC while at the same time it maintains itself. By E5.5, the distal ExE gives rise to intermediate ExE while at the same time it maintains itself. The core EPC has grown in size. At the gastrulation stage (E6.5), intermediate ExE gives rise to the proximal ExE and the core EPC gave rise to EPC derivative tissues. The boundary of ExE – EPC is at the RM initiation point. B) Pattern induction and maintenance is regulated by Fgf4 and Activin. Distal ExE identity is maintained by the simultaneous responsiveness to both Fgf4 and Nodal/Activin. In the absence of both pathways, distal ExE differentiates into EPC. In the presence of Activin, distal ExE differentiates into proximal ExE through intermediate ExE.

Our partial success in creating double transgenic TS cells by means of double lentivirus transduction might be due to epigenetic silencing occurring after long term culture, although this condition is unlikely since it was not observed in TS cells when using a different lentiviral backbone (Golding et al, 2010). However, the successful derivation of TS cells capable of expressing a histone H2B-linked GFP allows as to use this system for studies involving alterations of TS cells live morphology during differentiation and/or other experimental treatments. For example, by using our system not only we managed to recapitulate the published behavior of TS cells during differentiation (Tanaka et al, 1998) but we also observed for a first time a small but statistically significant increase in nuclear size one day after induction of differentiation which was not associated with concomitant increase in the chromatin content. In addition, using live microscopy and GFP exposure at day 4 of differentiation, we were able to link three morphologically different trophoblast cell types with differences in their nuclear sizes and chromatin content, identifying two different giant cell types with increased chromatin content and one smaller cell type which although had a bigger nucleus relative to control stem cells, its chromatin content appeared to be unaltered. In agreement to our findings, Simmons and coworkers have reported the existence of several different types of TGCs during differentiation (Simmons et al, 2007). In addition, *TpbpA* a marker of the diploid population of SpT and GlyT cells appears during culture of TS under differentiation conditions (Donnison et al, 2015). A weakness of our methodology can be seen when there is a difference in the proliferation rate between the control stem cells and the examined cell type. For example, faster proliferating cells are expected to have a higher number of cells passing through the G2 phase of the cycle per time, leading to a bias in the estimation of their chromatin content. This scenario should therefore be taken into account when examining different cell populations.

CHAPTER 6:

FUTURE EXPERIMENTS

6. Future experiments

The work done during the completion of this thesis has opened new interesting questions in trophoblast development. For example, it is still unknown whether the intermediate ExE can be identified by the expression of a specific gene. This is important to be done, not only to better describe ExE patterning but also in order to understand TS differentiation *in vitro*. One possible way to initiate this investigation is by culturing distal ExE explants in medium containing Activin for given times followed by RNA extraction for whole transcriptome RNA sequencing and comparison with control explants cultured in the presence of both Fgf2 and Activin as well as explants cultured in the absence of both growth factors.

A second question is to investigate the possible role of other signaling pathways in the ExE whose role is still poorly understood. These pathways could be the Notch and the wnt pathway. For example, by using live microscopy and a transgenic Notch detector, Nowotschin and coworkers were able to observe that the Notch pathway is transiently activated at the ExE around the E6.0 stage (Nowotschin et al, 2013). A role for wnt signaling is suggested by the necessity to include the small molecule inhibitor of wnt signaling XAV939 in order to successfully derive and maintain TS cells under defined culture conditions on fibronectin (Ohinata and Tsukiyama, 2014). In addition, *Wnt7b* expression has already been identified in the ExE at E6.5 (Yoon et al, 2012).

In addition to the above said experiments, the transgenic TS cells described here, could be employed for the detailed morphological and gene expression study of the different cell types of trophoblast cells appearing during *in vitro* differentiation as well as their precursors. Since our knowledge regarding the live morphology of differentiated trophoblast cell types is currently reduced, especially for precursors' morphology, this study should be of great interest. For this, the cellular morphologies appearing during the course of differentiation, should be identified and documented while in culture, in phase contrast and under the GFP filter, followed by fixation and then stained for the expression of markers of specific cell types. Time lapse microscopy should also contribute towards this aim.

CHAPTER 7:

REFERENCES

Abell AN, Granger DA, Johnson NL, Vincent-Jordan N, Dibble CF, Johnson GL (2009)
Trophoblast stem cell maintenance by fibroblast growth factor 4 requires MEKK4 activ ation of JunN-terminal kinase. *Mol Cell Biol*; 29(10):2748-61

Abell AN, Jordan NV, Huang W, Prat A, Midland AA, Johnson NL, Granger DA, Mieczkowski PA, Perou CM, Gomez SM, Li L, Johnson GL. (2011) MAP3K4/CBP-regulated H2B acetylation controls epithelial-mesenchymal transition in trophoblast stem cells. *Cell Stem Cell*; 8(5):525-37.

Adachi K, Nikaido I, Ohta H, OhtSuka S, Ura H, Kadota M, Wakayama T, Ueda HR, Niwa H (2013) Context-dependent wiring of Sox2 regulatory networks for self-renewal of embryonic and trophoblast stem cells. *Mol Cell*; 52(3):380-92.

Adamson SL, Lu Y, Whiteley KJ, Holmyard D, Hemberger M, Pfarrer C, Cross JC (2002) Interactions between trophoblast cells and the maternal and fetal circulation in the mouse placenta. *Dev Biol*.;250(2):358-73.

Ahmed K, Dehghani H, Rugg-Gunn P, Fussner E, Rossant J, Bazett-Jones DP. (2010) Global chromatin architecture reflects pluripotency and lineage commitment in the early mouse embryo. *PLoS One*; 5(5):e10531.

Ain R, Canham LN, Soares MJ (2003) Gestation stage-dependent intrauterine trophoblast cell invasion in the rat and mouse: novel endocrine phenotype and regulation. *Dev Biol*; 260(1):176-90.

Alam SM, Konno T, Dai G, Lu L, Wang D, Dunmore JH, Godwin AR, Soares MJ (2007)
A uterine decidual cell cytokine ensures pregnancy-dependent adaptations to a physiological stressor. *Development*;134(2):407-15.

Albano RM, Arell R, Beddington RS, Smith JC. (1994) Expression of inhibin subunits and follistatin during postimplantation mouse development: decidual expression of

activin and expression of follistatin in primitive streak, somites and hindbrain. *Development*; 120(4):803-13.

Al-Jameil N, Aziz Khan F, Fareed Khan M, Tabassum H (2014) A brief overview of preeclampsia. *J Clin Med Res*; 6(1):1-7.

Aoyama M, Sun-Wada GH, Yamamoto A, Yamamoto M, Hamada H, Wada Y (2012) Spatial restriction of bone morphogenetic protein signaling in mouse gastrula through the mVam2-dependent endocytic pathway. *Dev Cell*; 22(6):1163-75.

Arhel JN, Genovesio G, Kim KA, Miko S, Perret E, Olivo-Marin JC, Shorte S and Charneau P. (2006b) Quantitative 4D tracking of cytoplasmic and nuclear HIV-1 complexes. *Nat. Meth*; 3: 817-824

Arman E, Haffner-Krausz R, Chen Y, Heath JK, Lonai P. (1998) Targeted disruption of fibroblast growth factor (FGF) receptor 2 suggests a role for FGF signaling in pregastrulation mammalian development. *Proc Natl Acad Sci USA*; 95(9):5082-7.

Armulik A, Genove G, Beltsholtz C (2011) Pericytes: developmental, physiological, and pathological perspectives, problems, and promises. *Dev Cell* 21(2):193-215

Arnold SJ, Robertson EJ. (2009) Making a commitment: cell lineage allocation and axis patterning in the early mouse embryo. *Nat Rev Mol Cell Biol*; 10(2):91-103.

Ashkar AA, Croy BA (2001) Functions of uterine natural killer cells are mediated by interferon gamma production during murine pregnancy. *Semin Immunol*; 13(4):235-41.

Auman HJ, Nottoli T, Lakiza O, Winger Q, Donaldson S, Williams T. (2002) Transcription factor AP-2gamma is essential in the extra-embryonic lineages for early postimplantation development. *Development*; 129(11):2733-47.

Batlle E, Sancho E, Franci C, Dominguez D, Monfar M, Baulida J, Garcia De Herreros A. (2000) The transcription factor snail is a repressor of E-cadherin gene expression in epithelial tumour cells. *Nat Cell Biol*; 2(2):84-9.

Beck S, Le Good JA, Guzman M, Ben-Haim N, Roy K, Beermann F, Constam DB. (2002) Extraembryonic proteases regulate Nodal signalling during gastrulation. *Nat Cell Biol*; 4(12):981-5.

Bedzhov I, Leung CY, Bialecka M, Zernicka-Goetz M. (2014) In vitro culture of mouse blastocysts beyond the implantation stages. *Nat Protoc*; 9(12):2732-9

Bedzhov I, Zernicka-Goetz M (2014) Self-organizing properties of mouse pluripotent cells initiate morphogenesis upon implantation. *Cell*; 156(5):1032-44.

Ben-Haim N, Lu C, Guzman-Ayala M, Pescatore L, Mesnard D, Bischofberger M, Naef F, Robertson EJ, Constam DB (2006)
The nodal precursor acting via activin receptors induces mesoderm by maintaining a source of its convertases and BMP4. *Dev Cell*; 11(3):313-23.

Bevilacqua E, Lorenzon A.R, Bandeira C.L. (2014). Biology of the Ectoplacental Cone. In: A. Croy, A.T. Yamada, F.J. DeMayo and S. Lee Adamson, ed., *The Guide to Investigation of Mouse Pregnancy*, 1st ed. United States of America: Elsevier Inc, pp.113-124

Brennan J, Lu CC, Norris DP, Rodriguez TA, Beddington RS, Robertson EJ (2001) Nodal signalling in the epiblast patterns the early mouse embryo. *Nature*; 411(6840):965-9.

Brewer JR, Mazot P, Soriano P. (2016) Genetic insights into the mechanisms of Fgf signaling. *Genes Dev*; 30(7):751-71

Bulganova NA, Knust E. (2009) The Crumbs complex: from epithelial-cell polarity to retinal degeneration. *J Cell Sci*; 122(Pt 15):2587-96.

Burtscher I, Lickert H. (2009) Foxa2 regulates polarity and epithelialization in the endoderm germ layer of the mouse embryo. *Development*; 136(6):1029-38.

Cano A, Perez-Moreno MA, Rodrigo I, Locascio A, Blanco MJ, del Barrio MG, Portillo F, Nieto MA. (2000) The transcription factor snail controls epithelial-mesenchymal transitions by repressing E-cadherin expression. *Nat Cell Biol*; 2(2):76-83.

Charalambous C, Drakou K, Nicolaou S, Georgiades P. (2013) Novel spatiotemporal glycome changes in the murine placenta during placentation based on BS-I lectin binding patterns. *Anat Rec (Hoboken)*; 296(6):921-32.

Carver EA, Jiang R, Lan Y, Oram KF, Gridley T. (2001)
The mouse snail gene encodes a key regulator of the epithelial-mesenchymal transition. *Mol Cell Biol*; 21(23):8184-8.

Chakraborty D, Rumi MA, Konno T, Soares MJ (2011) Natural killer cells direct hemochorial placentation by regulating hypoxia-inducible factordependent trophoblast lineage decisions. *Proc Natl Acad Sci USA*;108(39):16295-300.

Chazaud C, Rossant J (2006) Disruption of early proximodistal patterning and AVE formation in Apc mutants. *Development*; 133(17):3379-87

Chen Z, Zhang J, Hatta K, Lima PD, Yadi H, Colucci F, Yamada AT, Croy BA (2012) DBA-lectin reactivity defines mouse uterine natural killer cell subsets with biased gene expression. *Biol Reprod*; 87(4):81.

Chhabra A, Lechner AJ, Ueno M, Acharya A, Van Handel B, Wang Y, Iruela-Arispe ML, Tallquist MD, Mikkola HK (2012)

Trophoblasts regulate the placental hematopoietic niche through PDGF-B signaling. *Dev Cell*; 22(3):651-9.

Chu J, Shen MM. (2010) Functional redundancy of EGF-CFC genes in epiblast and extraembryonic patterning during early mouse embryogenesis. *Dev Biol*; 342(1):63-73

Coffin, J. M. (1996**)**. Retroviridae: the viruses and their replication, p. 1767– 1847. *In* B. N. Fields, D. M. Knipe, and P. M. Howley (ed.), Fields virology. Lippincott Raven, Philadelphia, Pa.

Ciruna BG, Rossant J. (1999) Expression of the T-box gene Eomesodermin during early mouse development. *Mech Dev*; 81(1-2):199-203.

Coan PM, Conroy N, Burton GJ, Ferguson-Smith AC. (2006) Origin and characteristics of glycogen cells in the developing murine placenta. *Dev Dyn*; 235(12):3280-94.

Cockrell SA, Kafri T. (2007) Gene delivery by lentivirus vectors. *Mol Biotech*; 36:184-204

Constancia M, Hemberger M, Hughes J, Dean W, Ferguson- Smith A, Fundele R, Stewart F, Kelsey G, Fowden A, Sibley C, and Reik W. (2002) Placental-specific IGF-II is a major modulator of placental and fetal growth. *Nature*; 417: 945–948.

Corson LB, Yamanaka Y, Lai KM, Rossant J. (2003) Spatial and temporal patterns of ERK signaling during mouse embryogenesis. *Development*; 130(19):4527-37.

Coucouvanis E, Martin GR. (1995) Signals for death and survival: a two-step mechanism for cavitation in the vertebrate embryo. *Cell*; 83(2):279-87.

Croy BA, Gambel P, Rossant J, Wegmann TG. (1985) Characterization of murine decidual natural killer (NK) cells and their relevance to the success of pregnancy. *Cell Immunol*; 93(2):315-26.

de Sousa Lopes SM, Carvalho RL, van den Driesche S, Goumans MJ, ten Dijke P, Mummery CL. (2003) Distribution of phosphorylated Smad2 identifies target tissues of TGF beta ligands in mouse development. *Gene Expr Patterns*; 3(3):355-60.

Detmar J, Rennie MY, Whiteley KJ, Qu D, Taniuchi Y, Shang X, Casper RF, Adamson SL, Sled JG, Jurisicova A. (2008) Fetal growth restriction triggered by polycyclic aromatic hydrocarbons is associated with altered placental vasculature and AhR-dependent changes in cell death. *Am J Physiol Endocrinol Metab*; 295(2):E519-30

Donnison M, Beaton A, Davey HW, Broadhurst R, L'Huiller P, Pfeffer PL. (2005) Loss of the extraembryonic ectoderm in Elf5 mutants leads to defects in embryonic patterning. *Development*; 132(10):2299-308.

Donnison M, Broadhurst R, Pfeffer PL (2015) Elf5 and Ets2 maintain the mouse extraembryonic ectoderm in a dosage dependent synergistic manner. *Dev Biol*; 397(1):77-88.

Drakou K, Georgiades P. (2015) A serum-free and defined medium for the culture of mammalian postimplantation embryos. *Biochem Biophys Res Commun*; 468(4):813-9.

Dufait I, Liechtenstein T, Lanna A, Laranga R, Padella A, Bricogne C, Arce F, Kochan G, Breckpot K and Escors D. (2013) Lentiviral Vectors in Immunotherapy, Gene Therapy - Tools and Potential Applications, Dr. Francisco Martin (Ed.), InTech, DOI: 10.5772/50717. Available from: https://www.intechopen.com/books/gene-therapy-tools-and-potential-applications/lentiviral-vectors-in-immunotherapy

Dunn NR, Vincent SD, Oxburgh L, Robertson EJ, Bikoff EK. (2004) Combinatorial activities of Smad2 and Smad3 regulate mesoderm formation and patt erning in the mouse embryo. *Development*; 131(8):1717-28

Dupressoir A, Vernocher C, Bawa O, Harper F, Pierron G, Opolon P, Heidmann T (2009) Syncytin-A knockout mice demonstrate the critical role in placentation of a fusogenic, endogenous retrovirus-derived, envelope gene. *Proc Natl Acad Sci* USA;106(29):12127-32.

Dupressoir A, Vernochet C, Harper F, Guegan J, Dessen P, Pierron G, Heidmann T (2011) A pair of co-
opted retroviral envelope syncytin genes is required for formation of the two-layeredmurine placental syncytiotrophoblast. *Proc Natl Acad Sci* USA; 108(46):E1164-73.

Dupressoir A, Marceau G, Vernocher C, Benit L, Kanellopoulos C, Sapin V, Heidmann T (2005) Syncytin-A and syncytin-B, two fusogenic placenta specific murine envelope genes of retroviralorigin conserved in Muridae. *Proc Natl Acad Sci* USA; 102(3):725-30.

Erlebacher A, Price KA, Glimcher LH. (2004) Maintenance of mouse trophoblast stem cell proliferation by TGF-beta/activin. *Dev Biol*; 275(1):158-69.

Evans, M. J. and Kaufman, M. (1981) Establishment in culture of pluripotential cells from mouse embryos. *Nature*; 292:154-156.

Feldman B, Poueymirou W, Papaioannou VE, DeChiara TM, Goldfarb M. (1995) Requirement of FGF-4 for postimplantation mouse development. *Science*; 267(5195):246-9.

Ferrer-Vaquer A, Viotti M, Hadjantonakis AK. (2010)
Transitions between epithelial and mesenchymal states and the morphogenesis of the early mouse embryo. *Cell Adh Migr*; 4(3):447-57.

Frank D, Fortino W, Clark L, Musalo R, Wang W, Saxena A, Li CM, Reik W, Ludwig T, Tycko B. (2002) Placental overgrowth in mice lacking the imprinted gene Ipl. *Proc Natl Acad Sci* USA; 99(11):7490-5.

Frankenberg S, Smith L, Greenfield A, Zernicka-Goetz M. (2007) Novel gene expression patterns along the proximo-distal axis of the mouse embryo before gastrulation. *BMC Dev Biol*; 7:8.

Freed OE. (2002) HIV-1 replication. *Som. cell and Mol. Gen*. 26; 13-34.

Gabriel HD, Jung D, Butzler C, Temme A, Traub O, Winterhager E, and Willecke K. (1998) Transplacental uptake of glucose is decreased in embryonic lethal connexin26-deficient mice. *J Cell Biol*; 140:1453–1461

Garcia-Garcia MJ, Anderson KV. (2003)
Essential role of glycosaminoglycans in Fgf signaling during mouse gastrulation. *Cell*; 114(6):727-37.

Gardner RL. 1983. Origin and differentia- tion of extraembryonic tissues in the mouse. *Int Rev Exp Pathol*; 24:63-133.

Gardner RL, Papaioannou VE, and Barton SC. (1973). Origin of the ectoplacental cone and secondary giant cells in mouse blastocysts reconstituted from isolated trophectoderm and inner cell mass. *J. Embryol. Exp. Morphol*; 3(1,561-572.

Gasperowicz M, Surmann-Schmitt C, Hamada Y, OttoF, Cross JC (2013)
The transcriptional co-
repressor TLE3 regulates development of trophoblast giant cells lining maternal blood spaces in the mouse placenta. *Dev Biol*; 382(1):1-14

Gaynor LM, Colucci F (2017) Uterine Natural Killer Cells: Functional Distinctions and Influence on Pregnancy in Humans and Mice. *Front Immunol*; 8:467.

Geng Y, Yu Q, Sicinska E, Das M, Schneider JE, Bhattacharya S, Rideout WM, Bronson RT, Gardner H, Sicinski P. (2003) Cyclin E ablation in the mouse. *Cell*; 114(4):431-43.

Georgiades P, Ferguson-Smith AC, Burton GL. (2002) Comparative developmental anatomy of the murine and human definitive placentae. *Placenta*; 23(1):3-19.

Georgiades P, Rossant J. (2006) Ets2 is necessary in trophoblast for normal embryonic anteroposterior axis development. *Development*; 133(6):1059-68.

Golding MC, Zhang L, Mann MR. (2010)
Multiple epigenetic modifiers induce aggressive viral extinction in extraembryonic end oderm stem cells. *Cell Stem Cell*; 6(5):457-67.
Gonçalves CR, Antonini S, Vianna-Morgante AM, Machado-Santelli GM, Bevilacqua E. (2003) Developmental changes in the ploidy of mouse implanting trophoblast cells in vitro. *Histochemistry and cell biology*; *119*(3), pp.189-198

Gotoh N, Manova K, Tanaka S, Murohashi M, Hadari Y, Lee A, Hamada Y, Hiroe T, Ito M, Kurihara T, Nakazato H, Shibuya M, Lax I, Lacy E, Schlessinger J. (2005) The docking protein FRS2alpha is an essential component of multiple fibroblast growth factor responses during early mouse development. *Mol Cell Biol*; 25(10):4105-16.

Goumans MJ, Mummery C. (2000) Functional analysis of
the TGFbeta receptor/Smad pathway through gene ablation in mice. *Int. J. Dev Biol*; 44(3):253-65.

Guillemot F, Nagy A, Auerbach A, Rossant J, Joyner AL. (1994) Essential role of Mash-2 in extraembryonic development. *Nature*; 371(6495):333-6.

Günzel D, Yu ASL. (2013) Claudins and the Modulation of Tight Junction Permeability. *Physiological Reviews*; *93*(2): 525–569.

Gu Z, Nomura M, Simpson BB, Lei H, Feijen A, van den Eijnden-van Raaij J, Donahoe PK, Li E. (1998)
The type I activin receptor ActRIB is required for egg cylinder organization and gastrul ation in the mouse. *Genes Dev*; 12(6):844-57.

Guzman-Ayala M, Ben-Haim N, Beck S, Constam DB. (2004) Nodal protein processing and fibroblast growth factor 4 synergize to maintain a trophoblast stem cell microenvironment. *Proc Natl Acad Sci* USA; 101(44):15656-60.

Harrison SE, Sozen B, Christodoulou N, Kyprianou C, Zernicka-Goetz M. (2017) Assembly of embryonic and extraembryonic stem cells to mimic embryogenesis in vitro. *Science*; 356(6334).

Hu D, Cross JC (2010) Development and function of trophoblast giant cells in the rodent placenta. *Int J Dev Biol*; 54(2-3):341-54.

Hu D, Cross JC (2011) Ablation of Tpbpa-positive trophoblast precursors leads to defects in maternal spiral artery remodeling in the mouse placenta. *Dev Biol*; 358(1):231-9.

Hudson JW, Kozarova A, Cheung P, Macmillan JC, Swallow CJ, Cross JC, Dennis JW (2001) Late mitotic failure in mice lacking Sak, a polo-like kinase. *Curr Biol*; 11(6):441-6.

Hughes M, Dobric N, Scott IC, Starovic M, St-Pierre B, Egan SE, Kingdom JC, Cross JC. (2004) The Hand1, Stra13 and Gcm1 transcription factors override FGF signaling to promote terminal differentiation of trophoblast stem cells. *Dev Biol*; 271(1):26-37.

Hughes M, Natale BV, Simmons DG, Natale DR (2013) Ly6e expression is restricted to syncytiotrophoblast cells of the mouse placenta. *Placenta*;34(9):831-5.

Iguchi T, Tani N, Sato T, Fukatsu N, Ohta Y. (1993) Developmental changes in mouse placental cells from several stages of pregnancy in vivo and in vitro. *Biol Reprod*; 48(1):188-96.

Inoue S, Leblond CP, Laurie GW. (1983) Ultrastructure of Reichert's membrane, a multilayered basement membrane in the parietal wall of the rat yolk sac. *J Cell Biol*; 97(5 Pt 1):1524-37.

Ishikawa T, Yagyu K, Seguchi K. (1986) A scanning electron microscopic study of the surface morphology of visceral endoderm and ectoderm in postimplantation mouse embryos. *J Electron Microsc (Tokyo)*; 35(2):185-94.

Jackson D, Volpert OV, Bouck N, Linzer DI (1994) Stimulation and inhibition of angiogenesis by placental proliferin and proliferin- related protein. *Science.* 266(5190):1581-1584.

Jukkola PI, Rogers JT, Kaspar BK, Weeber EJ, Nishijima I. (2011) Secretin deficiency causes impairment in survival of neural progenitor cells in mice. *Hum Mol Genet*; 20(5):1000-7.

Kanda T, Sullivan KF, Wahl GM. (1998) Histone-GFP fusion protein enables sensitive analysis of chromosome dynamics in living mammalian cells. *Curr Biol*; 8(7):377-85.

Kawamura N, Sun-Wada GH, Aoyama M, Harada A, Takasuga S, Sasaki T, Wada Y. (2012) Delivery of endosomes to lysosomes via microautophagy in the visceral endoderm of mouse embryos. *Nat Commun*; 3:1071.

Kopp JL, Ormbee BD, Desler M, Rizzino A (2008) Small increases in the level of Sox2 trigger the differentiation of mouse embryonic stem cells. *Stem Cells*; 26(4):903-11

Kovacs CS, Lanske B, Hunzelman JL, Guo J, Karaplis AC, and Kronenberg HM. (1996) Parathyroid hormone-related peptide (PTHrP) regulates fetal- placental calcium transport through a receptor distinct from the PTH/PTHrP receptor. *Proc Natl Acad Sci* USA 93: 15233–15238.

Kredel S, Oswald F, Nienhaus K, Deuschle K, Roecker C, Wolff M, Heilker R, Nienhaus GU, Wiedenmann J. (2009) mRuby,
a bright monomeric red fluorescent protein for labeling of subcellular structures. *PLoS One*; 4(2):e4391.

Kubaczka C, Senner C, Arauzo-Bravo MJ, Sharma N, Kuckenberg P, Becker A, Zimmer A, Brustle O, Peitz M, Hemberger M, Schorle H. (2014) Derivation and maintenance of murine trophoblast stem cells under defined conditions. *Stem Cell Reports*; 2(2):232-42.

Kubaczka C, Senner CE, Cierlitza M, Arauzo-Bravo MJ, Kuckenberg P, Peitz M, Hemberger M, Schorle H. (2015) Direct Induction of Trophoblast Stem
Cells from Murine Fibroblasts. *Cell Stem Cell*; 17(5):557-68.

Kuehnel E, Kleff V, Stoianovska V, Kaiser S, Waldschuetz R, Herse F, Ploesch T, Winterhager E, Gellhaus A (2017) Placental-Specific Overexpression of sFlt
1 Alters Trophoblast Differentiation and NutrientTransporter Expression in
an IUGR Mouse Model. *J Cell Biochem*; 118(6):1316-1329

Kulandavelu S., Whiteley K.J., Bainbridge S.A., Qu D., Adamson SL. (2013) Fetal growth restriction triggered by polycyclic aromatic hydrocarbons is associated with altered placental vasculature and *AhR*-dependent changes in cell death. *Hypertension*; 61: 259-266

Kunath T, Arnaud D, Uy GD, Okamoto I, Chureau C, Yamanaka Y, Heard E, Gardner RL, Avner P, Rossant J. (2003) Imprinted X-inactivation in extra-embryonic endoderm cell lines from mouse blastocysts. *Development*; 132(7):1649-61.

Lamouille S, Xu J, Derynck R. (2014) Molecular mechanisms of epithelial-mesenchymal transition. *Nat Rev Mol Cell Biol*; 15(3):178-96.

Lanner F, Rossant J. (2010) The role of FGF/Erk signaling in pluripotent cells. *Development*; 137(20):3351-60.

Latos PA, Goncalves A, Oxley D, Mohammed H, Turro E, Hemberger M. (2015) Fgf and Esrrb integrate epigenetic and transcriptional networks that regulate self-renewal of trophoblast stem cells. *Nat Commun*; 6:7776.

Latos PA, Hemberger M. (2016) From the stem of the placental tree: trophoblast stem cells and their progeny. *Development*; 143(20):3650-3660.

Latos PA, Sienerth AR, Murray A, Senner CE, Muto M, Ikawa M, Oxley D, Burge S, Cox BJ, Hemberger M. (2015) Elf5-centered transcription factor hub controls trophoblast stem cell self-renewal and differentiation through stoichiometry-sensitive shifts in target gene networks. *Genes Dev*; 29(23):2435-48.

Le Good JA, Joubin K, Giraldez AJ, Ben-Haim N, Beck S, Chen Y, Schier AF, Constam DB. (2005) Nodal stability determines signaling range. *Curr Biol*; 15(1):31-6.

Lescisin KR, Varmuza S, Rossant J. (1988) Isolation and characterization of a novel trophoblast-specific cDNA in the mouse. *Genes Dev*; 2(12A):1639-46.

Lewis P, Hensel M, Emerman M. (1992) Human immunodeficiency virus infection of cells arrested in the cell cycle. *EMBO journal*; 11:3053-3058.

Li L, Liu C, Biechele S, Zhu Q, Song L, Lanner F, Jing N, Rossant J. (2013) Location of transient ectodermal progenitor potential in mouse development. *Development*; 140(22):4533-43.

Li M, Schwerbrock NM, Lenhart PM, Fritz-Six KL, Kadmiel M, Christine KS, Kraus DM, Espenschied ST, Willcockson HH, Mack CP, Caron KM (2013) Fetal-derived adrenomedullin mediates the innate immune milieu of the placenta. *J Clin Invest*; 123(6):2408-20.

Li P, Mao X, Ren Y, Liu P. (2015)
Epithelial cell polarity determinant CRB3 in cancer development. *Int J Biol Sci*; 11(1):31-7.

Liu P, Wakamiya M, Shea MJ, Albrecht U, Behringer RR, Bradley A. (1999) Requirement for Wnt3 in vertebrate axis formation. *Nat Genet*; 22(4):361-5.

Louvi A, Accili D, Efstratiadis A. (1997) Growth-promoting interaction of IGF-II with the insulin receptor during mouse embryonic development. *Dev Biol*; 189(1):33-48.

Luo J, Sladek R, Bader JA, Matthyssen A, Rossant J, Giguere V. (1997) Placental abnormalities in mouse embryos lacking the orphan nuclear receptor ERR-beta. *Nature*; 388(6644):778-82.

Ma GT, Linzer DI (2000) GATA-2 restricts prolactin-
like protein A expression to secondary trophoblast giant cells in the mouse. *Biol Reprod*; 63(2):570-4.

Manova K, De Leon V, Angeles M, Kalantry S, Giarre M, Attisano L, Wrana J, Bachvarova RF. (1995)
mRNAs for activin receptors II and IIB are expressed in mouse oocytes and in the epiblast of pregastrula and gastrula stage mouse embryos. *Mech Dev*; 49(1-2):3-11.

Manova K, Paynton BV, Bachvarova RF. (1992) Expression of activins and TGF beta 1 and beta 2 RNAs in early postimplantation mouse embryos and uterine decidua. *Mech Dev*; 36(3):141-52.

Martindilli DM, Risebro CA, Smart N, Franco-Viseras Mdel M, Rosario CO, Swallow CJ, Dennis JW, Riley PR (2007) Nucleolar release of Hand1 acts as
a molecular switch to determine cell fate. *Nat Cell Biol*; 9(10):1131-41.

Masui S, Nakatake Y, Toyooka Y, Shimosato D, Yagi R, Takahashi K, Okuda A, Matoba R, Sharov AA, Ko MS, Niwa H. (2007) Pluripotency governed by Sox2 via regulation of Oct3/4 expression in mouse embryonic stem cells. *Nat Cell Biol*; 9(6):625-35.

Matsuo I, Hiramatsu R. (2017) Mechanical perspectives on the anterior-posterior axis polarization of mouse implanted embryos. *Mech Dev*; 144(Pt A):62-70.

Matzuk MM, Kumar TR, Vassalli A, Bickenbach JR, Roop DR, Jaenisch R, Bradley A. (1995) Functional analysis of activins during mammalian development. *Nature*; 374(6520):354-6.

McBride MS, Schwartz DM, Panganiban TA. (1997) Efficient encapsidation of human immunodeficiency virus type 1 vectors and further characterization of *cis* elements required for encapsidation. *J Virol*; 4544-4554

McDonald D, Vodicka MA, Lucero G, Svitkina TM, Borisy GG, Emerman M, HopeTJ (2002) Visualization of the intracellular behavior of HIV in living cells. *J. Cell Biol*; 159: 441-452

Mehrotra P.K. (1984) Blastocyst attachment and morphogenesis of ectoplacental cone in mouse. *J. Biosci*; 6(2):43-52

Mesnard D, Guzman-Ayala M, Constam DB (2006)
Nodal specifies embryonic visceral endoderm and sustains pluripotent cells in the epiblast before overt axial patterning. *Development*; 133(13):2497-505.

Migeotte I, Omelchenko T, Hall A, Anderson KV (2010) Rac1-dependent collective cell migration is required for specification of the anterior-posterior body axis of the mouse. *PloS Biol*; 8(8): e1000442.

Miner JH, Li C, Mudd JL, Go G, Sutherland AE. (2004)
Compositional and structural requirements for laminin and basement membranes duri ng mouseembryo implantation and gastrulation. *Development*; 131(10):2247-56.

Moll W. (1985) Physiological aspects of placental ontogeny and phylogeny. *Placenta*; 6(2):141-54.

Morsut L, Yan KP, Enzo E, Aragona M, Soligo SM, Wendling O, Mark M, Khetchoumian K, Bressan G, Chambon P, Dupont S, Losson R, Piccolo S. (2010) Negative control of Smad activity by ectodermin/Tif1gamma patterns the mammalian embryo. *Development*; 137(15):2571-8.

Mould A, Morgan MA, Li L, Bikoff EK, Robertson EJ. (2012)
Blimp1/Prdm1 governs terminal differentiation of endovascular trophoblast giant cells and defines multipotent progenitors in the developing placenta. *Genes Dev*; 26(18):2063-74

Murohashi M, Nakamura T, Tanaka S, Ichise T, Yoshida N, Yamamoto T, Shibuya M, Schlessinger J, Gotoh N. (2010) An FGF4-FRS2alpha-
Cdx2 axis in trophoblast stem cells induces Bmp4 to regulate proper growth of early mouse embryos. *Stem Cells*; 28(1):113-21.

Murray A, Sienerth AR, Hemberger M, (2016) Plet1 is
an epigenetically regulated cell surface protein that provides essential cues to direct trophoblast stem cell differentiation. *Sci Rep*; 6:25112.

Myers AP, Corson LB, Rossant J, Baker JC. (2004) Characterization of mouse Rsk4 as an inhibitor of fibroblast growth factor-RAS-extracellular signal-regulated kinase signaling. *Mol Cell Biol*; 24(10):4255-66.

Nagai A, Takebe K, Nio-Kobayashi J, Takahashi-Iwanaga H, Iwanaga T. (2010) Cellular expression of the monocarboxylate transporter (MCT) family in the placenta of mice. *Placenta*; 31(2):126-33.

Nakao A, Afrakhte M, Moren A, Nakayama T, Christian JL, Heuchel R, Itoh S, Kawabata M, Heldin NE, Heldin CH, ten Dijke P. (1997) Identification of Smad7, a TGFbeta-inducible antagonist of TGF-beta signalling. *Nature*; 389(6651):631-5.

Nakayama H, Scott IC, Cross JC. (1998)
The transition to endoreduplication in trophoblast giant cells is regulated by the mSNA zinc finger transcription factor. *Dev Biol*.; 199(1):150-63.

Nardozza LM, Caetano AC, Zamarian AC, Mazzola JB, Silva CP, Marcal VM, Lobo TF, Peixoto AB, Araujo Junior E (2017) Fetal growth restriction: current knowledge. *Arch Gynecol Obstet*; 295(5):1061-1077

Natale DR, Hemberger M, Hughes M, Cross JC. (2009) Activin promotes differentiation of cultured mouse trophoblast stem cells towards a labyrinth cell fate. *Dev Biol*; 335(1):120-31.

Natale BV, Schweitzer C, Hughes M, Globisch MA, Kotadia R, Tremblay E, Vu P, Cross JC, Natale DRC. (2017) Sca-1 identifies a trophoblast population with multipotent potential in the mid-gestation mouse placenta. *Sci Rep*; 7(1):5575.

Nelson WJ. (2009) Remodeling epithelial cell organization: transitions between front-rear and apical-basal polarity. *Cold Spring Harb Perspect Biol*; 1(1):a000513.

Nelson AC, Mould AW, Bikoff EK, Robertson EJ (2016) Single-cell RNA-seq reveals cell type-specific transcriptional signatures at the maternal-foetal interface during pregnancy. *Nat Commun*; 7:11414

Ninomiya Y, Davies TJ, Gardner RL. (2005) Experimental analysis of the transdifferentiation of visceral to parietal endoderm in the mouse. *Dev Dyn*; 233(3):837-46.

Niwa H, Miyazaki J, Smith AG. (2000) Quantitative expression of Oct-3/4 defines differentiation, dedifferentiation or self-renewal of ES cells. *Nat Genet*; 24(4):372-6.

Noguchi M, Noguchi T, Watanabe M, Muramatsu T. (1982)
Localization of receptors for Dolichos biflorus agglutinin in early post implantation em bryos in mice. *J Embryol Exp Morphol*; 72:39-52.

Norris DP, Brennan J, Bikoff EK, Robertson EJ. (2002) The Foxh1-dependent autoregulatory enhancer controls the level of Nodal signals in the mouse embryo. *Development*; 129(14):3455-68.

Nowotschin S, Hadjantonakis AK. (2010) Cellular dynamics in the early mouse embryo: from axis formation to gastrulation. *Curr Opin Genet Dev*; 20(4):420-7.

Nowotschin S, Xenopoulos P, Schrode N, Hadjantonakis AK. (2013) A bright single-cell resolution live imaging reporter of Notch signaling in the mouse. *BMC Dev Biol*; 13:15.

Odiatis C, Georgiades P. (2010) New insights for Ets2 function in trophoblast using lentivirus-mediated gene knockdown in trophoblast stem cells. *Placenta*; 31(7):630-40.

Oh-McGinnis R, Bogutz AB, Lefebvre L (2011)
Partial loss of Ascl2 function affects all three layers of
the mature placenta and causes intrauterine growth restriction. *Dev Biol*; 351(2):277-86.

Ohinata Y, Tsukiyama T. (2014) Establishment of trophoblast stem cells under defined culture conditions in mice. *PLoS One*; 9(9):e107308.

Ornitz DM. (2000)
FGFs, heparan sulfate and FGFRs: complex interactions essential for development. Bioessays; 22(2):108-12.

Ornitz DM, Itoh N. (2001) Fibroblast growth factors. *Genome Biol*; 2(3):1-12

Outhwaite JE, McGuire V, Simmons DG (2015) Genetic ablation of placental sinusoidal trophoblast giant cells causes fetal growth restriction and embryonic lethality. *Placenta*; 36(8):951-5.

Paffaro VA Jr, Bizinotto MC, Joazeiro PP, Yamada AT (2003)
Subset classification of mouse uterine natural killer cells by DBA lectin reactivity. *Placenta*; 24(5):479-88.

Paikari A, D Belair C, Saw D and Blelloch R (2017)
The eutheria-specific miR-290 cluster modulates placental growth and maternal-fetal transport. *Development*; 144(20):3731-3743

Papadaki C, Alexiou M, Cecena G, Verykokakis M, Bilitou A, Cross JC, Oshima RG, Mavrothalassitis G. (2007) Transcriptional repressor erf determines extraembryonic ectoderm differentiation. *Mol Cell Biol*; 27(14):5201-13

Papanayotou C, Collignon J (2014) Activin/Nodal signalling before implantation: setting the stage for embryo patterning. *Philos Trans R Soc Lond B Biol Sci*; 369(1657)

Parast MM, Aeder S, Sutherland AE. (2001) Trophoblast giant-cell differentiation involves changes in cytoskeleton and cell motility. *Dev Biol*; 230(1):43-60.

Parisi T, Beck AR, Rougier N, McNeil T, Lucian L, Werb Z, Amati B. (2003)
Cyclins E1 and E2 are required for endoreplication in placental trophoblast giant cells. *EMBO J*; 22(18):4794-803.

Pearton DJ, Smith CS, Redgate E, van Leeuwen J, Donnison M, Pfeffer PL. (2014) Elf5 counteracts precocious trophoblast differentiation by maintaining Sox2 and 3 and inhibitingHand1 expression. *Dev Biol*; 392(2):344-57.

Pereira PN, Dobreva MP, Graham L, Huylebroeck D, Lawson KA, Zwijsen AN. (2011) Amnion formation in the mouse embryo: the single amniochorionic fold model. *BMC Dev Biol*; 11:48.

Polydorou C, Georgiades P. (2014) Ets2-dependent trophoblast signalling is required for gastrulation progression after primitive streak initiation. *Nat Commun*; 4:1658.

Rai A, Cross JC (2014) Development of the hemochorial maternal vascular spaces in the placenta through endothelial and vasculogenic mimicry. *Dev Biol*; 387(2):131-41.

Rai A, Cross JC (2015) Three-dimensional cultures of trophoblast stem cells autonomously develop vascular-like spaceslined by trophoblast giant cells. *Dev Biol*; 398(1):110-9.

Rampon C, Bouillot S, Climescu-Haulica A, Prandini MH, Cand F, Vandenbrouck Y, Huber P. (2008) Protocadherin 12 deficiency alters morphogenesis and transcriptional profile of the placenta. *Physiol Genomics*; 34(2):193-204.

Rampon C, Prandini MH, Bouillot S, Pointu H, Tillet E, Frank R, Vernet M, Huber P. (2005) Protocadherin 12 (VE-cadherin 2) is expressed in endothelial, trophoblast, and mesangial cells. *Exp Cell Res*; 302(1):48-60.

Rayon T, Menchero S, Rollan I, Ors I, Helness A, Crespo M, Nieto A, Azuara V, Rossant J, Manzanares M. (2016) Distinct mechanisms regulate Cdx2 expression in the blastocyst and in trophoblast stem cells. *Sci. Rep*; 6:27139.

Reinius S. (1965) Morphology of the mouse embryo, from the time of implantation to mesoderm formation. *Z Zellforch Mikrosk Anat*; 68(5):711-23.

Rhodes KE, Gekas C, Wang Y, Lux CT, Francis CS, Chan DN, Conway S, Orkin SH, Yoder MC, Mikkola HK (2008) The emergence of hematopoietic stem cells is initiated in the placental vasculature in the absence of circulation. *Cell Stem Cell*; 2(3):252-63.

Richardson L, Torres-Padilla ME, Zernicka-Goetz M. (2006) Regionalised signalling within the extraembryonic ectoderm regulates anterior visceral endoderm positioning in the mouse embryo. *Mech Dev*; 123(4):288-96.

Riedl J, Crevenna AH, Kessenbrock K, Yu JH, Neukirchen D, Bista M, Bradke F, Jenne D, Holak TA, Werb Z, Sixt M, Wedlich-Soldner R. (2008) Lifeact: a versatile marker to visualize F-actin. *Nat Methods*; 5(7):605-7.

Riley P, Anson-Cartwright L, Cross JC. (1998) The Hand1 bHLH transcription factor is essential for placentation and cardiac morphogenesis. *Nat Genet*; 18(3):271-5.

Robertson GG. (1942) An analysis of the development of homozygous yellow mouse embryos. *PhD Thesis*, Yale University, New Haven, Connecticut, United States of America

Rodig SJ, Meraz MA, White JM, Lampe PA, Riley JK, Arthur CD, King KL, Sheehan KC, Yin L, Pennica D, Johnson Jr EM, Schreiber RD (1998). Disruption of the Jak1 gene demonstrates obligatory and nonredundant roles of the Jaks in cytokine-induced biologic responses. *Cell*; 93:373–383

Rossant J, Ofer L. (1977) Properties of extra-embryonic ectoderm isolated from postimplantation mouse embryos. *J Embryol Exp Morphol*; 39:183-94.

Rossant J, Tam PP. (2009) Blastocyst lineage formation, early embryonic asymmetries and axis patterning in the mouse. *Development*; 136(5):701-13.

Russ AP, Wattler S, Colledge WH, Aparicio SA, Carlton MB, Pearce JJ, Barton SC, Surani MA, Ryan K, Nehls MC, Wilson V, Evans MJ (2000)

Eomesodermin is required for mouse trophoblast development and mesoderm formati on. *Nature*; 404(6773):95-9.

Saba-El-Leil MK, Vella FD, Vernay B, Voisin L, Chen L, Labrecque N, Ang SL, Meloche S. (2003) An essential function of the mitogen-activated protein kinase Erk2 in mouse trophoblast development. *EMBO Rep*; 4(10):964-8.

Salamat M, Miosge N, Herken R. (1995) Development of Reichert's membrane in the early mouse embryo. *Anat. Embryol*; 192: 275-281.

Scott IC, Anson-Cartwright L, Riley P, Reda D, Cross JC. (2000) The HAND1 basic helix-loop-helix transcription factor regulates trophoblast differentiation via multiple mechanisms. *Mol Cell Biol*; 20(2):530-41.

Screen M, Dean W, Cross JC, Hemberger M. (2008) Cathepsin proteases have distinct roles in trophoblast function and vascular remodelling. *Development*; 135(19):3311-20.

Sebastiano V, Dalvai M, Gentile L, Schubart K, Sutter J, Wu GM, Tapia N, Esch D, Ju JY, Hubner K, Bravo MJ, Scholer HR, Cavaleri F, Mattias P. (2010) Oct1 regulates trophoblast development during early mouse embryogenesis. *Development*; 137(21):3551-60.

Shimokawa K, Kimura-Yoshida C, Nagai N, Mukai K, Matsubara K, Watanabe H, Matsuda Y, Mochida K, Matsuo I. (2011) Cell surface heparan sulfate chains regulate local reception of FGF signaling in the mouse embryo. *Dev Cell*; 21(2):257-72.

Shin BC, Suzuki T, Matsuzaki T, Tanaka S, Kuraoka A, Shibata Y, Takata K. (1996) Immunolocalization of GLUT1 and connexin 26 in the rat placenta. *Cell Tissue Res*; 285(1):83-9.

Shin BC, Fujikura K, Suzuki T, Tanaka S, Takata K. (1997) Glucose transporter GLUT3 in the rat placental barrier: a possible machinery for the transplacental transfer of glucose. *Endocrinology*; 138(9):3997-4004.

Simmons DG. (2014). Biology of the Ectoplacental Cone. In: A. Croy, A.T. Yamada, F.J. DeMayo and S. Lee Adamson, ed., *The Guide to Investigation of Mouse Pregnancy*, 1st ed. United States of America: Elsevier Inc, pp.143-161

Simmons DG, Fortier AL, Cross JC. (2007) Diverse subtypes and developmental origins of trophoblast giant cells in the mouse placenta. *Dev Biol*; 304(2):567-78.

Simmons DG, Natale DR, Begay V, Hughes M, Leutz A, Cross JC. (2008) Early patterning of the chorion leads to the trilaminar trophoblast cell structure in the placental labyrinth. *Development*; 135(12):2083-91.

Simmons DG, Rawn S, Davies A, Hughes M, Cross JC (2008)
Spatial and temporal expression of the 23 murine Prolactin/Placental Lactogen-related genes is not associated with their position in the locus. *BMC Genomics*; 9:352.

Soares MJ, Konno T, Alam SM. (2007) The prolactin family: effectors of pregnancy-dependent adaptations. *Trends Endocrinol Metab*; 18(3):114-21.

Soares ML, Torres-Padilla ME, Zernicka-Goetz M. (2008)
Bone morphogenetic protein 4 signaling regulates development of the anterior visceral endoderm in the mouse embryo. *Dev Growth Differ*; 50(7):615-21.

Spruce T, Pernaute B, Di-Gregorio A, Cobb BS, Merkenschlager M, Manzanares M, Rodriguez TA (2010) An early developmental role for miRNAs in the maintenance of extraembryonic stem cells in the mouse embryo. *Dev Cell*; 19(2):207-19.

Stower MJ, Srinivas S. (2014) Heading forwards: anterior visceral endoderm migration in patterning the mouse embryo. *Philos Trans R Soc Lond B Biol Sci*; 369(1657).

Strumpf D, Mao CA, Yamanaka Y, Ralston A, Chawengsaksophak K, Beck F, Rossant J. (2005) Cdx2 is required for correct cell fate specification and differentiation of trophectoderm in the mouse blastocyst. *Development*; 132(9):2093-102.

Sun X, Meyers EN, Lewandoski M, Martin GR. (1999) Targeted disruption of Fgf8 causes failure of cell migration in the gastrulating mouse embryo. *Genes Dev*; 13(14):1834-46.

Tabata T, Takei Y. (2004) Morphogens, their identification and regulation. *Development*; 131(4):703-12.

Takahashi Y, Takahashi M, Carpino N, Jou ST, Chao JR, Tanaka S, Shigeyoshi Y, Parganas E, Ihle JN (2008)
Leukemia inhibitory factor regulates trophoblast giant cell differentiation via Janus kin ase 1-signaltransducer and activator of transcription 3-suppressor of cytokine signaling 3 pathway. *Mol Endocrinol*; 22(7):1673-81.

Takeichi M. (2014)
Dynamic contacts: rearranging adherens junctions to drive epithelial remodelling. *Nat Rev Mol Cell Biol*; 15(6):397-410.

Tam PP, Loebel DA. (2007) Gene function in mouse embryogenesis: get set for gastrulation. *Nat Rev Genet*; 8(5):368-81

Tanaka M, Puchyr M, Gertsenstein M, Harpal K, Jaenisch R, Rossant J, Nagy A. (1999) Parental origin-specific expression of Mash2 is established at the time of implantation with its imprinting mechanism highly resistant to genome-wide demethylation. *Mech Dev*; 87(1-2):129-42.

Tanaka S, Kunath T, Hadjantonakis AK, Nagy A, Rossant J. (1998) Promotion of trophoblast stem cell proliferation by FGF4. *Science*; 282(5396):2072-5.

Telesnitsky A, Goff SP. (1997) Reverse transcription and the generation of the retroviral DNA. In: Coffin JM, Hughes SH, Varmus HE eds. Retroviruses. *Cold Spring Harbor Laboratory Press*; 121-160.

Tesser RB, Scherholz PL, do Nascimento L, Katz SG. (2010) Trophoblast glycogen cells differentiate early in the mouse ectoplacental cone: putative role during placentation. *Histochem Cell Biol*; 134(1):83-92.

Thiery JP, Acloque H, Huang RY, Nieto MA. (2009) Epithelial-mesenchymal transitions in development and disease. *Cell*; 139(5):871-90.

Tremblay KD, Hoodless PA, Bikoff EK, Robertson EJ. (2000) Formation of the definitive endoderm in mouse is a Smad2-dependent process. *Development*; 127(14):3079-90.

Trichas G, Joyce B, Crompton LA, Wilkins V, Clements M, Tada M, Rodriguez TA, Srinivas S. (2011) Nodal dependent differential localisation of dishevelled-2 demarcates regions of differing cell behaviour in the visceral endoderm. *PloS Biol*; 9(2):e1001019.

Tortelote GG, Hernandez-Hernandez JM, Quaresma AJ, Nickerson JA, Imbalzano AN, Rivera-Perez JA (2013) Wnt3 function in the epiblast is required for the maintenance but not the initiation of gastrulation in mice. *Dev Biol*; ;374(1):164-73.

Tunster SJ, McNamara GI, Creeth HDJ, John RM (2016) Increased dosage of the imprinted Ascl2 gene restrains two key endocrine lineages of the mouse Placenta. *Dev Biol*; 418(1):55-65.

Tunster SJ, Tycko B, John RM (2010)
The imprinted Phlda2 gene regulates extraembryonic energy stores. *Mol Cell Biol*; 30(1):295-306

Uehara M, Yashiro K, Takaoka K, Yamamoto M, Hamada H. (2009)
Removal of maternal retinoic acid by embryonic CYP26 is
required for correct Nodal expressionduring early embryonic patterning. *Genes Dev*; 23(14):1689-98.

Ueno M, Lee LK, Chhabra A, Kim YJ, Sasidharan R, Van Handel B, Wang Y, Kamata M, Kamran P, Sereti KI, Ardehali R, Jiang M, Mikkola HK (2013) c-Met-dependent multipotent labyrinth trophoblast progenitors establish placental exchange interface. *Dev Cell*;27(4):373-86.

Uez N, Lickert H, Kohlhase J, de Angelis MH, Kuhn R, Wurst W, Floss T. (2008) Sall4 isoforms act during proximal-distal and anterior-posterior axis formation in the mouse embryo. *Genesis*; 46(9):463-77.

Uy GD, Downs KM, Gardner RL. (2002) Inhibition of trophoblast stem cell potential in chorionic ectoderm coincides with occlusion of the ectoplacental cavity in the mouse. *Development*; 129(16):3913-24.

Vassalli A, Matzuk MM, Gardner HA, Lee KF, Jaenisch R. (1994)
Activin/inhibin beta B subunit gene disruption leads to defects in eyelid development a nd female reproduction. *Genes Dev*; 8(4):414-27.

Venditti CC, Casselman R, Murphy MS, Adamson SL, Sled JG, Smith GN. (2013) Chronic carbon monoxide inhalation during pregnancy augments uterine artery blood flow and uteroplacental vascular growth in mice. *Am J Physiol Regul Integr Comp Physiol*; 305(8):R939-48.

Vinot S, Le T, Ohno S, Pawson T, Maro B, Louvet-Vallee S. (2005)
Asymmetric distribution of PAR proteins in the mouse embryo begins at the 8-cell stage during compaction. *Dev Biol*; 282(2):307-19.

Walentin K, Hinze C, Schmidt-Ott KM. (2016)
The basal chorionic trophoblast cell layer:
An emerging coordinator of placenta development. *Bioessays*; 38(3):254-65.

Waldrip WR, Bikoff EK, Hoodless PA, Wrana JL, Robertson EJ. (1998) Smad2 signaling in extraembryonic tissues determines anterior-posterior polarity of the early mouse embryo. *Cell*; 92(6):797-808.

Wang GP, Ciuffi A, Leipzig J, Berry CC, Bushman FD. (2007)
HIV integration site selection: analysis by massively parallel pyrosequencing reveals association with epigenetic modifications. *Genome Res*; 17(8):1186-94.

Watson ED, Cross JC (2005) Development of structures and transport functions in the mouse placenta. *Physiology* (Bethesda);20:180-93

Whiteman EL, Liu CJ, Fearon ER, Margolis B. (2008)
The transcription factor snail represses Crumbs3 expression and disrupts apico-basal polarity complexes. *Oncogene*; 27(27):3875-9.

Williams M, Burdsal C, Periasamy A, Lewandoski M, Sutherland A. (2012)
Mouse primitive streak forms in situ by initiation of epithelial to mesenchymal transition without migration of a cell population. *Dev Dyn*; 241(2):270-83

Winnier G, Blessing M, Labosky PA, Hogan BL (1995) Bone morphogenetic protein-4 is required for mesoderm formation and patterning in the mouse. *Genes Dev*; 9(17):2105-16.

Yamamoto M, Saijoh Y, Perea-Gomez A, Shawlot W, Behringer RR, Ang SL, Hamada H, Meno C (2004) Nodal antagonists regulate formation of the anteroposterior axis of the mouse embryo. *Nature*; 428(6981):387-92.

Yang W, Klaman LD, Chen B, Araki T, Harada H, Thomas SM, George EL, Neel BG. (2006)
An Shp2/SFK/Ras/Erk signaling pathway controls trophoblast stem cell survival. *Dev Cell*; 10(3):317-27

Yang X, Letterio JJ, Lechleider RJ, Chen L, Hayman R, Gu H, Roberts AB, Deng C. (1999b)
Targeted disruption of SMAD3 results in impaired mucosal immunity and diminished T cell responsiveness to TGF-beta. *EMBO*; 18(5):1280-91.

Yoon Y, Cowley DO, Gallant J, Jones SN, Van Dyke T, Rivera-Perez JA. (2012) Conditional Aurora A deficiency differentially affects early mouse embryo patterning. *Dev Biol*; 371(1):77-85.

Yoon Y, Huang T, Tortelote GG, Wakamiya M, Hadjantonakis AK, Behringer RR, Rivera-Perez JA (2015) Extra-embryonic Wnt3 regulates the establishment of the primitive streak in mice. *Dev Biol*; 403(1):80-8.

Zhu Y, Li B, Wu T, Ye L, Zeng Y, Zhang Y (2017) Cell cycle and histone modification genes were decreased in placenta tissue from unexplained early miscarriage. *Gene*; 636:17-22.

Zimmer Y, Givol D, Yavon A. (1993) Multiple structural elements determine ligand binding of fibroblast growth factor receptors. Evidence that both Ig domain 2 and 3 define receptor specificity. *J Biol Chem*; 268(11):7899-903.

Zwijsen A, van Rooijen MA, Goumans MJ, Dewulf N, Bosman EA, ten Dijke P, Mummery CL, Huylebroeck D. (2000) Expression of the inhibitory Smad7 in early mouse development and upregulation during embryonic vasculogenesis. *Dev Dyn*; 218(4):663-70.

CHAPTER 8:

APPENDIX

8. Appendix

Gene	Forward primer	Reverse primer	Source
Spry 4	5'-CATGACTGAGCTGGGATTCA-3'	5'-TTTACACAGACGTGGAGCGA-3'	https://mouseprimerdepot.nci.nih.gov
Smad7	5'-CTTCTCCTCCCAGTATGCCA-3'	5'-GAACGAATTATCTGGCCCCT-3'	https://mouseprimerdepot.nci.nih.gov
Gapdh	5'-TTGATGGCAACAATCTCCAC-3'	5'-CGTCCCGTAGACAAAATGGT-3'	https://mouseprimerdepot.nci.nih.gov

Table 8.1: List of Real Time PCR primers used in this study

Gene	**Forward primer** (restriction enzyme added)	**Reverse primer** (restriction enzyme added)	**Annealing temperature**
Sprouty4	5'-TTATA-CTCGAG-GGGAACACAGGCTCTCACAAACAG-3' (XhoI)	5'-TTATA-GAATTC-ATGTGTGCTGCCCACACGCCTC-3' (EcoRI)	65^{o}c
Smad7	5'-TATTA-CTCGAG-GTCAGCACTGCCAAGCATGG-3' (XhoI)	5'-TATAT-GAATTC-CTCGCTGGTCTACAGAGCTC-3' (EcoRI)	60^{o}c
Secretin	5'-TATTA-gaattc-TGTTGCTGCTGCTGCTCT-3' (EcoRI)	5'-TATTA-ctcgag-GGTGGCCTGGTTGTTTCA-3' (XhoI)	55^{o}c
Cldn4	5'-TATAT-ctcgag-TGCTGCAGTTGCCCACCTC-3' (XhoI)	5'-TATTA-gaattc-CCATGGCAGAGCCCACCG-3' (EcoRI)	60^{o}c

Table 8.2: List of primer pairs used for template derivation

Materials used in this study

- **Growth factors**

Human Fgf2 protein NBP2-34921, Novus
Activin A, human A4941-5UG, Sigma

- **Small molecule inhibitors**

SU5402 (potent FGFR and VEGFR inhibitor), 3300, TOCRIS
PD161570 (selective FGFR inhibitor), 3724, TOCRIS
A83-01 (selective inhibitor of TGF-bRI, ALK4 and ALK7), 2939, TOCRIS
SB431542 (potent and selective inhibitor of ALK5, ALK4 and ALK7), 1614, TOCRIS

- **Cell culture reagents (including embryo and explants)**

Fetal Bovine Serum, 10500, Gibco
4-well cell culture plate, 30004, SPL
35mm plate, 20035, SPL
Neurobasal®-A medium (1x) 12349-015 Gibco
DMEM (1x) 31053-028 Gibco
DMEM (1x) 41965-039 Gibco
F-12 Nut Mix (1x) + GlutaMAX™-I, 31765-027, Gibco
Sodium Pyruvate, 11360, Gibco
RPMI Medium 1640 (1x) + GlutaMAX™-I, 61870-010, Gibco
T-75 Corning™ Falcon™ Tissue Culture Treated Flasks, Catalogue Number: 353136
Trypsin-EDTA (0,05%), Cat number: 25-300-062, Gibco
Matrigel® matrix, REF 356230, CORNING
Mitomycin C from *Streptomyces caespitosus*, catalogue number: M4287, Sigma-Aldrich

- **Lentivirus**

Filter Flask, 150 ml, PES, 0.45µm, sc-200310 UltraCruz®
Filters (for virus filtration): 150ml, 0.45um, PES, filter unit, sc-200310, Santa Cruz
Corning 0.45um Cellulose Acetate filters (low protein binding), Catalogue number: 431155
Ultracentrifuge Sorvall WX, Ultra 80 (@25000rpm, 4c, 1:35min)
Sorvall ultracentrifuge tubes, 36ml (filled with 31-32 ml), Catalogue number 03141
Polybrene®, sc-134220, Santa Cruz

- **Immunochemistry - Antibodies – Lectins - Secondaries**

pErk: Phospho-p44/42 MAPK (Erk1/2) (Thr202/Tyr204) Antibody #9101, Cell Signaling technology
Collagen IV alpha 1, Biotin labeled: Novus (NB120-6581)
Par6B: santa cruz (sc-67393)
Cdx2: BioGenex (AM392-10M)
Lectin, Biotin labeled, From Bandeiraea simplicifolia BS-I, L3759-1MG, Sigma
Lectin, Biotin labeled, From Dolichos biflorus, L6533-5MG, Sigma
Streptavidin-peroxidase from Jackson ImmunoResearch, Cat nr: 016-030-084
Streptavidin-cy3 from Jackson ImmunoResearch, Cat nr: 016-160-084
Anti-Rabbit-Alexa 488 from Jackson ImmunoResearch Cat nr: 111-545-003
Anti-Rat-Alexa-488 from Jackson ImmunoResearch, Cat nr: 112-545-003

Goat serum, G9023-5ML, Sigma
DAB substrate kit, ab94665, Abcam
TOPRO™-3 Iodide (642/661), Catalog number T3605, Thermo Fisher
Hoechst 33342, trihydrochloride trihydrate, H3570, Invitrogen
Triton® X-100, T8787-250ML, Sigma

- ***In situ* hybridization**

UltraPure™ Formamide, Redistilled, 15516-026, Invitrogen
Glutaraldehyde solution, Grade II, 25% G6257-10ML, Sigma
BM Purple AP Substrate precipitating, 11442074001, Roche
INT/BCIP Stock Solution, 11 681 460 001, Roche
tRNA, 10109495001, Roche
T_7 RNA Polymerase, 10881767001, Roche
DIG RNA labeling Mix, 10x conc, 11277073910, Roche
Proteinase K, recombinant PCR Grade, 03115879001, Roche
T_3 RNA Polymerase, 11 031 163 001, Roche
RNase A, REF 10109169001, Roche
DEPC-treated water, 46-2224, Invitrogen

- **Subcloning and general molecular biology procedures**

TAE 50x, UltraPure DNA typing grade, 24710-030, Invitrogen
Agarose Calbiochem, 2125
1kb Plus DNA Ladder TrackIt™, 10488-085, Invitrogen
Ampicillin sodium salt, A9518-5G, Sigma-Aldrich
Phenol:$ChCl_3$:IAA (25:24:1) pH 6.6/7.9, AM9730, Ambion
Distilled water DNase/RNase free, 11977-035, Gibco
Subcloning Efficiency™ DH5α™ Competent Cells, Catalogue number: 18265017 Invitrogen
NucleoBond Xtra Midi Ref. 740410.50 Mackerey Nagel
DEPC, D5758-50ML, Sigma

- **Microscopes**

Zeiss stereoscope, Stemi 2000-C
Zeiss Axiovert 200M inverted microscope

- **General histology**

Glass coverslipes 12 mm round (100), CS-12R, Cat: 64-0702, Warner Instruments
SUPERFROST® PLUS, Thermo Scientific
wax (histoplast) 6774006, Thermo Scientific